THERMOECONOMIC ANALYSIS OF REFRIGERATION SYSTEM

Thesis Submitted
in Partial Fulfillment of the Requirements for the
Degree of

DOCTOR OF PHILOSOPHY

in

Mechanical Engineering

by

SUNIL KUMAR GUPTA

(2K16/PhD/ME/17)

Under the Supervision of

Prof. B.B. Arora
Professor

Prof. Akhilesh Arora
Professor

Department of Mechanical Engineering
Delhi Technological University

Department of Mechanical Engineering
DELHI TECHNOLOGICAL UNIVERSITY
(Formerly Delhi College of Engineering)
Shahbad Daulatpur, Main Bawana Road, Delhi-110042. India

October, 2024

CANDIDATE'S DECLARATION

I, Sunil Kumar Gupta, (2K16/PhD/ME/17) hereby declare that the thesis entitled ***"Thermoeconomic Analysis of Refrigeration System"*** submitted by me, is an original and authentic work carried out by me under the supervision of **Prof. B.B. Arora, and Prof. Akhilesh Arora**, Professors, Department of Mechanical Engineering, Delhi Technological University, Delhi for the award of the degree of **Doctor of Philosophy** in **Mechanical Engineering**. I further declare that the work reported in this thesis has not been submitted and will not be submitted, either in part or in full, for the award of any other degree or diploma in this Institute or any other Institute or University.

Place: Delhi

Date:

SUNIL KUMAR GUPTA
(2K16/PhD/ME/17)
PhD Scholar
Department of Mechanical Engineering
Delhi Technological University.

CERTIFICATE

Certified that **Sunil Kumar Gupta** (2K16/PhD/ME/17) has carried out his research work presented in this thesis entitled **"Thermoeconomic Analysis of Refrigeration System"** for the award of degree of **Doctor of Philosophy** from Delhi Technological University New Delhi, under our supervision. The thesis embodies results of original work, and studies are carried out by the student himself and the contents of the thesis do not form the basis for the award of any other degree to the candidate or to anybody else from this or any other University/Institution.

Prof. B. B. Arora
(Professor)
Department of Mechanical Engineering
Delhi Technological University, Delhi.

Prof. Akhilesh Arora
(Professor)
Department of Mechanical Engineering
Delhi Technological University, Delhi.

Date:

ACKNOWLEDGEMENTS

First and foremost, I am thankful to almighty GOD for keeping me fit, healthy and energetic during entire course of my Ph. D. work.

With pleasure, I would like to express my deepest gratitude to my supervisors Prof. B. B. Arora, Professor and Head of Department and Prof. Akhilesh Arora, Professor, Department of Mechanical Engineering, Delhi Technological University for their proficient guidance, intelligent approach, constructive critique, whole hearted and ever available help, which has been the primary impetus behind the research. Without the wise advice and able guidance, it would have been impossible to complete the thesis in this manner.

I would like to express my gratitude to Prof. Prateek Sharma, Vice chancellor, Delhi Technological University, Delhi for providing this opportunity to carry out my work in this prestigious institute.

I wish to record my thanks and gratitude to Prof. Vipin Kumar (DTU, Delhi) and Prof. S. Maji (DTU, Delhi) for offering me the necessary and timely advice. I owe special thanks to my colleagues Dr. A.K. Ahluwalia and Dr. Jaji Varghese who provided valuable suggestions on books and literature which enriched and enhanced the level of my research. I offer my heartfelt thanks to my friends Mr. Pritpal Singh, Mr. Rachit Saxena and Mr. Deepak Saini, who supported and motivated me at times of mental fatigue.

I am greatly indebted to my parents for their love and blessings to see me scaling greater heights of life. One who matters most in my Ph.D work is my wife Smt. Rachna Varshney without whose motivation and encouragement, pursuit of this Ph.D work would have never been possible. I thank her for her care and relieving me entirely from the family affairs. Last but not the least I am thankful to my daughter Shreya and son Piyush who imparted me immense energy to work.

October, 2024 **Sunil Kumar Gupta**

ABSTRACT

The application of refrigeration and air-conditioning on a large scale is responsible to produce green-house gases and is a threatening issue concerning global warming. The vapor-compression refrigeration system based conventional split air conditioners (CAC) draw a significant amount of gross electrical energy and pose a very serious concern by degrading the environment. Improving the energy efficiency could reduce this damage. With the growing concerns to reduce energy consumption and environmental impact, increasingly significant need is felt for efficient and sustainable cooling technologies.

This study assesses the performance of a split air conditioner with and without the implementation of direct evaporative cooling (DEC) for the condenser. A thorough thermo-economic evaluation is conducted for a 5.25 kW capacity split air conditioner (SAC) integrated with direct evaporative cooling, focusing on performance, energy consumption, coefficient of performance (COP), and economic viability.

The reduction in ambient air temperature through evaporative cooling is calculated under various outdoor conditions for New Delhi. The enhanced heat exchange between the evaporatively cooled condenser and ambient air contributes to reduced power input and improved COP. A numerical model is developed to determine the decrease in condenser inlet air temperature resulting from direct evaporative cooling.

The multi-objective optimization is carried out with Box-Behnken design (BBD) technique using response surface methodology. The objective functions include COP, total cost rate (TCR), and total exergy destruction ($\dot{E}_{D,t}$). Design variables include ambient temperature (T_a =30ºC-45ºC), relative humidity (RH =20%-80%),

and evaporator temperature (T_e =3ºC-12ºC). Cooling capacity, life duration, operation hours, interest rate, maintenance factor, and electricity price for the system are considered to be constants. The proposed system significantly enhances air conditioner performance, achieving improvement in the refrigerating effect and saving in work input by 11.59% and 23.53%, respectively in average design conditions (T_a = 37.5℃, relative humidity = 50%, T_e = 7.5℃). For the whole range of inputs, the *COP* enhances by 3.53 to 65.21% while total cost rate reduces by 2.23% – 23.2% compared to conventional SAC. The influence of ambient temperature is more significant than other input parameters.

Thermoeconomic optimization results in a maximized *COP* enhancement of 64.23%, along with a 22.91% reduction in TCR and a 54.45% reduction in total exergy destruction ($\dot{E}_{D,t}$).

The water consumption to energy-saving ratio for different cooling months (April to September) vary from 5.5 to 9.8L/kWh. The direct evaporative cooling (DEC) system demonstrates significant energy savings in hot-dry and warm-humid climates of New Delhi, India, with respective average annual savings of electrical energy as 47.17% and 12.11%.

The thermoeconomic performance and sustainability of DEC-SAC are notably improved compared to conventional SAC, especially in hot-dry climates. The simple payback period for the proposed system ranges from 1.21 to 2.99 years, depending on the operating conditions. Sustainability indices indicate a substantial environmental improvement with the modified DEC-SAC system.

Among the various alternatives available, direct evaporative cooling (DEC) stands out as a promising solution due to its energy-efficient operation and minimal environmental impact.

CONTENTS

LIST OF TABLES

LIST OF FIGURES

LIST OF SYMBOLS AND ABBREVIATIONS

Notations

A	area (m^2)
B	width of cooling pad (m)
COP	coefficient of performance (-)
CSAC	conventional split air conditioner
C	cost rate (₹. $year^{-1}$)
CF_{net}	net cash flow (₹. $year^{-1}$)
C_p	specific heat (kJ $Kg^{-1}K^{-1}$)
d	diameter of heat exchanger tubes (m^{-1})
H	height of cooling pad (m)
DEC	direct evaporative cooler
E	exergy (kW)
F	surface area (m^2)
h	enthalpy (kJ kg^{-1})
H	water head (m)
h_c	heat transfer coefficient (kW $m^{-2}K^{-1}$)
h_M	mass transfer coefficient (kW $m^{-2}s^{-1}$)
i	interest rate (%)
IRR	internal rate of return (%)
L_e	Lewis number (-)
L_w	Latent heat of water (kJ kg^{-1})
$\dot{m}$	mass flow rate ($kg.s^{-1}$)
n	life period (year)
N	annual operation hours (h. $year^{-1}$)

NPV	net present value (₹)
P	pressure (kPa)
$\dot{P}$	power (kW)
q	refrigerating effect (kJ kg^{-1})
$\dot{q}_l$	latent heat transfer rate (kW)
$\dot{q}_s$	sensible heat transfer rate (kW)
Q	cooling capacity(kW)
r	discount rate per annum (%)
RH	relative humidity (%)
s	entropy (kJ.$kg^{-1}K^{-1}$)
SPP	simple payback period (year)
T	temperature (°C)
TCR	total cost rate (₹.h^{-1})
U	overall heat transfer (kW.$m^{-2}K^{-1}$)
V	air velocity across the cooling pad (m s^{-1})
$\dot{V}_p$	compressor swept volume (m^3 s^{-1})
w	specific work (kJ kg^{-1})
W	power input (kW)
x	dryness fraction (-)

Greek symbols

δ	thickness of cooling pad (m)
ε	cooling pad efficiency, saturation efficiency (-)
ζ	capital recovery factor (-)
η	pump efficiency (-)

η_s	compressor isentropic efficiency (-)
η_{vol}	compressor volumetric efficiency (-)
ν	specific volume (m^3 kg^{-1})
ξ	pore surface coefficient per unit pad volume (m^2/m^3)
ρ	density (kg m^{-3})
φ	maintenance factor (-)
ω	specific humidity (kg/kg of dry air)
Δ	difference
Ψ	exergy ratio (-)

Subscripts

a	air
c	compressor
CAP	capital
D	destruction
EL	unit electricity (kWh)
e	evaporator
ENV	environmental
i	inlet, inside
INV	investment
k	condenser
LM	log mean
o	outlet, outdoor
OP	operating cost
p	pump
r	refrigerant

R	room
ref	refrigeration
s	saturation
sh	superheat
t	total
v	expansion valve
w	water
0	dead state
1,2,3,4	various state points of CSAC refrigeration cycle
1,2’,3’,4’	various state points of DEC SAC refrigeration cycle

CHAPTER 1

INTRODUCTION

This chapter provides background of refrigeration and air conditioning sector. It gives an account of energy consumption and environmental impact of refrigeration equipment. The energy efficiency with exergy efficiency and economic considerations in air- conditioning is also discussed. At the end, the organisation of this thesis is presented.

1.1 Background

The refrigeration and air conditioning sector significantly contribute to environmental degradation by CO_2 gas emissions through the widespread use of vapor compression refrigeration systems. Consequently, there is a persistent need to enhance the efficiency of these systems and mitigate their environmental impact [1]. In addition to considering the thermodynamic performance of a refrigerant, the choice of a refrigerant for a specific application should also involve an evaluation of its environmental impact. Metrics such as Total Equivalent Warming Impact (TEWI) and Life Cycle Climate Performance (LCCP) play a critical role in assessing the overall influence of systems or processes that utilize energy input and indirectly affect the environment. LCCP analysis aims to identify the most environmentally sustainable outcome by achieving a proper balance among factors like low charge, low Global Warming Potential (GWP), and energy efficiency [2].

1.2 Simple Vapor Compression Refrigeration Cycle

The fundamental vapor compression refrigeration cycle serves as a core process in refrigeration and air conditioning systems, facilitating the transfer of heat from a low-temperature space to a higher-temperature sink. Comprising four primary components - a compressor, condenser, expansion valve, and evaporator - the cycle initiates with the compressor. The compressor elevates low-pressure, low-temperature vapor refrigerant to a high-pressure, high-temperature gas. The high-energy gas proceeds to the condenser, where it releases heat to the outdoor air and undergoes a phase change, transitioning into a high-pressure liquid. This liquid refrigerant moves through the expansion valve, experiencing a remarkable pressure drop that results in a temperature decrease. The resulting cold, low-pressure liquid enters the evaporator, absorbing heat from the cooled space and transforming into a low-pressure vapor. The vapor then returns to the compressor, marking the commencement of the cycle once again.

This continuous process facilitates the transfer of heat, allowing the refrigeration system to maintain a desired temperature within a controlled space. Figures 1.1 (a) to (c) depict the schematic, P-h and T-s diagrams of simple vapor compression refrigeration cycle.

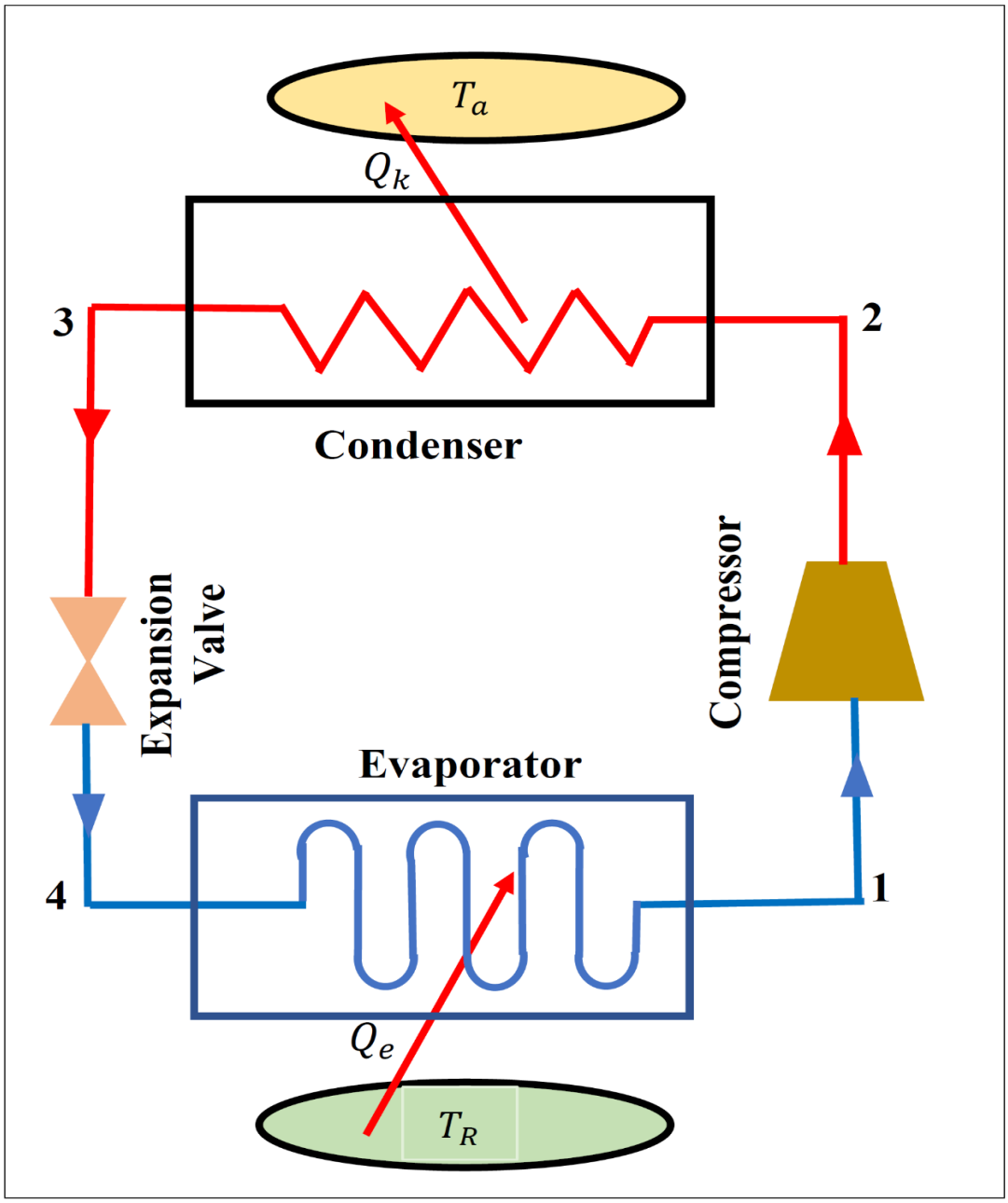
T_a
Q_k
3
2
Condenser
Expansion Valve
Compressor
Evaporator
4
1
Q_e
T_R

(a)

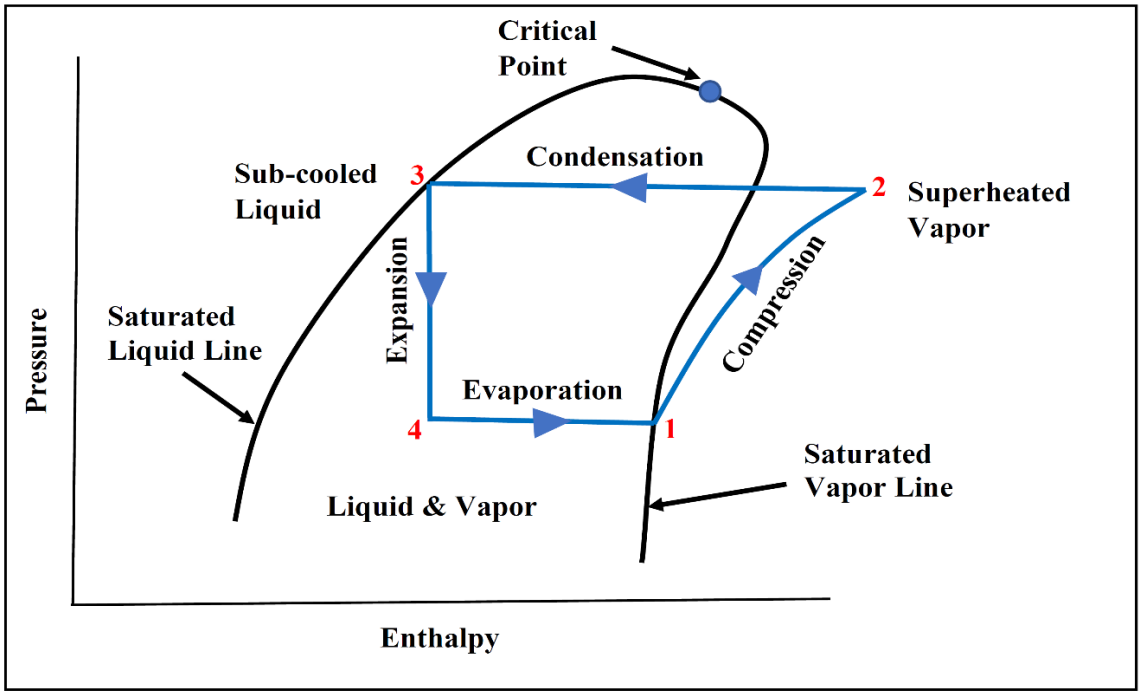

(b)

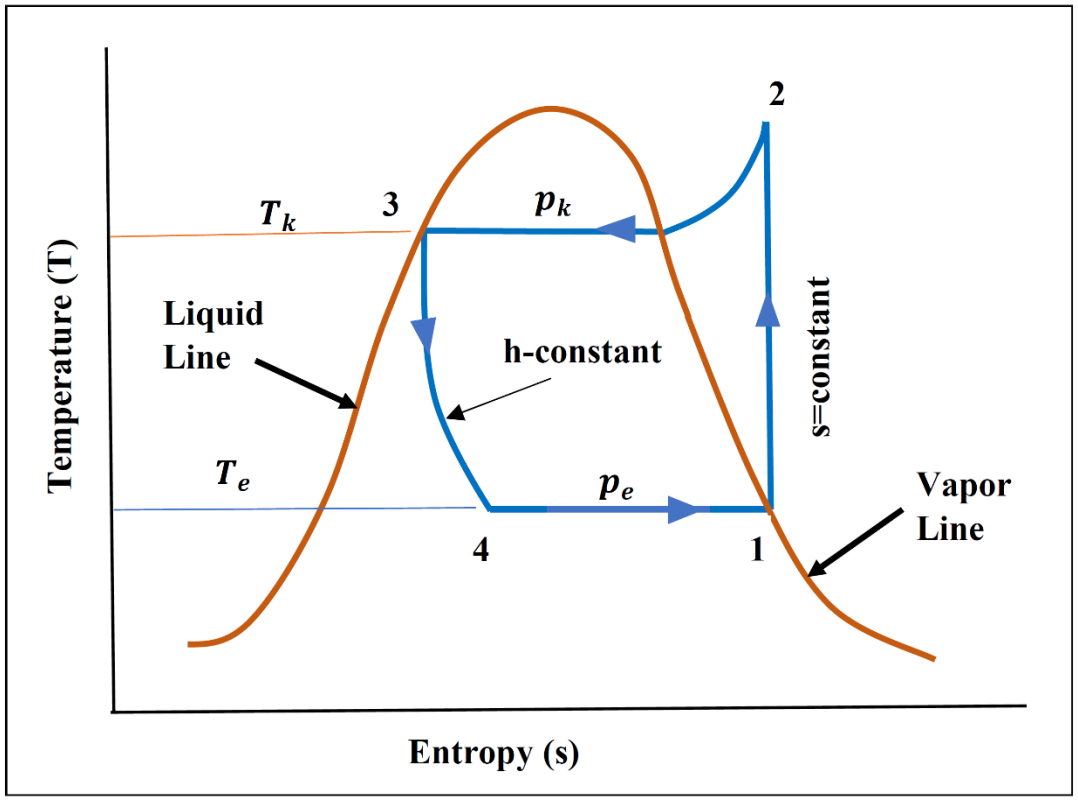

(c)

Fig. 1.1 (a) Schematic, (b) P-h and (c) T-s diagrams of Simple Refrigeration Cycle

1.3 Energy and Environmental Concern of Air Conditioning

The surge in electrical energy consumption by the refrigeration industry, emitting 7.8% of greenhouse gases and contributing 37% to global warming [3], underscores the need for efficiency improvements. Air conditioners in commercial and domestic premises of Malaysia consume over 50% and 30% of electrical energy, respectively [4]. In India, air conditioners (ACs) account for a larger share of electricity consumption due to climatic variations than other gadgets [5], with about 42% of electric energy used by households in heating, ventilation, and air conditioning (HVAC) systems [6]. According to 'India Cooling Action Plan' report (2019), India's total primary energy supply (TPES) for cooling in the year 2022-23 is as shown in Fig.1.2. Space cooling energy consumption by equipment for the year 2017-18 and projections for 2037-38 are shown in Fig.1.3 (a) and (b), respectively [7].

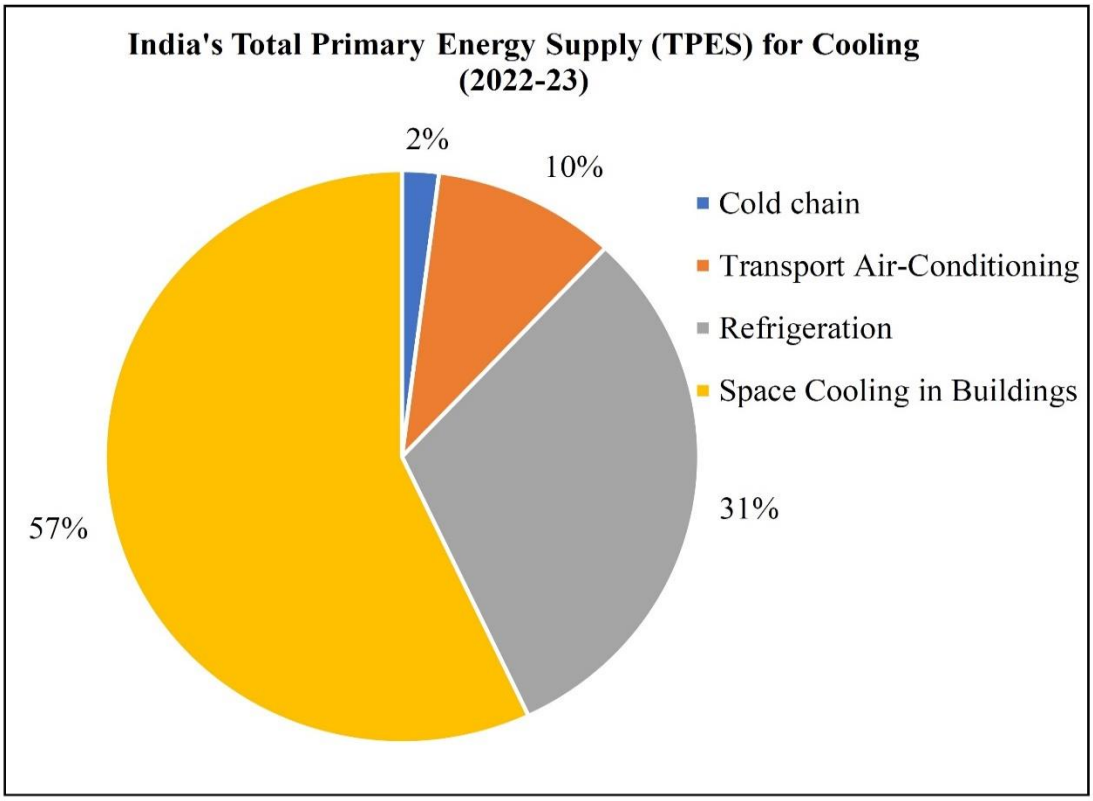

Fig. 1.2 India's Total Primary Energy Supply (TPES) for Cooling (2022-23)

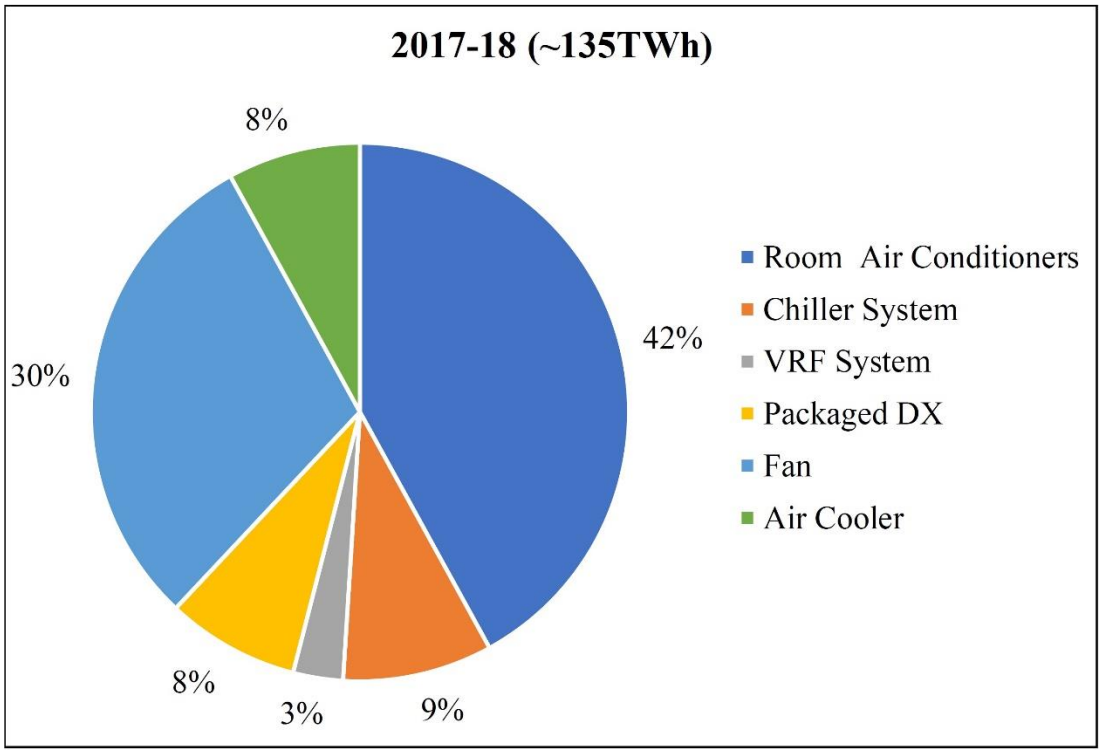

(a)

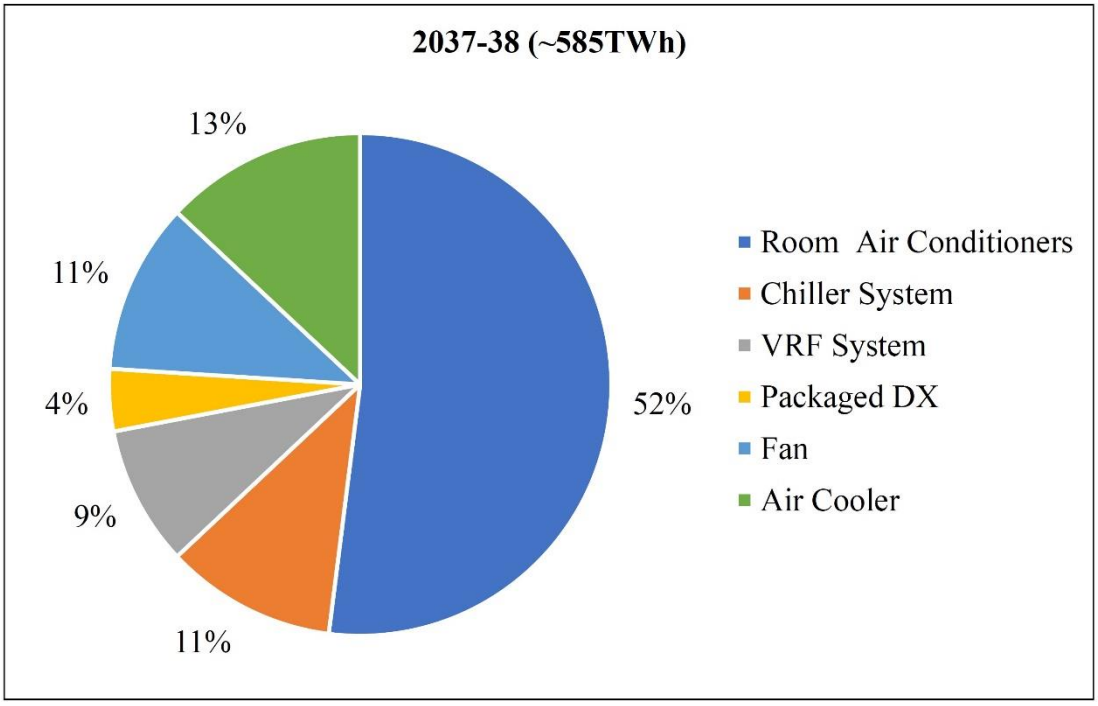

(b)

Fig.1.3 Space Cooling Energy Consumption by Equipment (a) 2017-18, (b) 2037-38 [7]

The increase in global temperatures and burgeoning economies have heightened the demand for increased cooling. According to the International Institute of Refrigeration (IIR), approximately 1.1 billion domestic air conditioners are currently in use worldwide [3]. Factors such as rapid population growth, urbanization, and climate change-induced rising temperatures have exponentially increased the need for cooling systems, especially air conditioners. The widely adopted vapor compression refrigeration system, prevalent in most refrigeration, air-conditioning, and heat-pumping equipment, is known for its high energy consumption [8]. Refrigeration and air conditioning systems collectively account for about one-third of the world's total energy consumption [9].

The surge in electrical energy consumption has significant repercussions on the environment. Over the past few decades, the air-conditioning industry has experienced rapid growth, with a notable demand for small systems in households, shops, offices, and other settings. Unfortunately, despite providing immediate comfort, these systems contribute to CO_2 emissions posing a considerable threat in terms of global warming by utilizing high GWP substances in the vapor compression refrigeration cycle. The global refrigeration industry is responsible for emitting 7.8% of greenhouse gases, with a substantial 37% contribution to global warming, primarily from fluorinated refrigerants [3]. Projections indicate a potential doubling of emissions by 2050 compared to the 2016 baseline [10]. If efficiency gains are not realized, the energy consumption for space cooling is expected to more than double by 2040, driven by increased activity and air conditioning usage [11]. Therefore, there is a pressing need for more efficient air conditioners, not only to reduce energy consumption but also to mitigate greenhouse gas emissions.

1.4 Transition to Environment Friendly Refrigerants

Traditionally, refrigeration systems relied on halogenated compounds such as chloro-fluoro carbons (CFCs) and hydro chloro-fluoro carbons (HCFCs) due to their favorable thermo-physical and thermodynamic properties. However, the chlorine content in these compounds led to ozone layer depletion and contributing to global warming through the greenhouse effect [12]. Recent research aimed at enhancing the efficiency of vapor compression refrigeration systems has focused on developing new

technologies and utilizing alternative refrigerants, either pure or mixtures, to achieve improved performance while addressing environmental concerns [13]. Hydrofluorocarbons (HFCs) like R-32, natural refrigerants such as hydrocarbons (HC) like R-600a, and more recently, hydro-fluoro-olefins (HFO) like R-1234yf, have been tested as substitutes for CFCs and HCFCs due to their shorter atmospheric lifetimes, leading to reduced ozone depletion and greenhouse gas impact [14]. The use of mixed refrigerants, comprising two or more components, offers an avenue to tailor fluid properties for specific applications with acceptable environmental attributes. International environmental agreements like the Kyoto Protocol (1997) and the Montreal Protocol (1987) underscore the necessity of adopting new refrigerants to mitigate ozone depletion and global warming [15].

The quest for more efficient vapor compression refrigeration systems (VCRS) has prompted the introduction of new refrigerants to enhance energetic performance and diminish environmental impact. The utilization of high GWP refrigerants has spurred efforts to identify substitutes that are both environmentally friendly and energy-efficient [16]. Despite experimenting with various alternative refrigerants, the focus remains on finding substitutes with shorter atmospheric lifespans to mitigate global warming. The primary consideration when introducing replacement refrigerants is the energetic and exergetic optimization of the system. Developed nations have embraced R410A, a blend refrigerant, as a key substitute for HCFC-22. However, R32, a single-component gas devoid of chlorine content and ozone layer depletion (ODP=0), emerges as an environmentally friendly alternative. Despite R410A having a global warming potential (GWP) three times that of R32, it is hindered by its zeotropic nature [17]. Conversely, R32, being non-toxic and chemically inert, stands out as a readily available and efficient commercial product. Concerns persist about R32's discharge temperature from the compressor during extreme cooling and heating operations [18], as well as its mild flammability (Class 2L under refrigerant standards ASHRAE 34). Medium-pressure refrigerants have demonstrated superior efficiency compared to high-pressure ones at elevated ambient temperatures [2]. The properties of most commonly used refrigerant in residential air-conditioners are listed in Table 1.1.

Table 1.1 Thermophysical properties of refrigerants (Genetron properties software v14.1)

Property	R32	R410A	R454B
Chemical name	Difluoro methane	Difluoro methane(R32)/ Pentafluoro ethane(R125) (w/w=50/50)	Difluoro methane(R32)/ 2,3,3,3-tetrafluoro propene(R1234yf) (w/w=68.9/31.1)
Chemical formula	CH_2F_2	CH_2F_2/CHF_2CF_2	$CH_2F_2/C_3H_2F_4$
Molecular weight(kg/kmol)	52.024	72.585	62.2
Critical temperature (C)	78.4	70.17	77
Critical pressure (MPa)	5.186	4.77	5.014
GWP	675	2088	466
Safety Class	A2L	A1	A2L
Temp Glide (K)		1.5	0.05

In a comparison between R410A and R32, R410A slightly surpasses R22 in terms of refrigerating effect (higher by 3.44%) and discharge pressure (lower by 2.46%) [19]. However, R410A consumes more compressor power and exhibits a lower average coefficient of performance (COP) than R22 [20]. An investigation considering different evaporation temperatures was conducted by Domanski et al. [21] to match the capacity of R22. At a 7ºC evaporation temperature, both R32 and R410A demonstrated greater capacity than R22, with R32 holding a 14.5% capacity advantage. Importantly, R32 exhibited similar performance when analyzing evaporator effects. In theoretical analyses, R32 exhibited a superior coefficient of

performance (COP) in both heating (5%) and cooling (6%) when compared to R410A [17]. Studies conducted by Bobbo et al. [22] indicated that R454B outperformed R410A in terms of COP and exergetic efficiency, particularly considering variable isentropic efficiency of the compressor. Additionally, Nan Zheng's [23] research revealed that R454B demonstrated a higher COP than R410A under specific temperature conditions (T_e=10°C and T_k=45°C). In summary, the quest for refrigerants that are both environmentally friendly and energy-efficient continues, with R32, R454B, and other alternatives showing promise in enhancing the performance of vapor compression refrigeration systems.

1.5 Challenges and Alternatives in Cooling Technology

The rising global temperatures and expanding economies are driving an increased demand for cooling solutions. Refrigeration equipment, including air-conditioners and refrigerators, has become essential for consumers, enhancing their quality of life and providing more leisure time [24]. Refrigeration and air conditioning systems play a major role in global energy demand, representing approximately 25-30% of total energy consumption worldwide [25]. The HVAC (Heating, Ventilating, and Air Conditioning) systems alone contribute to 20–40% of the total energy consumption in developed countries [9]. The dominant share of the refrigeration, air conditioning, and heat-pumping load is managed by vapor compression systems, known for their high energy consumption [26], [27]. In India, the domestic sector alone consumes about 42% of electric energy for running HVAC systems [6]. Missaoui et al. [28] enhanced the thermal efficiency of a helical coil by modifying its shape. The variable pitch coil exhibited a notable improvement, with a 36.48% increase in the

average heat transfer coefficient and a 16.17% increase in the average coefficient of performance (COP) compared to a normal coil. In another study, Missaoui et al. [29] aimed to enhance the precision of numerical results and reduce computational time in simulating a heat pump water heater utilizing immersed helically coiled tubes. They explored the impact of storage tank dimensions and copper coil pitch on the heating process. The findings highlighted the influence of time step size on the accuracy of results, indicating a clear trend towards decreased precision. N. Dai and S. Li [30] carried out a numerical investigation of performance analysis on heat pump water heater (HPWH). A combined model, integrating a vapor-compression cycle and a water heater, was developed to assess the performance of a heat pump water heater (HPWH). The evaluation focused on three key characteristics: water temperature distribution, heat transfer coefficient, and coefficient of performance (COP). The performance of a variable-diameter coil was compared to that of a constant-diameter coil. Results revealed a 19.06% increase in the heat transfer coefficient for the variable-diameter coil and a 3.97% higher average COP for this specific coil configuration.

Reduction in the indoor temperature by employing non-mechanical methods is called passive cooling. Passive cooling plays a vital role in alleviating the environmental impact on the buildings. The indoor cooling load can lower to a great extent by employing passive cooling techniques. Thus, the size and running duration of the air conditioner gets reduced [31]. Shading is one of the passive techniques which do not require any energy source and protect the building from solar heat gains [32]. Many researchers have used different methods to describe the effect of passive cooling on reduction of indoor temperatures. Kumar et al. [33], found a decrease of

nearly 2.5°C-4.5°C in the room temperature with solar shading. Further reductions of 4.4-6.8°C in the indoor temperature were recorded with insulation and regulated air flow rate. The insulation of outer wall produces barriers to the heat transferred into the conditioned room. Insulation also isolates the inner wall surfaces from the effect of the outdoor conditions. The passive cooling effect lowers DBT and help supply air take more room heat load compared to the Normal AC, which improves energy efficiency of the AC unit [25]. Majumdar [34] found that implementing a 40 mm thick expanded polystyrene insulation on walls and vermiculite concrete insulation on the roof led to a potential reduction in air conditioning loads by approximately 15%.

To address the escalating energy consumption and its environmental impact, a pressing need exists to enhance the energy efficiency of existing air conditioning technology. Scientists and engineers are currently investigating alternative cooling approaches that promise enhanced energy efficiency while minimizing environmental impacts.

1.6 Energy Efficiency and Economic Considerations

During the period from April to September, most regions in India experience intense heat and humidity, with ambient temperatures ranging from 30 to 44°C and relative humidity between 18.1% and 80.1% [35]. These conditions create discomfort for individuals, hampering efficient work. Consequently, the adoption of comfort air conditioning becomes essential to counter the adverse consequences of such extreme climate.

Given the environmental concerns associated with GHG emissions and global warming, enhancing the efficiency of refrigeration systems becomes imperative. The

coefficient of performance (COP) serves as a metric for measuring the energy efficiency of refrigeration systems, and various studies have explored methods to reduce energy consumption in these systems. Strategies include substituting older air conditioners having low efficiency with high efficiency machines, placing auxiliary heat exchangers, or decreasing heat exchanger areas [36],[37],[38].

Energy efficiency and thermal comfort stand out as crucial factors that determine the effectiveness of air-conditioning units. Yang et al. [39], presented the effective energy performance factor for thermal comfort, referred to as effective energy efficiency ratio/coefficient of performance. This metric is defined as the proportion of the effective cooling/heating capacity (considering factors like spacing ratio, effective working period, likelihood of dissatisfaction, and cooling/heating capacity) to the overall electric consumption. Conclusively the proposed index, which integrates considerations of both indoor environment and energy performance, suggests that optimal performance is achieved with a smaller set-point temperature, inflated supply airspeed, and an elevated vertical supply air angle and also contribute to the creation of more comfortable and uniform environments.

Improving the energy efficiency and performance of refrigeration cycles can be achieved through variable speed technology [40]. A research by Ha and Jeong [41] demonstrated a 21% reduction in annual power consumption with a variable-speed compressor compared to a fixed-speed compressor. Substantial electricity savings were realized by replacing less energy-efficient air conditioners with inverter ACs featuring variable frequency compressors [42]. The Energy Efficiency Rating (EER) of the compressor significantly influences system performance and economics [24]. Investments in equipment improvement, particularly in electric motors, evaporators,

and compressors, resulted in a noticeable reduction in energy costs [43]. Optimization of energy savings requires careful consideration of the variable-speed compressor's cost, ensuring it does not exceed specific thresholds [44]. The energy-saving effects of employing an inverter air conditioner primarily stem from variations in daily or seasonal temperatures and cooling loads. In various climates, inverter technology has demonstrated energy savings ranging from 18.3% to 51.7%. Notably, these savings are more pronounced during non-peak summer months and in part load operations.

Manufacturers assert that inverter air conditioners are more than 50% more efficient than their non-inverter counterparts. Consumers have the option to select from a range of energy-efficient inverter air conditioners with enhanced features compared to non-inverter models. However, the higher efficiency is accompanied by increased product costs, attributed to technological advancements in components such as compressors. The additional expense incurred by consumers during the initial purchase is expected to be offset by lower operating costs over the product's lifespan. A more energy-efficient air conditioner consumes less power, leading to reduced monthly electricity bills compared to less efficient alternatives. While air conditioners are generally considered expensive due to their high initial and running costs, their acquisition has become a necessity in the current climatic scenario. Opting for a more efficient product entails an additional investment but results in reduced electricity consumption and subsequently lower monthly energy bills. Over the past two decades, significant strides in refrigeration technology have enhanced energy efficiency. However, ongoing efforts are essential to meet international environmental standards and ensure sustainable improvements in the efficiency of refrigeration systems.

Elevated cooling loads are linked to higher product costs per unit of cooling capacity, even as the energy cost per unit of cooling load decreases [45]. Studies have shown that the investment in more efficient components becomes justified when electricity prices are on the higher side [46]. A pioneering approach was developed to provide small consumer of Makassar region, Indonesia, a choice for reducing the electrical energy cost (EEC). A pre-cooling model (PM) was practiced to forestall an unpredicted surge in electricity cost. The finding of research described that the EEC for AC reduces by up to 31.03% [47].

Thermodynamic optimization can impact an increase in the initial investment, leading to improved energy efficiency and energy conservation. However, excessively high investment is not favorable to consumers. Thermo-economic optimization based on a life cycle cost approach becomes more relevant with higher annual operating hours and varying interest rates [48].

1.7 Exergy Efficiency

The exploration of system parameter variations influencing exergy losses revealed notable improvements in exergy efficiency and reductions in compression exergy losses when substituting R404A and R406A [49]. In a two-stage Vapor Compression Refrigeration (VCR) system assessing the ideal inter-stage temperature/pressure for refrigerants HCFC22, R410A, and R717, a higher efficiency deficit was identified in the condenser compared to other components [50]. Comparing two potential alternatives, R438A and a new refrigerant mixture M1 (R32/R125/R600A), their energy and exergy efficiency were found to be lower than that of R22. However, R438A emerged as a preferable option since both its coefficient

of performance (COP) and exergy efficiency were higher than those of M1 [51]. Results from a computational model suggested that alternate refrigerants R407C and R410A do not match the performance of R22. Nonetheless, R410A, with its high COP and low exergy destruction rate (EDR), proved to be a superior alternative compared to R407C [52]. Proposed strategies to enhance exergy efficiency include increasing the reference state temperature, staging in compression, taking care of the compressor, choosing a suitable refrigerant, and ensuring proper sealing. Sub-cooling up to 5ºC and minimizing the temperature difference between the evaporator and condenser contribute to improved exergy efficiency [53]. Optimal degrees of subcooling for initial cost savings range from 2ºC to 6ºC, while total exergy destruction is recommended to be kept between 4ºC and 7ºC for R134a, R22, R410A, and R717 in vapor-compression refrigeration systems. The rise in total exergy destruction is attributed to increased heat-exchanger area and implicit friction loss [54].

The compressor is identified as the primary source of maximum exergy destruction [24]. The whole system output is optimized when fully charged, although COP diminishes when there is high amount of compressor work expenditure. To achieve an optimal balance between exergy efficiency and energy savings, it is recommended to operate the system with variable refrigerant flow during periods of reduced actual requirements [55]. Significant impacts on exergy efficiency are observed by adjusting the evaporator and condenser temperatures [56]. In air conditioning, HFO1234yf has been found to be more exergy efficient than HFC134a, with the compressor identified as the major contributor to exergy destruction [16]. Notably, the compressor's exergy destruction rate with HFO1234yf was determined to be lower than that calculated for HFC134a [57].

1.8 Objectives and Scope of the Present Work

This research work aims to conduct a thorough thermo-economic assessment of air conditioners integrated with direct evaporative cooling across a wide range of Indian climates, specifically in New Delhi. The scope and primary objectives, which contribute to the novelty of this work, include:

1. Investigating the impact of ambient conditions (spanning a wide range of temperature and humidity) on the Coefficient of Performance (COP) and exergy destruction of the proposed Direct Evaporative Cooling Split Air Conditioner (DEC-SAC) system.
2. Assessing the sustainability of DEC-SAC based on the reduction in energy consumption compared to Conventional Split Air Conditioners (CSAC).
3. Analyzing the environmental impact of DEC-SAC.
4. Conducting an economic assessment of DEC-SAC.
5. Performing a multi-objective optimization of the proposed system.

In conclusion, this research work endeavors to fill the existing gap in understanding the thermo-economic aspects of air conditioners incorporating direct evaporative cooling. Through a comprehensive analysis, it is intended to provide valuable insights for informed decision-making by researchers, engineers, and policymakers in their quest for sustainable cooling solutions. Ultimately, this research will contribute to the progression of energy-efficient technologies, fostering the transition towards a more sustainable and environmentally conscious future.

1.9 Configuration of Thesis

The thesis consists of seven chapters which are summarized below:

Chapter 1: Introduction

This chapter expresses the background of the refrigeration system. The energy, exergy and environmental issues of conventional vapor compression systems have been discussed. The energy demands and improvement in refrigeration industry are discussed. The motivation for undertaking the present research is presented. In the end, the overall organization of the whole thesis is highlighted.

Chapter 2: Literature Review

This chapter encompasses the information about contributions and development in the field of air conditioning system by different researchers. It is tried to include the most significant outcomes of the described works in terms of set-up, method, process, input parameters, output response, and the achievements of the study. It also highlights the shortfalls in literature and accordingly, the objectives of the present study are showcased.

Chapter 3 The System and Methodology

The system employed and modifications incorporated therein for the analysis are described in detail. The methodology adopted and numerical modelling is elucidated.

Chapter 4: Model Validation

The model is validated against the experimental results in this chapter. The statistical outcomes for the model fitness are also described.

Chapter 5: Results and Discussion

The obtained results are discussed in details. The thermodynamic, economic and environmental performance comparisons are presented under different sections. Also, the performance optimization results are presented.

Chapter 6: Conclusions and Directions for Future Research

The main findings from the present work are summarized in this chapter. Also, the appropriate recommendations and suggestions for further work are mentioned.

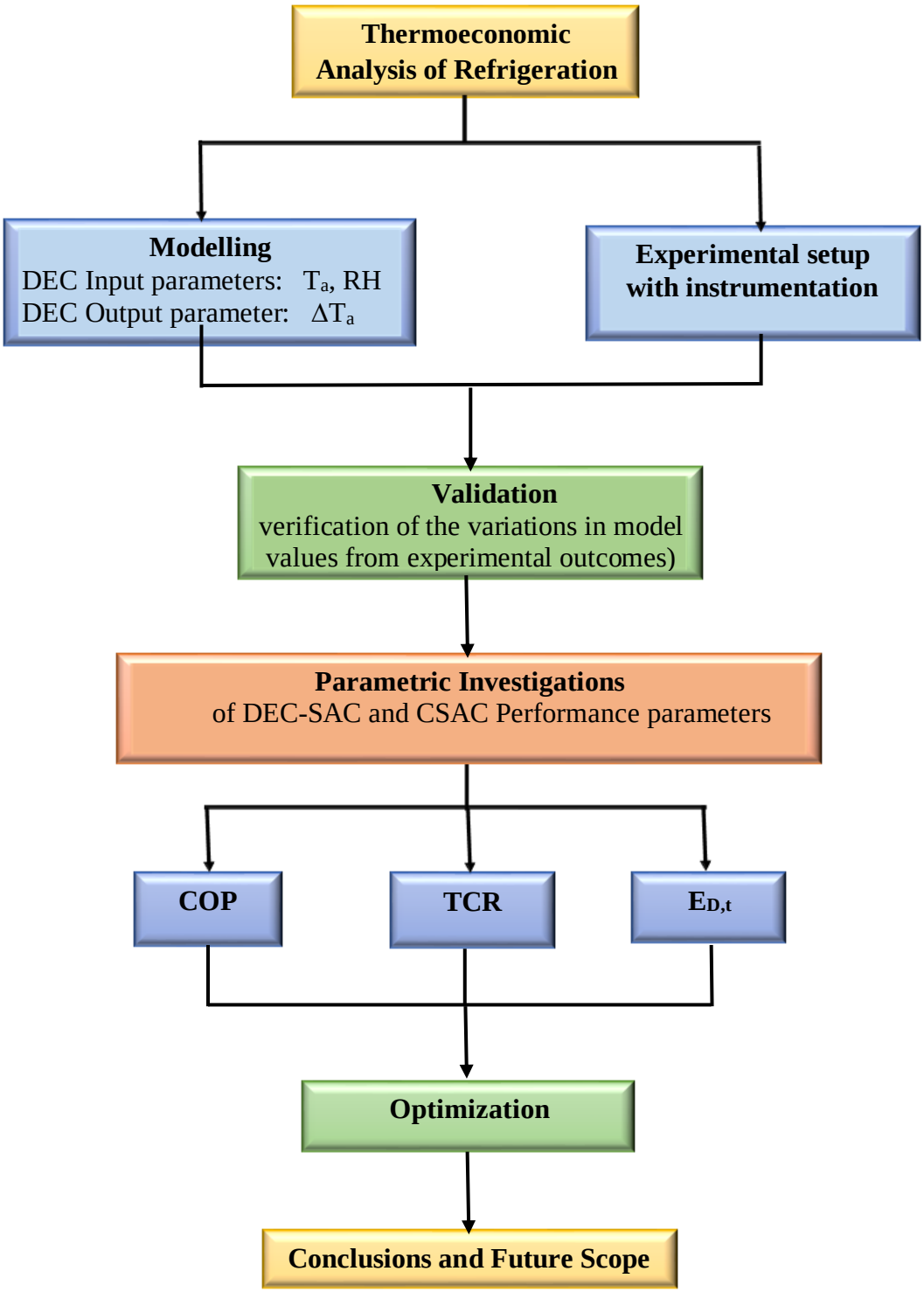

Fig.1.4 Flow diagram of thesis work

CHAPTER 2

LITERATURE REVIEW

This chapter reports the findings of the comprehensive literature survey. It covers the investigation of vapor compression-based refrigeration system and latest improvements in refrigeration technology. The literature review thoroughly illustrates the impact of ambient environments and evaporative cooling on the performance of air conditioning system.

2.1 Methods adopted for increasing efficiency of Refrigeration Systems

Strategies such as subcooling, internal heat exchangers, and liquid-suction heat exchangers and variable speed compressors have been explored to enhance efficiency in various refrigeration systems.

In a vapor compression cycle, subcooling, achieved through methods like liquid cooling below saturation temperature, internal heat exchanger (IHX), or mechanical subcooling, has been identified as an effective strategy to enhance efficiency [58]. Generally, subcooling of liquid refrigerant takes place during its travel along the liquid line in a vapor compression refrigeration system (VCRS), either by dispersing heat to the surrounding air or while storing in the liquid receiver [59]. The regenerative cycle significantly impacts cycle performance under identical operating conditions [60]. Subcooling (Fig.2.1) has been linked to increased COP, as evidenced by studies such as [61]. The utilization of liquid-suction or internal heat exchangers proves advantageous for enhancing refrigeration system performance across various

refrigerants [62]. In automotive air conditioning systems, the use of an internal heat exchanger achieved up to a 4.6% enhancement in COP [63]. Yau and Pean [4] applied a suction line heat exchanger (SLHX) in a 29.3 kW split air-cooled ducted air conditioner using R22 refrigerant. Their investigation into the system's performance under varying weather conditions concluded that with every 1°C increase in ambient temperature, the COP decreased by 2%.

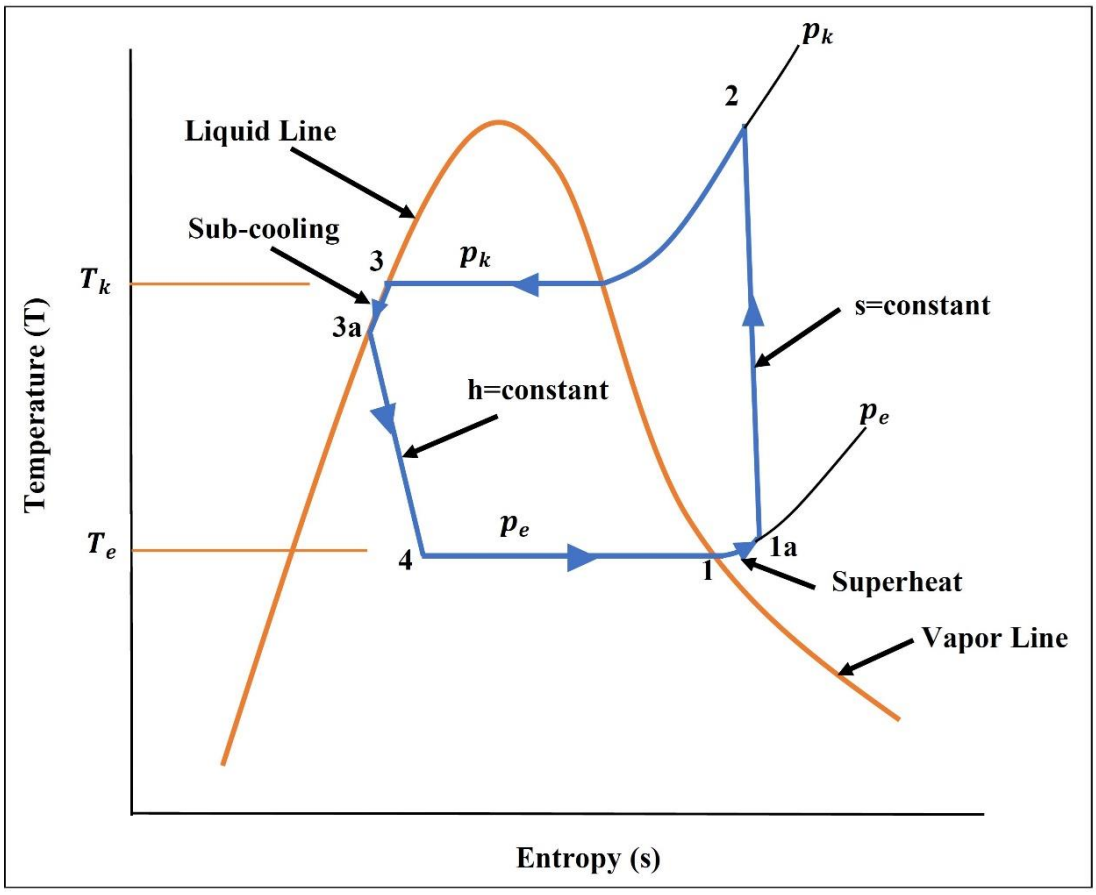

Fig.2.1 Sub-cooled Refrigeration Cycle on T-s diagram

In a separate study, Pottker and Hrnjak [58] examined the impact of condenser subcooling on a 3.5 kW split air conditioning system. The findings demonstrated that

subcooling optimized COP by striking a balance between refrigerating effect and specific compressor work. Additionally, Yang and Yeh [64] utilized a sub-cooler in a 400 kW vapor-compression refrigeration system, observing an improvement in system efficiency with higher levels of subcooling. The optimal degrees of subcooling, aimed at cost savings, ranged from 2-6℃ for refrigerants R134a, R22, R410A, and R717, with lower cooling water temperatures significantly enhancing condenser performance. A desiccant based system was examined for building air-conditioning during a whole cooling period in Adana, Turkey. The highest monthly average COP was 0.78 in October and lowest as 0.22 in July. The average seasonal COP of the system was found as 0.43 [65].

The utilization of variable speed technology significantly enhances the energy efficiency and performance of refrigeration cycles [40]. Experimental findings indicate that variable speed compressors outperform fixed-speed compressors in moderate and warm weather conditions, resulting in energy savings. Ha & Jeong [41] demonstrated a 21% reduction in yearly power consumption when using a variable speed compressor compared to a constantly run compressor. Substantial electricity savings are achieved by substituting low energy-efficiency air conditioning system with higher energy-efficient inverter air-conditioners encompassing a changeable frequency compressor [42]. The integration of a variable frequency compressor leads to more significant improvements in Coefficient of Performance (COP) by 32.64% and exergy efficiency by 23.32%. Experiments have shown that modified decentralized optimization can reduce energy consumption by 6% compared to conventional on/off control [66]. It was observed that increasing compressor frequency leads to an increase in the total exergy destruction of the refrigeration system,

accompanied by a decrease in compressor suction pressure. Elevating compressor frequency with a higher compressor speed results in higher power consumption by the compressor, leading to a decrease in COP [67]. In air conditioning applications, higher seasonal efficiencies can be achieved with variable-speed compressors using pulse width modulation (PWM) inverters and conventional induction motors compared to fixed-speed ACs [68]. According to Jabardo et al. [69], a variable-speed compressor, equipped with a capacity control device, effectively maintains a constant cooling load throughout its operation. The widespread adoption of variable-speed compressors in air conditioners is attributed to their high efficiency and thermal load adjustment capabilities. In the case of an air conditioning unit with variable refrigerant flow (VRF), it achieved up to 40% energy savings compared to a fixed-volume AC at moderate temperatures but consumed more power in elevated temperature conditions. VRF technology proves advantageous in regions where part-load conditions prevail for most operating periods, providing energy savings specifically at part-load conditions. Unlike a constant volume system, the electrical consumption in a VRF system only varies when there is a change in the system's heat load [70].

2.2 Impact of Ambient Temperature on Refrigeration Systems

Heating, ventilating, air conditioning, and refrigeration (HVACR) equipment find applications in various sectors, including industry, hotels, malls, hospitals, homes, and transportation. The widespread adoption of split air-conditioners (SAC) has significantly impacted global energy consumption. As air conditioning systems operate under sundry climate situations and atmospheric temperatures, it is essential to study the influence of environmental temperature how the system performs. Oruç

and Devecioğlu [71] examined a split-type air conditioner (2.05 kW cooling capacity with refrigerant R22) and observed a 32% increase in power consumption when the ambient temperature rose from 25℃ to 35℃. Strategies for reducing energy consumption include the replacement of old and inefficient air conditioners with more efficient units [36], the integration of additional heat exchangers [72], or the enhancement of heat exchanger area [38].

2.3 Evaporative Cooling employed in Air Conditioning Systems

The condenser in the vapor compression refrigeration cycle is critical component which remarkably influences global performance and the coefficient of performance (COP) of the system. The performance and energy usage of the condenser significantly impact refrigeration systems, with dependence on surrounding temperature variations, cabinet temperature, and heat load [73]. Temperature fluctuations in the condenser have a notable impact on the irreversibility rate of the overall vapor compression refrigeration cycle [74], [75]. Improving the coefficient of performance (COP) involves enhancing the heat transfer from the condenser to the adjacent environment [76].

In the realm of comfort-air conditioning, the decision between direct evaporative cooling options and vapor compression-based air conditioning systems is contingent on the existing humidity levels. Direct evaporative cooling is less effective in extending comfort in a situation of elevated outdoor humidity levels [77], making vapor-compression refrigeration-based air conditioning systems more appropriate for humid situations. Two primary methods of evaporative cooling are namely direct evaporative cooling (DEC) and indirect evaporative cooling (IEC). Evaporative

condensers have been acknowledged as energy-efficient and ecologically sound for air conditioning, as stated by Liu et al. [78]. This recognition has led many users to adopt evaporatively cooled systems, both direct and indirect, to lower the air temperature at the condenser inlet. A well-established and widely used method used in air conditioning is direct evaporative cooling (DEC), operating on the principle of converting sensible heat to latent heat. The DEC incorporates a fan which pulls hot outside air through a porous wet material, promoting evaporation that absorbs sensible heat and lowers the dry bulb temperature of the air. On the other side, the indirect evaporative cooling (IEC) serves as a pre-cooling unit for air conditioning systems in humid seasons. It involves utilizing evaporative cooling of outdoor air (secondary air) to cool the primary air entering the conditioned space.

Various theoretical and experimental studies underscore the use of environmentally welcoming evaporatively cooled air conditioning to curtail energy outlay and operating costs. These studies encompass experimental data on the performance of indirect evaporative cooling (IEC) units, direct evaporative cooling (DEC) systems, and combinations like IEC/DEC in diverse climates and conditions. The continuous exploration of innovative solutions and optimization strategies is essential for achieving more efficient and economically viable refrigeration and air conditioning systems.

The effectiveness of a direct evaporative cooling (DEC) system typically ranges from 70–90% [79] [80]. Indirect evaporative cooler (IEC) effectiveness is generally lower, around 40–60% [81], as IEC cools the air sensibly without absorbing moisture from the process air. However, it garners more attention than a direct evaporative system. In climates with significant variations, IEC effectiveness ranges

from 55-61%, and IEC/DEC effectiveness varies between 108–111%. The wet bulb depression strongly influences the effectiveness of the IEC unit, with regions having high wet-bulb depression exhibiting greater effectiveness than areas with low wet-bulb depression. While DEC systems prove useful for most of the hot season, IEC/DEC systems can achieve a higher level of comfort conditions by providing lower dry bulb and wet bulb temperatures [82].

Delfani et al. [83] investigated the application of pre-cooled air from an indirect evaporative cooling system in a packaged unit air conditioner, demonstrating experimental data indicating a substantial reduction of up to 75% in cooling load and 55% in energy consumption. In a separate study, Yan et al. [84] conducted tests on an 8.3kW rated capacity SAC using an indirect evaporative cooler (IEC) to examine the effects of ambient air dry bulb temperature (DBT) and relative humidity (RH) on system performance. The coefficient of performance improved in hot-dry climates ($T \leq 33$°C, $RH \leq 60\%$), while in humid environments ($T \geq 30$°C, $RH > 50\%$), additional moisture was introduced into the cooling space from outdoors. Thiangchanta et al. [85] implemented a pre-cooling system in a 1.5-ton split air conditioner (SAC) with an indoor temperature set at 25°C to 27°C and 70% relative humidity. The pre-cooling system resulted in 26.6% lower energy consumption and a 74.3% increase in heat rejection by the condenser compared to a conventional SAC.

Yang et al. [86] conducted experiments on a 60kW AC condenser using water spray indirect evaporative cooling, achieving a reduction in air temperature ranging from 6.7 to 13.1°C and a higher RH of 28.3 to 31.3% at the condenser inlet. The system realized a 22% reduction in energy input with a 42.6% increase in the coefficient of performance. Additionally, Heidarinejad [87] utilized a plastic wet surface as an IEC

unit and a cellulose pad as a DEC unit, achieving approximately 66% power savings with 108 to 111% effectiveness of IEC/DEC compared to traditional vapor compression systems. Yang et al. [88] implemented external-cooling indirect evaporative cooling as an efficient energy-saving technology, utilizing air–water finned coils connected to a packed cooling tower through water pipes. The study investigated the impact of four selected parameters—ambient temperature, ambient humidity ratio, total number of transfer units, and fresh air flow rate — while assessing the summer energy-saving potential in three different cities. The analysis indicates that the newly configured dew point exhibited optimal performance under conditions of high temperature, high humidity, and a substantial fresh air flowrate. The hybrid system incorporating this innovative dew point cooler achieved the highest energy-saving rate in both humid and arid climates, ranging from 19.1% to 48.5% when compared to a pure mechanical vapor compression system. Rao and Datta [89] assessed the improvement in cooling, temperature reduction, and environmental impact using different combinations of IEC, DEC, and dry expansion (DX) air conditioning in an 8-story residential building. The IEC-DEC-DX combination achieved up to 25% energy savings over the conventional DX system, and the auxiliary costs were recoverable within four years.

The effectiveness of a direct evaporative cooling (DEC) system typically ranges from 70–90%, while indirect evaporative cooler (IEC) effectiveness is generally lower, around 40–60%. However, IEC garners more attention than a direct evaporative system, especially in climates with significant variations. Direct Evaporative Coolers (DECs) have several advantages such as a user-friendly, cost-effective, small, and easy installation, therefore, they are frequently used for space

cooling in hot and dry climates. DEC's cost-effectiveness makes it a suitable application for residential premises.

Direct evaporative cooling (DEC) is a traditional and widely utilized method in evaporative air conditioning. DEC operates by converting sensible heat to latent heat. This approach makes use of a fan that pulls hot ambient air into an envelope through a porous wet material. The water absorbs the sensible heat of the air to evaporate, and thus the air DBT gets reduced. An experiment was undertaken by Vaisi and Taheri [90] to lower the water and energy consumption of DECs in a hot-dry condition. They obtained a daily reduction of 23.8 liters (nearly 56%) water, and the duration of system operation was reduced by 55% causing a cut of 67.5 W/hr in energy consumption. Based on the total systems under operation in Tehran, Iran, about 6.2 million litres of water saving could be achieved. The correlation between inlet water temperature, air speed, and heat transfer were established for the performance of cooling pads in DEC. They claimed increase of heat transfer in the vicinity of water tank and lowering the RH of the inlet air across the wet pad resulted in lowering the inlet water and pad exit temperatures. The water demand ranged from 9.64×10^{-4} to 1.46×10^{-3} kg/s. The lower inlet water temperature had remarkable improvement of the evaporation efficiency ranging from 56.4% to 80.96% [91].

Hybrid evaporative vapor compression (HEVC) cycles and coupling air conditioners with direct evaporative coolers showcase innovative approaches to enhance energy efficiency in various climates [92][93]. Krarti et al.[94] carried both experiment and simulation studies to assess the energy efficiency and cost benefits of hybrid systems in Saudi Arabia. They concluded that COP of the hybrid systems could be twice that of conventional air conditioner particularly at high ambient temperatures.

They also assessed that the hybrid systems could gain annual energy reductions of 51 TWh and 38 million tons in CO_2 emissions while additional cost recovering within a year's time. An evaporative cooler was installed ahead of condensing unit of an air-source heat pump (ASHP). The energy simulations demonstrated 8.87% decrease of energy expenditure by the modified system than that of the conventional ASHP when the evaporative cooling was done at 72% RH [95]. Advanced systems, such as dew point coolers and three-fluid heat exchangers, have been proposed as effective methods to regulate air temperature and enhance energy efficiency in air conditioning systems [96].

Theoretical investigation and evaluation of the energy-saving capabilities of an innovative Hybrid Air Conditioning system (HAC) in a hot-dry climate were conducted by Yang et al. [97]. The HAC was integrated with a conventional air conditioning system and includes an independent fresh air conditioner with a network of heat exchangers, such as a packed bed and three air-to-water cooling coils. This fresh air conditioner can adapt to various climate conditions by adjusting the network connections. In hot-dry climates, the network can act as an external dew-point evaporative cooler (DPEC) utilizing exhaust air as the working gas, pre-cooled in one of the three cooling coils. The remaining two coils serve for fresh air cooling, operating either in parallel mode (HAC-P) or series mode (HAC-S). Additionally, a sprayer was designed for effective fresh air humidification before the DPEC process. For parametric analysis, five independent parameters are considered: air-to-water heat capacity ratio, ambient temperature and humidity, characteristic number of heat transfer units of internal heat exchangers, and fresh air flow rate. The study specifically focused on assessing the energy-saving potential during the summer period (June to

August). The results indicate energy-saving rates ranging between 42.5% and 64.0% compared to conventional systems.

Jacob et al. [92] proposed a hybrid evaporative vapor compression (HEVC) cycle, combining adiabatic latent cooling with the vapor compression cycle (VCC), suitable for various global climates. Their study concluded that the suggested 3.5kW HEVC system could achieve energy savings exceeding 20% in hot arid climates, while increasing household water consumption by around 80% in arid conditions. Z. Yang et al. [93] implemented a hybrid air conditioning system by coupling an air conditioner (3150W capacity) with a fresh air ventilator and direct evaporative cooler. This system led to energy reductions ranging from 6.4% to 50.2% in different Chinese cities, along with improvements in seasonal energy efficiency ratios ranging from 6.9% to 98.9%.

Eidan et al. [98] implemented direct evaporative air cooling before the condenser to enhance the performance of a 7 kW (2-ton cooling capacity) air conditioner in extremely hot weather, where the highest dry bulb temperature (DBT) reached up to 55°C. They observed a 5% to 7.5% increase in cooling capacity and a 0.12A to 0.16A reduction in electrical current per unit decrease in temperature. Çag and Ali [99] improved the coefficient of performance (COP) and cooling capacity of the evaporatively cooled condenser of an ISAC (2.64 kW cooling capacity) by 10.2% to 35.3% and 5.8% to 18.6%, respectively, while decreasing energy consumption by 4% to 12.4%. They emphasized the significant impact of ambient temperature and relative humidity on COP, refrigerating capacity, and energy input of ISAC when using an evaporatively cooled condenser. Ambient temperature had a more pronounced effect on energy consumption, making the proposed system recommended for regions with wider temperature variations.

Sheng and Nnanna [100] employed direct evaporative cooling (DEC) to investigate the effects of air velocity, DBT, and water inlet temperature on the cooling performance of an HVAC system. They found that DEC cooling efficiency increased with higher air DBT, lower air velocity, and lower water inlet temperature. Al-badri and Al-waaly [101] utilized a direct evaporative cooler (DEC) in a vapor compression refrigeration system, determining DEC effectiveness through a performance factor. Their experimental design considered inlet air DBT (30 to 45°C), relative humidity (20-80%), water subcooling (1 to 8°C), and air-water ratio (2.2 to 9.1). Significant improvement in the system was achieved, especially in relatively low humidity conditions. DEC proved applicable even in very humid climates by adjusting the chilled water temperature and reducing the air-to-water mass flow ratio.

Ketwong et al. [80] conducted a simulation study on a DEC-cooled 1TR AC unit for hot–dry and hot–humid climates in Thailand. They explored the effects of inlet air DBT, inlet water temperature, and water-air ratio on the air temperature at the DEC outlet. The increased energy efficiency ratio (EER) ranged from 3.40 to 4.22 in hot–dry conditions and from 3.30 to 3.94 in hot–humid conditions, compared to 3.01 for the standalone system. The cost of the DEC was recovered in 2.87 years. In another study, [102] integrated a 1.5TR window air conditioner with an evaporative cooler for operation in the hot-dry climate of Bhopal, India. They achieved maximum cooling load savings of 64.19% at lower outdoor temperatures and a minimum saving of 27.36% at higher outdoor temperatures. The system was deemed suitable for the hot-dry climate, saving 646.8 kWh of energy from March to May, with an estimated payback period of 6.6 years.

Martinez et al. [103] utilized cooling pads of varying thicknesses to enhance energy efficiency through direct evaporative cooling of ambient air at the condenser inlet of a 2500W capacity air conditioner in the environmental conditions of Spain (ambient temperature, Ta, <30℃). Employing a 100mm thick cooling pad, they achieved a significant decrease in the condenser inlet temperature and a 10.6% increase in coefficient of performance (COP). With the cooling pad, the compressor consumed 11.4% less energy, and cooling capacity increased by 1.8%.

A Dew point cooler has the capability to lower the process air temperature below the wet bulb and approach the dew point of the working air inlet, thus providing an enhanced cooling effect compared to conventional systems [96]. Pakari and Ghani [104] observed that the wet-bulb effectiveness of a counter-flow dew point evaporative cooler could reach up to 125%. Investigating a dew-point evaporative cooler combined with an air conditioner at different outdoor temperatures and specific humidity, Chauhan and Rajput [105] found that the maximum saving of cooling load reached 60.93% for 46℃ and 6 g/kg specific humidity. In hot-dry climates, monthly energy savings were 192.31 kW h, and in hot and moderately humid climates, it was 124.38 kW h.

Chenjiyu Liang et al. [106] introduced an air conditioning system incorporating a three-fluid heat exchanger to control the air temperature in the conditioned space by adjusting the air and cooling water volumes. The proposed system demonstrated a total energy saving rate of 15.8% during the cooling season.

In an alternative approach to enhance the performance of a 5.3 kW to 7 kW split air conditioning system, Wang et al. [107] utilized evaporative cooling to bring down the condenser inlet air temperature by 2.4℃ to 6.6℃, resulting in a COP increase

ranging from 6.1% to 18%. Sarntichartsak and Thepa [108] examined the performance of an R-410A inverter air conditioner system (3.5 kW capacity) with an evaporatively cooled unit, observing an 18.32% improvement in COP at the lowest compressor frequency (30Hz) and a water flow rate of 200 l/h. Çag and Ali [99] compared the performance of a split-type air conditioner with an evaporatively cooled condenser to a conventional air-cooled condenser, noting a COP increase of 10.2%–35.3%, with a significant impact from ambient relative humidity and temperature. The maximum coefficient of performance was observed for high ambient temperature (35–40°C) and low relative humidity levels (20–40% RH).

Hajidavalloo and Eghtedari [109] integrated an evaporative cooler into the outdoor unit of a 1.5-ton split air conditioner. Experiments conducted at different ambient temperatures (35 to 49°C) and relative humidity (12 to 40%) demonstrated potential reductions in power consumption and improvements in COP of approximately 20% and 50%, respectively. Chauhan and Rajput [35] conducted experiments on a 6.5 kW capacity air conditioner, integrating a direct evaporative cooler. A maximum savings of 23.8% were obtained in energy consumption when the ambient temperature, and the relative humidity were 43.3°C and 18.1%, respectively, while no energy savings occurred in humid climates.

It is concluded that efficiency and performance in energy conversion devices, such as refrigerating machines and heat pumps, are traditionally assessed based on energy considerations. Analyzing these systems from an energy perspective is crucial to optimize performance, enhance energy savings (economic factors), and mitigate environmental impacts.

2.4 Summary of Literature Survey and Research Gaps

The vast literature survey indicates the following research gaps:

1. ***Limited Range of Environmental Conditions***

   The existing studies have predominantly focused on a trivial limit of outdoor temperature and relative humidity. There is a need for research that explores the performance of air conditioning systems using direct evaporative cooling (DEC) under a broader spectrum of environmental conditions to enhance the applicability of findings.

2. ***Neglect of Exergy and Economic Aspects***

   The previous research has primarily concentrated on the energy performance of air conditioners with DEC, neglecting the crucial considerations of exergy and economic aspects. Future studies should address these gaps to provide a comprehensive understanding of the overall efficiency and economic viability of such systems.

3. ***Lack of Multi-objective Optimization***

   The absence of multi-objective optimization in existing studies is a significant gap. Future research should focus on conducting a thorough multi-objective optimization to recognize the optimal variables for air conditioning systems, considering factors beyond energy efficiency, such as exergy, economic aspects, and environmental impacts.

4. ***Limited Integration of Thermoeconomic Analysis***

   While the pursuit of thermoeconomic analysis is acknowledged as beneficial, there is a gap in integrating this approach into existing studies on air conditioning systems. Research should aim to bridge this gap by incorporating

thermoeconomic analysis to assess the true efficiency, sustainability, and cost-effectiveness of refrigeration technology.

5. ***Absence of Comprehensive Environmental Considerations***

   There is a need for research that comprehensively incorporates environmental considerations into the analysis of air conditioning systems, ensuring a holistic understanding of their impact on sustainability.

2.5 Motivation

The survey reveals that most of the existing studies have been confined to a limited scope of outdoor temperature and relative humidity. The prime concentration of these studies was to assess the energy performance of air conditioning system utilizing direct evaporative cooler (DEC). Besides, these investigations have neglected the consideration of exergy and economic dimensions within these systems. Additionally, the critical step of conducting a multi-objective optimization to recognize optimal system variables has been overlooked.

The intricate nature of refrigeration systems presents opportunities for innovation and advancement. Engaging in thermoeconomic analysis unravels the core elements of efficiency, sustainability, and cost-effectiveness in refrigeration technology, integrating thermodynamics, economics, and environmental considerations. Such endeavors have the potential to revolutionize the approaches we take to cool, preserve, and foster sustainability in our world.

With this objective, this work aims to carry out the "**Thermoeconomic Analysis of Refrigeration System"**.

CHAPTER 3

THE SYSTEM AND METHODOLOGY

This chapter describes the conventional and modified system. The methodology used in this work and the modelling of direct evaporative cooling with refrigeration cycle is described in detail. The thermodynamic, economic and environmental aspects are also analyzed.

3.1 System Description

The system in the present work is a traditional split air conditioner (SAC) having a cooling capacity of 1.5 Ton (5.25 kW). The air conditioner works on vapor compression refrigeration (VCR) cycle. The refrigerant R32 is selected as working fluid for the refrigeration cycle. In the conventional system evaporator is placed indoors and air-cooled condenser is located outside. The schematic diagram (Figure 3.1) shows the system with its main components i.e., evaporator, compressor, condenser, and expansion valve.

The input mechanical energy required to run the vapor compression refrigeration system is obtained by an electric motor which drives the compressor. The evaporator exchanges the heat of the surrounding room air, while the condenser interacts with the ambient air outside. The thermodynamic performance of the system is assessed by varying the room temperature based on the different comfort conditions. Besides variation in the cooling space temperature, the outside ambient air temperature also differs according to the climate, system location, etc..

The refrigerant is pushed out by the compressor (2) at high-temperature/high-pressure. This refrigerant vapor is converted into high temperature liquid in the condenser (3). The hot liquid refrigerant is then allowed to expand while passing through an expansion valve/capillary tube (4). Now the refrigerant enters the evaporator as a low-temperature/low-pressure liquid-vapour mixture. The refrigerant during its travel in the evaporator (1) absorbs the latent heat of room ambient air and in turn cools the indoor space. In the evaporator, the refrigerant goes back to the compressor (2) and the cycle is repeated.

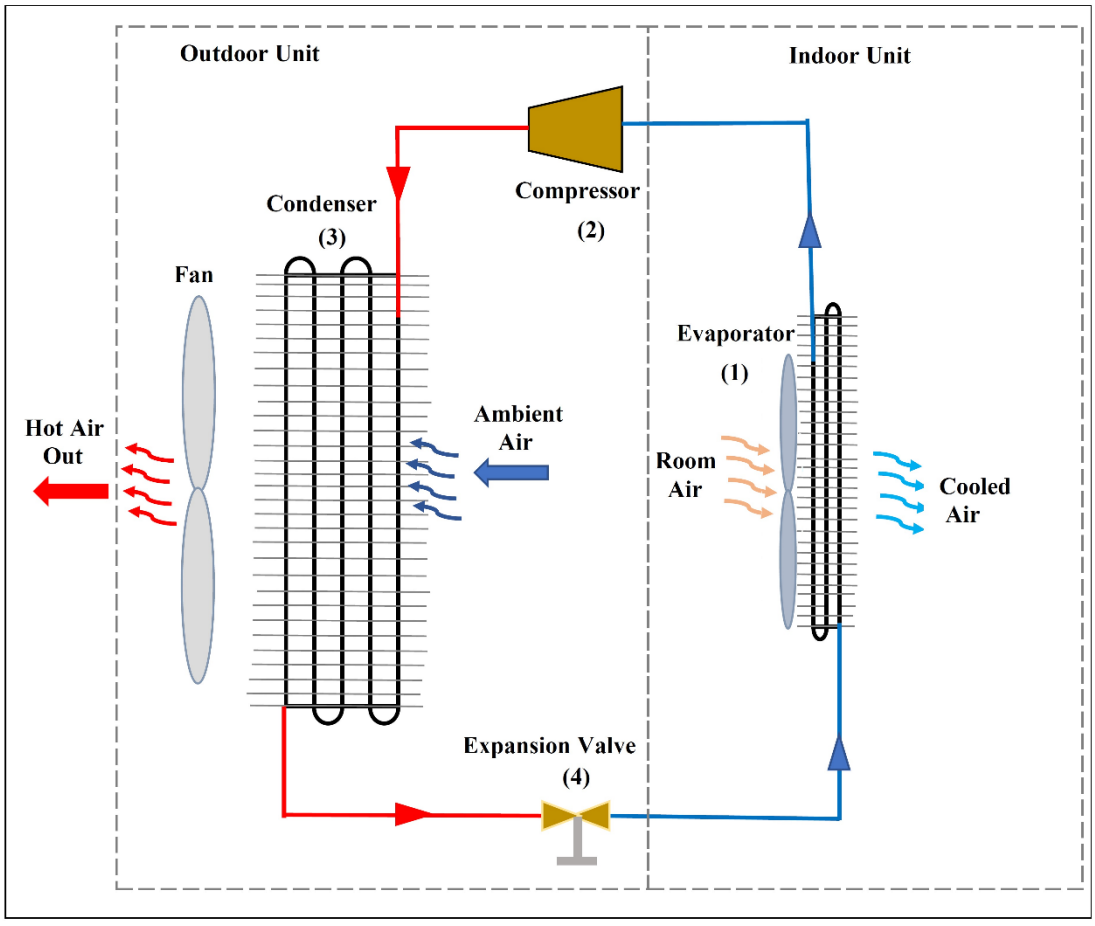

Fig.3.1 Schematic diagram of conventional SAC

It is well known fact that lower pressure ratio results in reduced compressor work. To obtain lower pressure ratio, a modest superheat is allowed at the vapor suction. This arrangement results in higher evaporator temperature and pressure. Also, the liquid subcooling is done prior to its entry into the capillary so that large heat gain is possible in the evaporator.

In the proposed DEC-SAC system, a direct evaporative cooler (DEC) combines with the condensing unit of the conventional split air conditioner (SAC) as shown in Fig. 3.2.

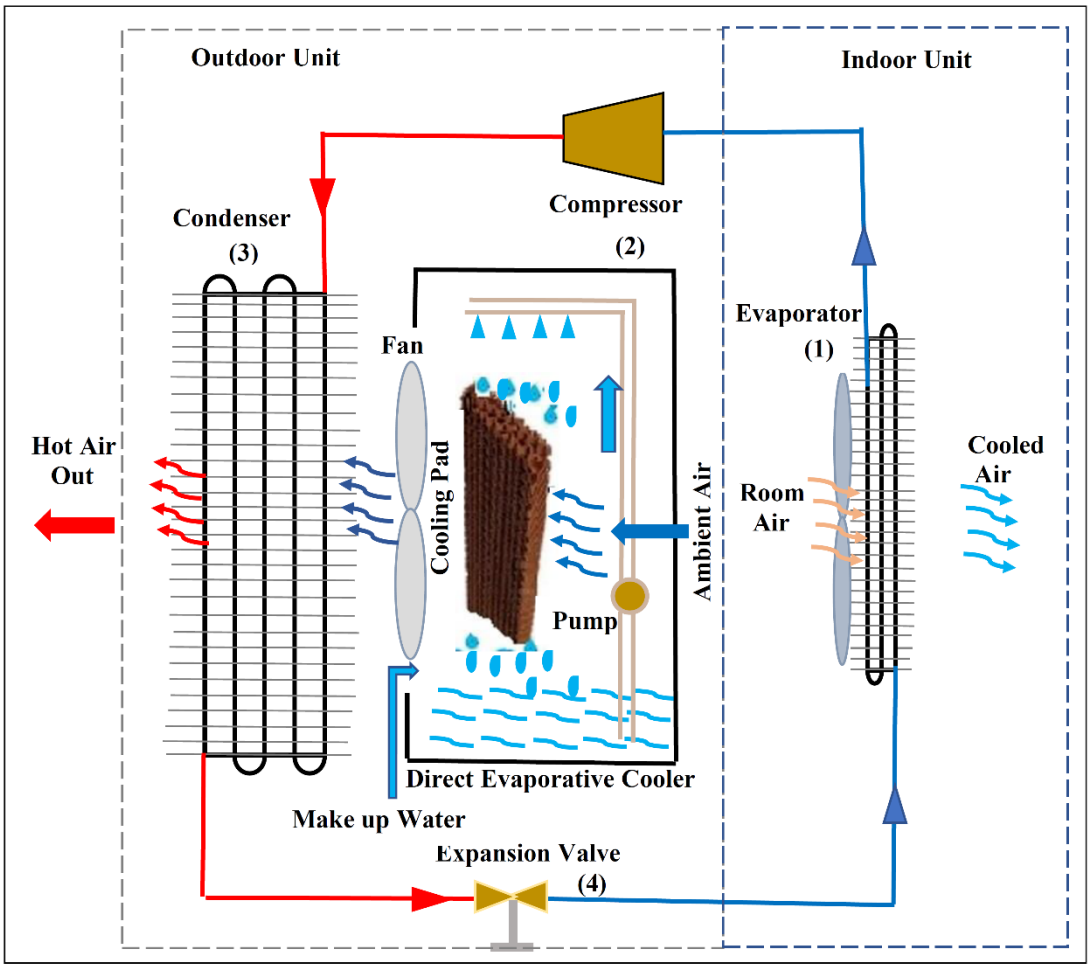

Fig. 3.2 Schematic diagram of DEC-SAC

The DEC section has a water tank made of galvanized iron sheet, a pump for water circulation, and a cooling pad to retain water. DEC makes use of water condensed on the evaporator surface and is drained through a pipe to the water tank. There is an arrangement for make-up water when the condensate amount depletes, especially in hot-dry conditions. The water soaked in the cooling pad vaporizes by retaining the latent heat from the non-saturated ambient air. Thus, a reduction of the outlet air temperature results.

The condenser fan is placed behind the condensing coils and in front of the DEC. The function of the condenser is to dissipate the cooling room heat absorbed by the evaporator outside to the ambient air. The axial fan sucks the cooled ambient air through pads, and blows over the condensing coils. This cooled air takes away the heat of hot refrigerant inside the condensing coils and pass it to the outdoor ambient air thus, lowering the condenser temperature. The experimental setup with outdoor unit and indoor unit are shown as Plate 1 and Plate 2, respectively.

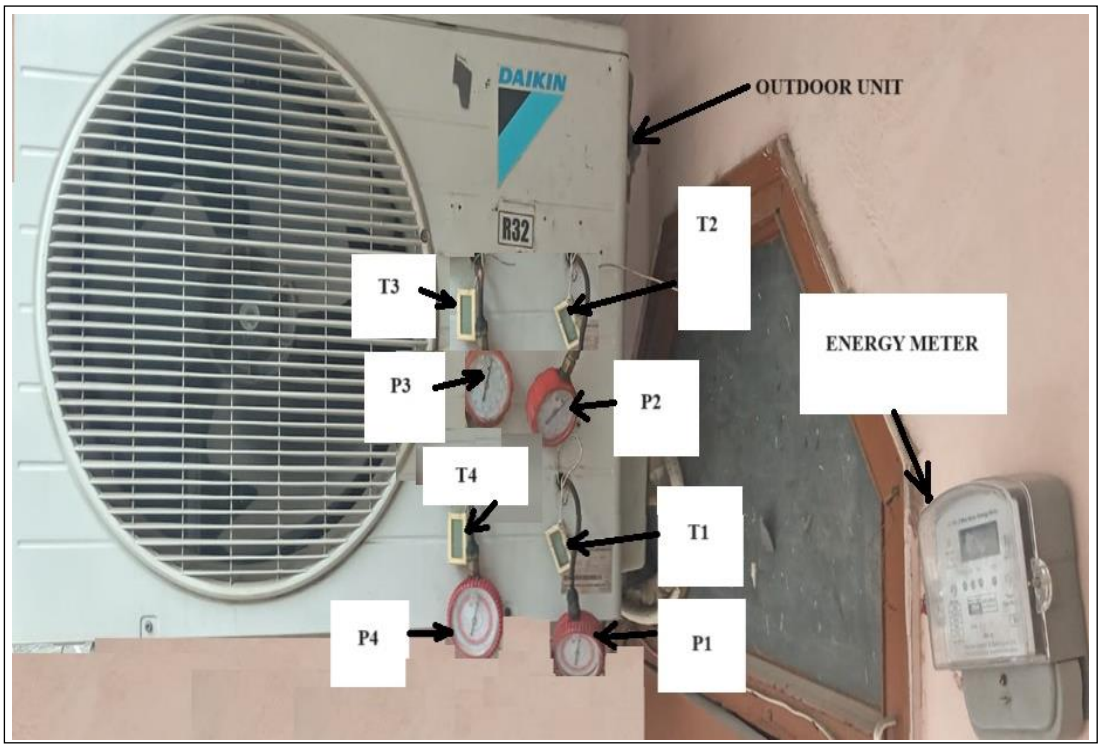

Plate 1 Outdoor Unit (P-Pressure Gauges, T- Temperature Sensors)
(P1, T1- Evaporator outlet; P2, T2 – Compressor outlet; P3, T3- Condenser outlet; P4, T4- Expansion outlet)

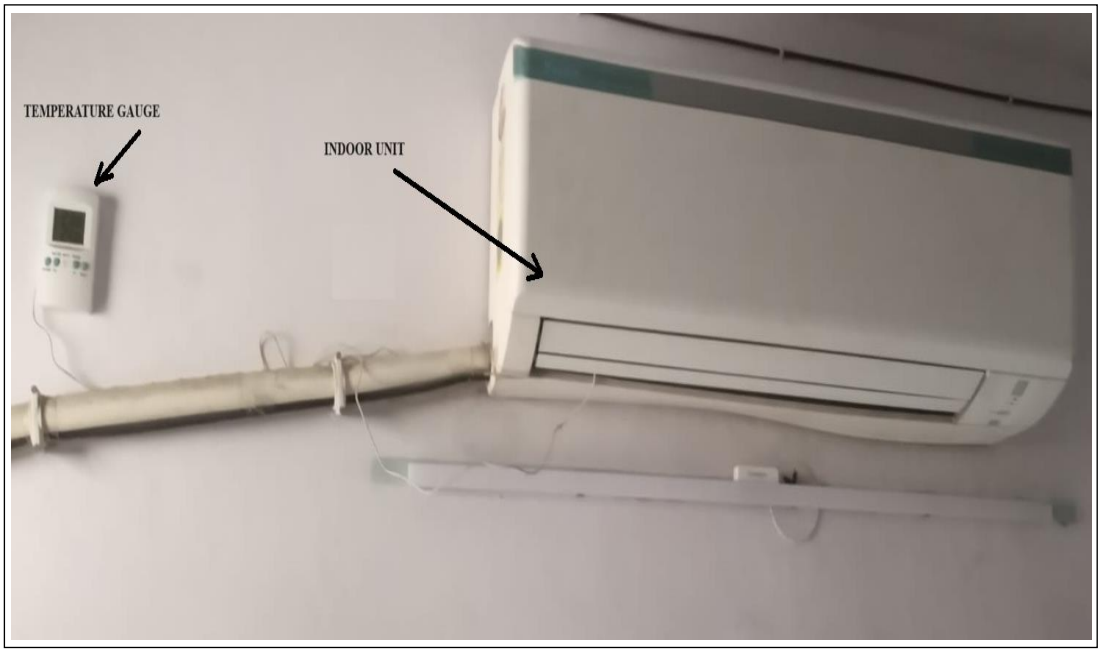

Plate 2 Indoor unit with temperature gauge for cooling coil and room temperatures

3.2 Methodology

This section explains the methodology and modelling of direct evaporative cooler and vapor compression refrigeration cycle.

The methodology for evaluating the potential theoretical performance of the DEC-SAC involves the following steps:

1. Conducting a modeling of the direct evaporative cooler (DEC) to calculate the decrease in the oudoor air temperature at the DEC outlet with rational conventions.
2. Utilizing Genetron Properties software [110] to compute the thermodynamic and transport properties of the refrigerant in both CSAC and DEC-SAC systems.
3. Calculating the exergy destruction in various components of both the CSAC and DEC-SAC.
4. Determining sustainability indices for both the CSAC and DEC-SAC.
5. Estimating the costs associated with both the CSAC and DEC-SAC.
6. Computing the energy savings and CO_2 emissions for the DEC-SAC in comparison to the CSAC.
7. Developing prediction equations using the box-Behnken design technique of response surface methodology with the assistance of Design Expert software.
8. Comparing simulated results with prediction equations and validating them against experimental results.
9. Obtaining optimal parameters for achieving an optimized system.

3.2.1 DEC modelling

The evaporative cooling pad comprises porous cellulose paper, facilitating air entry from surroundings at one end and exit at the other end. A water circulating pump is utilized to convey water from the reservoir tank to the cooler pad, ensuring complete wetting. Excess water accumulates in the bottom tray beneath the pad and is recirculated, with a provision for water makeup when the level drops below a certain mark.

During the process, the sensible heat from the air is absorbed by the water, leading to evaporation and cooling of the adjacent air. Also, the wet-bulb temperature of air represents the saturation capacity of water vaporization. As the temperature of air entering the condenser decreases, the rate of thermal dissipation through condensation rises. The condensing pressure falls below saturation value by the evaporative cooling, inducing sub-cooling [107].

Continuous water sprinkling maintains the cooling pad consistently moist during DEC operation. The water volume per unit time is regulated to keep the water temperature at the entry equal to the exit temperature (T_w) across the cooler pad. Applying this approach, sensible heat is minimized reflecting the authentic system performance in actual environmental conditions. Assumptions include constant thermodynamic properties of water and air through the entirely wetted cooler pad. Water gains the sensible heat of the air and is evaporated, and, in response, the air cools down while absorbing latent heat from the water.

The modeling considers the following assumptions:

1. The heat exchange due to conduction between water and air is negligible.

2. The heat transfer to the surroundings, as well as variations in kinetic and potential energies are overlooked.
3. The cooling pad is perfectly wetted by the water.
4. The water addition is carried at the same temperature as that of the wet-bulb temperature of surrounding air.
5. The thermodynamic properties for water and air are considered steady state during the complete moistening of cooler pad.
6. The convection heat and mass transfer coefficients are taken as constant.

A theoretical model was formulated, and system performance was simulated within specified constraints using the Genetron Properties software developed by Honeywell.

3.2.2 Mathematical Modelling

The following equation describes the energy and mass balance for the thermal exchange between air and water across the cooling pad (Fig. 3.3) under steady-state conditions.

$$\sum \dot{m}_i h_i = \sum \dot{m}_o h_o \tag{3.1}$$

The sensible heat lost by the air while advancing a small depth dx (diagram) of the cooler pad can be expressed by Wu et al. [79]:

$$d\dot{q}_s = -\dot{m}_a . C_{p,a} . dT = -h_c . dF . (T_a - T_w) \tag{3.2}$$

Here, the pad configuration factor, $dF = \xi . B . H . dx$

ξ is defined as the pore surface coefficient of the pad medium having breadth B and depth H per unit pad volume, contingent to the configuration of pad module.

Also, the latent heat added into the air while the water evaporation takes place is computed by Eq. (3.3),

$$d\dot{q}_l = d\dot{m}_w . L_w = h_m . dF . (\omega_s - \omega_a) \qquad [79] \qquad (3.3)$$

The convective heat transfer coefficient (h_c) and mass transfer coefficient (h_m) for moist air on the water film surface remain constant. The water loss attributed to evaporation is regarded as the evaporative cooler's water consumption. In the absence of thermal exchange from the vicinity, the sensible heat loss of the air is equal to the latent heat addition as water vapors, i.e.,

$$d\dot{q}_s = d\dot{q}_l \qquad (3.4)$$

In the relationship, $L_e = \frac{h_c}{h_m C_{p,a}}$ given by Alaa Ruhma et al. [101], considering Lewis number, L_e=1, we get

$$\frac{h_c}{h_m} = C_{p,a} \qquad (3.5)$$

The Eq. (3.1) to (3.5) are solved to obtain the temperature of air at the exit expressed by Eq. (3.6).

$$T_{a,dec} = T_s + (T_a - T_w) . exp\left(\frac{-h_c . \xi . \text{B.H.} \delta}{\dot{m}_a . C_{p,a}}\right) \qquad (3.6)$$

Where $T_{a,}$ $T_{a,dec}$, T_s and T_w are temperatures of outside air, condenser inlet air, saturated outside air and water, respectively. Also ‘δ’ is the is the thickness of cooling pad.

The cooling and humidification of air closely approximate an isenthalpic process. The water temperature (T_w) can be considered approximately equal to the wet-bulb temperature (T_s) of air, as suggested by Wu et al. [79]. The value of $'T_s'$ for different relative humidity is determined using a psychrometric calculator [111] at

various dry bulb temperatures (T_a). Subsequently, the evaporative cooling efficiency can be articulated in relation to the characteristics of the pad material as follows:

$$\eta = 1 - \exp\left(-\alpha \frac{\delta}{V^{0.35}}\right) \tag{3.7}$$

where $\alpha = \frac{A.\xi}{\rho_a.C_{p,a}}$

In the given equation, δ represents the thickness of the cooling pad, and V denotes the mean air velocity. Wu et al. [79] assigned the values to A, V and n in the equation as 25.2, 2 ms^{-1}, and 0.65, respectively, for the specific pad material. The selection of the cooling pad material is based on its ability to retain water and permit the passage of incoming air with minimal pressure drop.

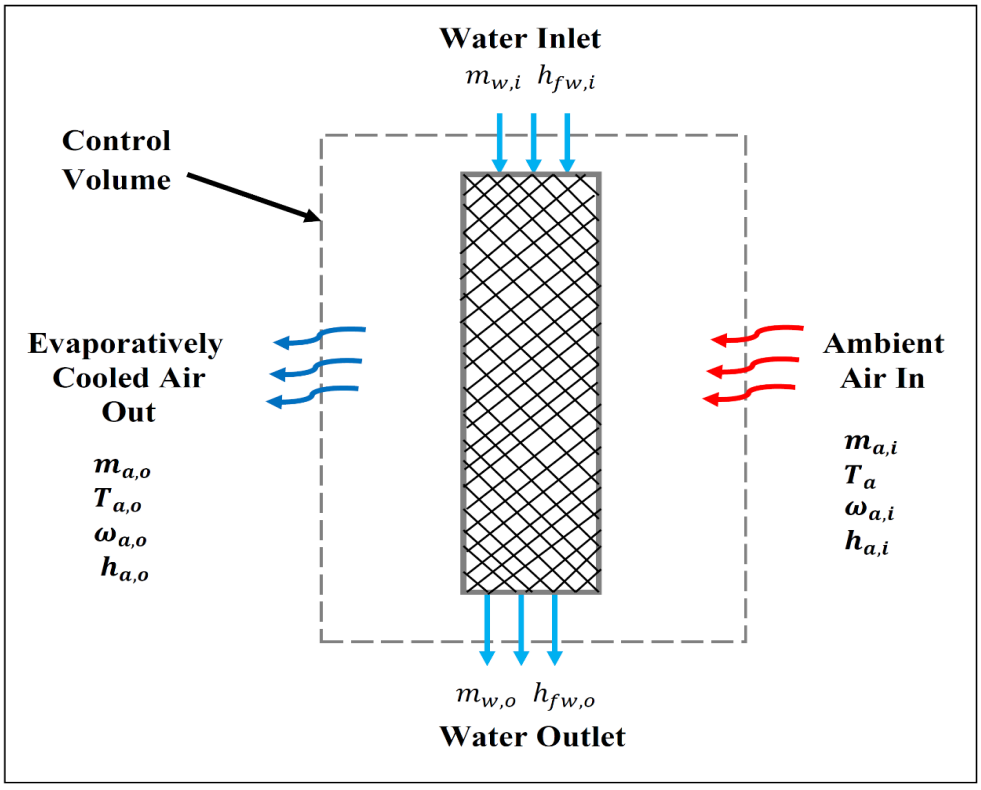

Fig. 3.3 Thermal heat and mass equilibrium across cooling pad

The thermo-hygrometer and anemometer used in the study are shown in Plate 3 and Plate 4, respectively. The range and least count of measuring devices are tabulated in Table 3.1.

Plate 3 Thermo-Hygrometer

Plate 4 Anemometer

Table 3.1 Range and accuracy of the measurement devices

Device	Range	Minimum Reading
Pressure transmitter	0-800 psi	5psi
Temperature sensor	0-150°C	0.1°C
Hygrometer (RH)	0-100%	1%
Anemometer	0-5m/s	0.1m/s
Energy meter	0-9999kWh	0.1kWh
Infrared Thermometer	(-)50- 550°C	0.1°C

Cellulose based cooling pads are used in the cooler. Geometry and specifications of the pad are displayed in Fig. 3.4.

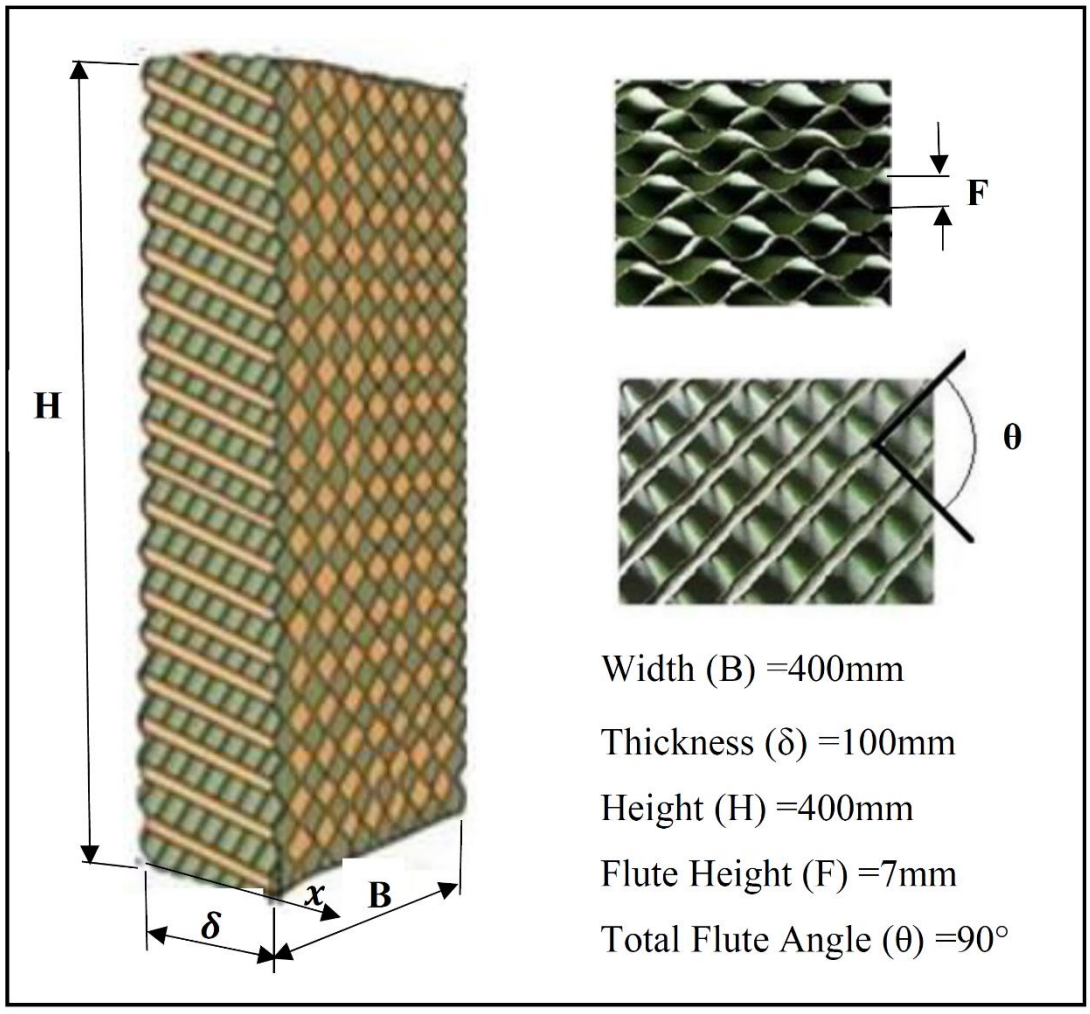

Fig. 3.4 Geometry and specification of cooling pad

3.2.3 Determining the process of conventional and evaporative cooling during condensation

In regions with very hot and humid air, characterized by high humidity levels or a low wet-bulb depression (the difference between dry and wet-bulb temperatures),

the effectiveness of the direct evaporative cooler (DEC) experiences a significant reduction [101]. Before assessing the performance of the DEC-SAC, an investigation into the impact of ambient air conditions ($T_a \; and \; RH$) on the evaporative cooler is conducted.

On the psychometric chart (Fig. 3.5), process lines 1-1e and 2-2e illustrate the enthalpy varies during traditional and evaporatively cooled condensation, respectively. A liquid phase of the refrigerant is obtained as the condenser releases the heat from the refrigerant vapor to the external air. The adiabatic process (constant enthalpy) represented by process lines 1 to 2 reflects the latent heat transfer through water evaporation to the air transferring across the pad. As a result, the DEC lowers the air temperature from state 1 to state 2, accompanied by an increase in specific humidity from ω_1 to ω_2.

The cooled air exiting the DEC then flows over the condenser coil, where the air temperature rises due to sensible heat gained from the refrigerant, as indicated by process line 2-2e. The heat exchange processes in the condensers of the conventional SAC and DEC-SAC follow process lines 1-1e and 1-2-2e, respectively.

Assuming negligible heat flux from the surroundings to the DEC, the air undergoes cooling and humidification with constant enthalpy. In other words, the air loses a certain amount of sensible heat while gaining an equal amount of latent heat through water evaporation.

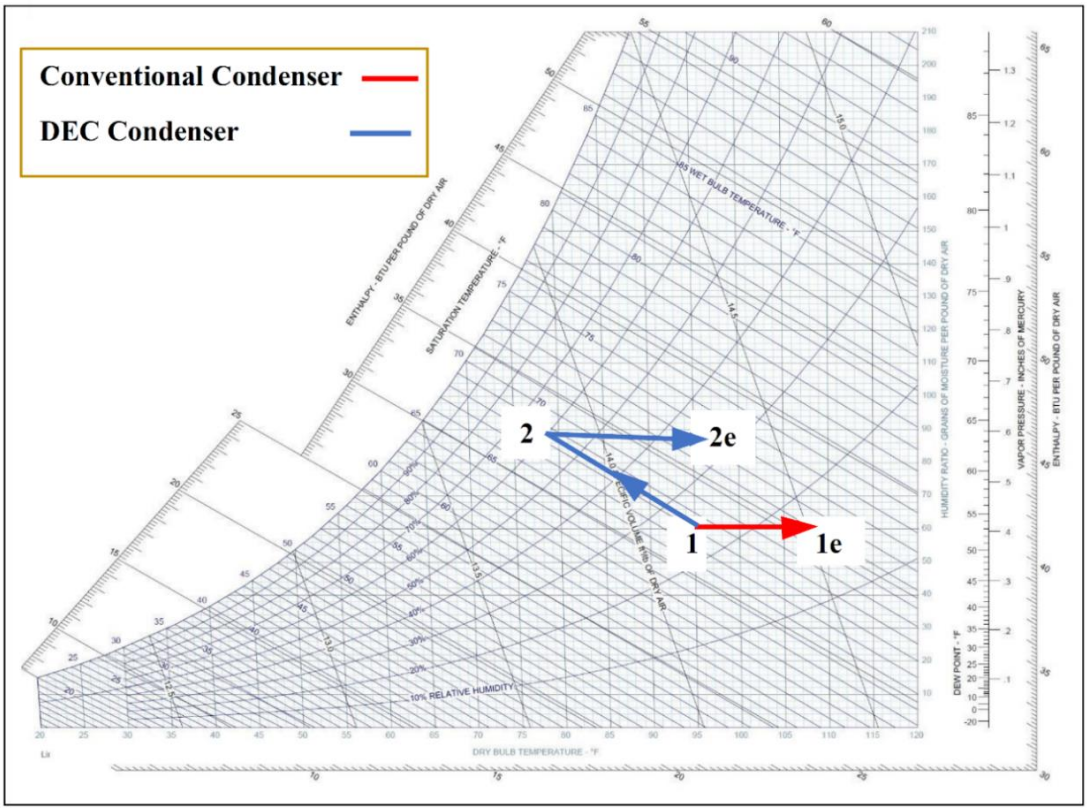

Fig. 3.5 Psychrometric variations in CSAC and DEC SAC

3.3 Experimental Performance of DEC

The evaluation of DEC performance considers the design parameters outlined in Table 3.2. The inlet water temperature (T_w) is typically set slightly higher than the air's saturation temperature (T_s), with a specific assumption of being 5°C greater than T_s. A water circulation pump with a 12W power rating (commonly available in the market) maintains a constant flow rate of 1.2 m^3h^{-1}.

Table 3.2 Design parameters for DEC

T_a (°C)[a]	30-45
RH (%)[a]	20-80
T_w (°C)[b]	$\approx T_s$
Saturation efficiency, ε[b]	0.65

[a][35], [b][79]

In Figure 3.6, the impact of T_a on the temperature reduction variation (ΔT_a) is illustrated for different saturation conditions (T_s) at varying relative humidity levels (20-80%). As the outdoor temperature rises from 30 to 45°C, the decline in dry-bulb temperature increases from 4°C to 14°C. The observation indicates that a higher ambient temperature contributes to a more substantial reduction in the cooling pad outlet temperature. In the DEC, air undergoes heat exchange with water before passing through the condenser. A higher air temperature enhances the water-air temperature differential at the pad, thereby improving the air-cooling effect. Notably, the temperature reduction is more pronounced at higher ambient temperatures compared to lower temperatures.

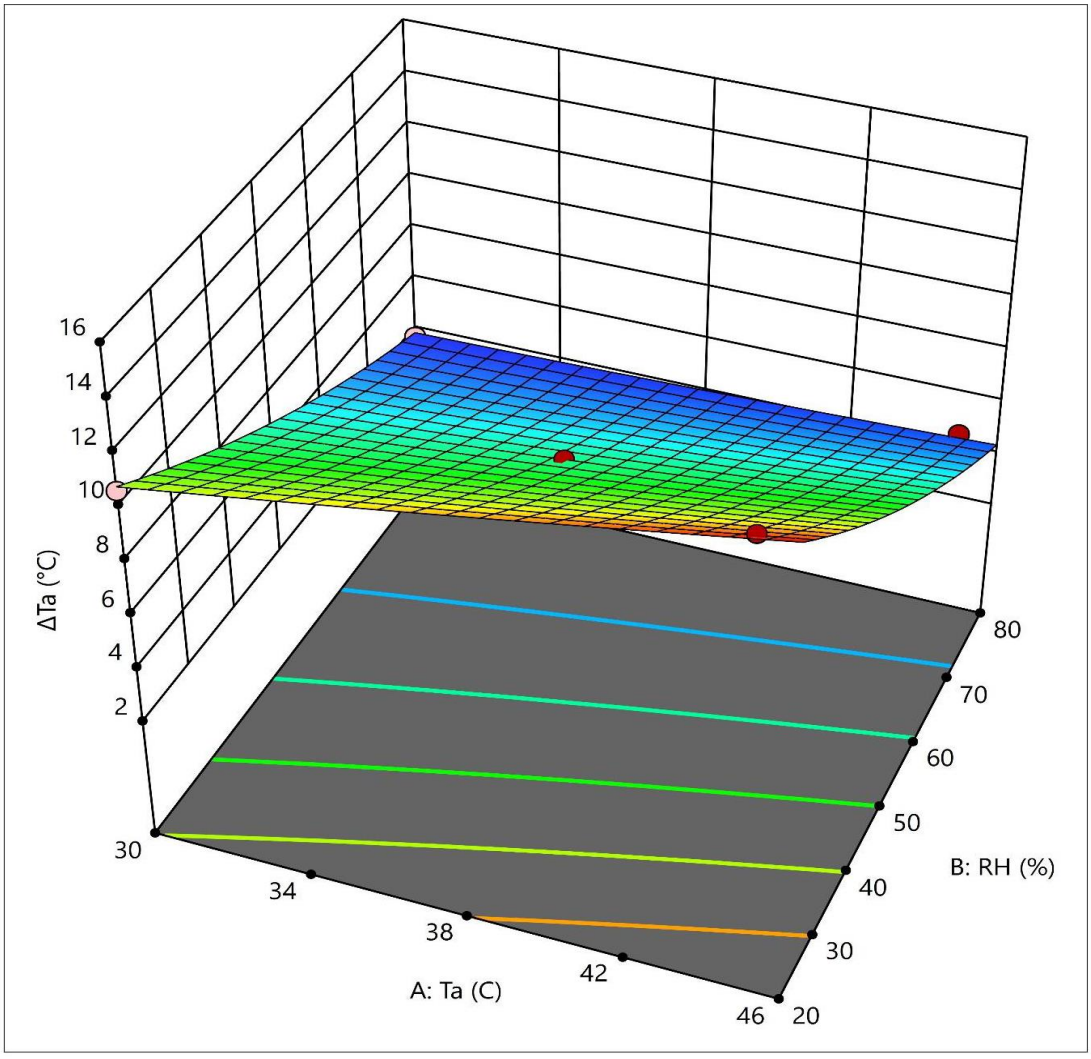

Fig. 3.6 Effect of ambient conditions on evaporative cooling degree

Additionally, the above figure reveals that a higher humidity level has a limited impact on decreasing the dry-bulb temperature. This phenomenon occurs because, as the air approaches saturation conditions, the sensible heat reduction of air diminishes due to a lower water evaporation rate. Consequently, ΔT_a decreases for higher relative humidity (80%) compared to lower relative humidity (20%) across the entire range of inlet air temperatures.

3.4 Refrigeration Cycle Analysis

Figure 3.7 illustrates the refrigeration cycles with and without evaporative cooling on the pressure-enthalpy curve. In these cycles, the evaporator and condenser interact with the surrounding room air and ambient air, respectively. The conventional air-cooled cycle and the evaporatively cooled cycle are depicted by 1-2-3-4-1 and 1-2'-3'-4'-1, respectively. Both cycles assume ideal condenser and evaporator conditions with effectiveness as unity and no heat or pressure losses. To evaluate the performance of the thermodynamic cycle, energy and exergy analyses are conducted.

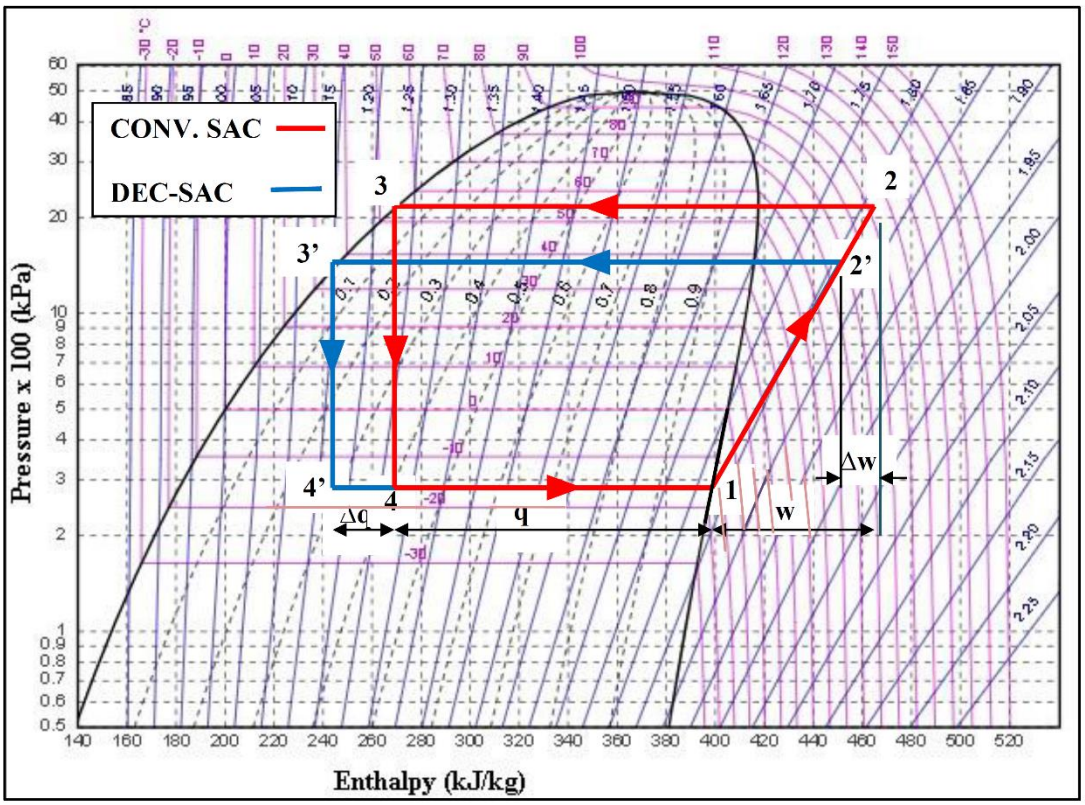

Fig. 3.7 P-h curves for CSAC and DEC-SAC

The coefficient of performance (COP) serves as the primary thermodynamic parameter for comparing the efficiency of different refrigerants. The COP of the cycle without evaporative cooling is determined by Eq. (3.8).

$$COP = \frac{q}{w} \tag{3.8}$$

Where $'q'$ is the amount of cooling produced and $'w'$ is the compressor work.

The COP' of the cycle with evaporative cooling can be represented by Eq. (3.9).

$$COP' = \frac{q+\Delta q}{W+\Delta W} \tag{3.9}$$

Enhancement in cooling effect due to evaporative cooling, $\Delta q/q$ is expressed by Eq. (3.10).

$$\frac{\Delta q}{q} = \frac{(h_4 - h_{4'})}{(h_1 - h_4)} \tag{3.10}$$

The lower compression ratio due to decrease in condenser temperature/pressure leads to a reduction in power consumption. The reduction in the specific work of compression relative to that without evaporative cooling is expressed by the Eq. (3.11),

$$\frac{\Delta w}{w} = \frac{(h_2 - h_{2'})}{(h_2 - h_1)} \tag{3.11}$$

The actual refrigeration cycles for CSAC and DEC-SAC are displayed in Fig. 3.8. The cooling capacity at evaporator temperature T_e, is given by following expression [52],

$$\dot{Q}_e = \dot{m}_r(h_1 - h_4) \tag{3.12}$$

The refrigerant's mass flow rate ($\dot{m}_r$) is calculated using the following relationship,

$$\dot{m}_r = \frac{\dot{V}_p}{v_1}\eta_{vol} \tag{3.13}$$

Where $\dot{V}_p$ represents the swept volume, v_1 is the vapor specific volume entering the compressor, η_{vol} denotes the compressor volumetric efficiency. The rotary compressor's isentropic and volumetric efficiencies can be approximated as follows [92],

$$\eta_s = 0.764 - 0.0465\,\frac{P_k}{P_e} \tag{3.14}$$

$$\eta_{vol} = 1.091 - 0.0691\,\frac{P_k}{P_e} \tag{3.15}$$

The refrigerant enthalpy at the evaporator exit (h_1) is the enthalpy of the refrigerant at a given evaporation pressure ($f[P_e, T_1]$; $T_1 = T_e + \Delta T_{sh}$). Also, the refrigerant liquid enthalpy is $h_4 = h_3$ at the condenser pressure ($f[P_k, x_3]$; where $x_3 = 0$). The enthalpy at the compressor exit (h_2), is calculated using the compressor isentropic efficiency, η_s and the enthalpy for isentropic compression ($h_{2s} = (f[P_k, s_{2s}]$; $where\ s_{2s} = s_1 = f[P_e, T_1]$), in the following relationship,

$$h_2 = h_1 + \eta_s(h_{2s} - h_1) \tag{3.16}$$

The power input (W) is determined using the expression,

$$W = \dot{m}_r(h_2 - h_1) \tag{3.17}$$

The Genetron Properties software [110] computes thermodynamic and transport properties of refrigerant (R32) using the NIST Refprop database.

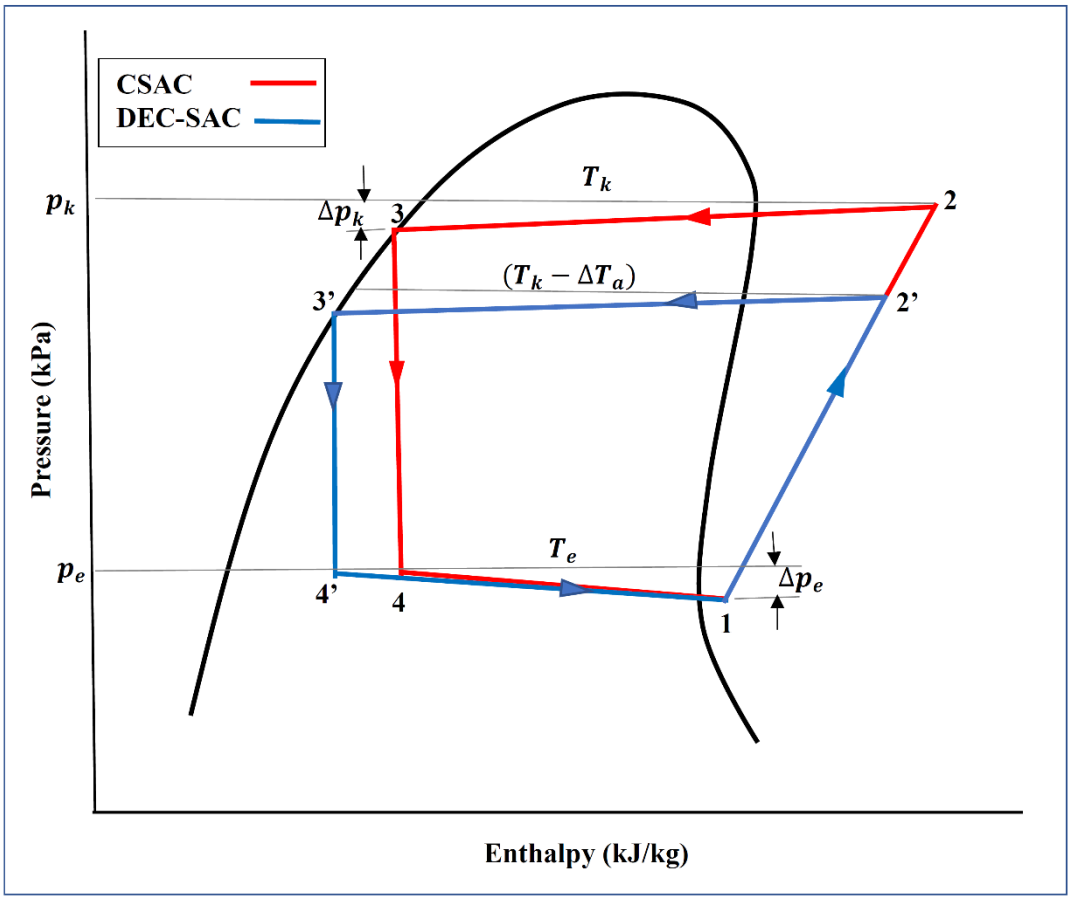

Fig. 3.8 Actual VCR cycles for CSAC and DEC-SAC

3.5 Exergy and Sustainability

Energy primarily focuses on the system, whereas exergy considers both the system and the environment. As a result, any changes in either the system or the environment lead to alterations in exergy potential. Through the analysis of exergy transfers, we can pinpoint the irreversibility or exergy destruction occurring within the system's components. This analysis proves valuable in identifying components that contribute more to exergy destruction than others. The equations provided in Table 3.3 are employed to evaluate the contribution of system components to exergy destruction. The rated power for both the condenser and evaporator fans is 65W each, following

the specifications of Daikin make split air conditioner model no. RL50TV16U3, while the water lifting pump draws 12W.

Table 3.3 Exergy destruction assessment in various components of SAC

Component	**Exergy destruction**	**Eq.**
Evaporator	$E_{D,e} = \left(\dot{m}_r(h_1 - h_4) - T_0\left(\dot{m}_r(s_1 - s_4)\right) - (1 - \frac{T_0}{T_e}\right) Q_e + P_{fan,e}$	(3.18)
Compressor	$E_{D,c} = P + \dot{m}_r[(h_1 - h_2) - T_0(s_1 - s_2)] = \dot{m}_r T_0(s_2 - s_1)$	(3.19)
Condenser	$E_{D,k} = \left(\dot{m}_r(h_2 - h_3) - T_0\left(\dot{m}_r(s_2 - s_3)\right) - (1 - \frac{T_0}{T_k}\right) Q_k + P_{fan,k} + P_{pump}$	(3.20)
Exp. Valve	$E_{D,v} = \dot{m}_r T_0(s_4 - s_3)$	(3.21)
System	$E_{D,t} = E_{D,e} + E_{D,c} + E_{D,k} + E_{D,v}$	(3.22)

Note: points 2, 3, and 4 are replaced by 2', 3', and 4', respectively, in case of DEC SAC (Fig.3.8)

The emission of greenhouse gases (mainly CO_2) causes global warming, which is responsible for climate change. The direct and indirect contribution of carbon dioxide poses a potential threat to the environment. Thus, low-carbon energy options, such as reduction in electrical energy by increasing efficiency of the systems, are helpful to lower the impact on the environment.

The sustainability index (SI) is used to compare the environmental degradation by evaporatively cooled SAC and conventionally cooled SAC. Here, sustainability index is given by Rosen and Dincer [112] as under,

$$\text{Sustainability index} = \frac{1}{(1-\psi)} \tag{3.23}$$

where $\psi = \frac{W-\dot{E}_{D,t}}{W}$, is the exergy ratio.

A high value of the sustainability index (SI) indicates efficient energy utilization which leads to the reduction in greenhouse gas emissions and degradation of the environment.

3.6 Economic Model

The economic modelling of DEC-SAC to replace CSAC is described in this section.

3.6.1 Modelling of heat exchangers

The efficiency of a heat exchanger is dependent upon the heat transfer coefficient (U) and surface area (A), typically consolidated as the heat exchange capacity (UA). To facilitate essential heat exchange, reducing the area can be a strategy to minimize costs. Hence, the dimensions of the heat exchanger constitute a crucial parameter influencing the overall cost of the system [38].

Evaporator

The Eq. (3.24) calculates the evaporator area [113],

$$A_e = \frac{Q_e}{F_e U_e * \Delta T_{LM\,e}} \tag{3.24}$$

The overall heat transfer coefficient for the evaporator, U_e, is calculated by Eq. (3.25) [114],

$$U_e = \left\{\left(\frac{1}{\eta_0 d_o}\right) + \left(\frac{d_o}{2K_{wall}} ln\left(\frac{d_o}{d_i}\right)\right) + \left(\frac{d_o}{d_i}\right)\left(\frac{1}{d_i}\right)\right\}^{-1} \tag{3.25}$$

where the value of the thermal conductivity (K_{wall}) of tube and fin material (copper) is taken as 385 W/m K. The cross-flow correction factor (F_e) and fin efficiency (η_o) are assumed to be 0.9 and 0.8 respectively, which can be applicable for tube-fin type compact heat exchanger [113].

As can be seen in Fig.3.9, room air enters the evaporator at $T_{R,i}$ and leaves after cooling at $T_{R,o}$ ($T_{R,o}$>T_e). Log mean temperature difference thus, is found as,

$$\Delta T_{LM\,e} \frac{(T_{R,i}-T_e)-(T_{R,o}-T_e)}{ln\left(\frac{(T_{R,i}-T_e)}{(T_{R,o}-T_e)}\right)} \tag{3.26}$$

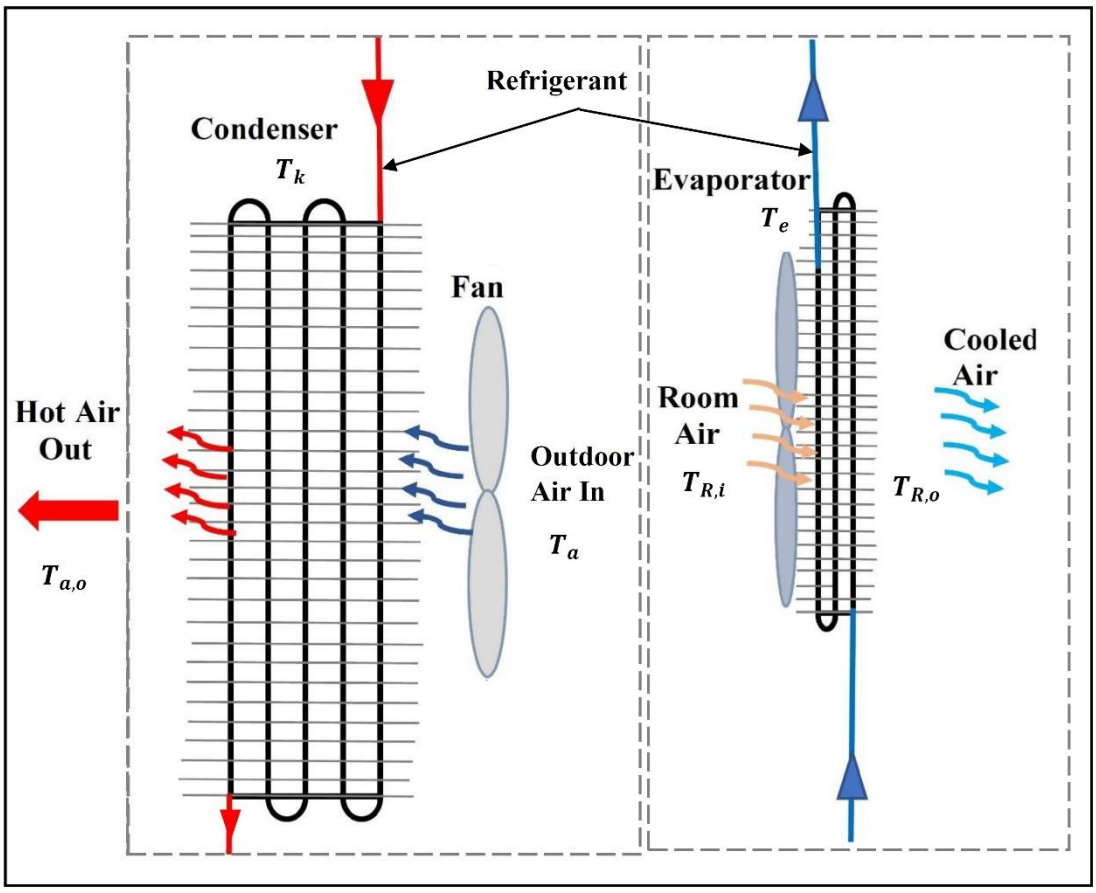

Fig. 3.9 Heat transfer processes in the condenser and evaporator of SAC system

Condenser

The condenser, serving as another compact heat exchanger within the system, requires careful consideration in determining its surface area. This aspect is critical due to the substantial amount of heat that needs to be dissipated to the ambient air. The calculation for the surface area of the condenser is obtained as follows:

$$A_k = \frac{Q_k}{U_k * \Delta T_{LM\,k}} \tag{3.27}$$

The overall heat transfer coefficient for the condenser, U_k, based on the outside surface of the tube is given by Florides and Kalogiro [115] as,

$$U_k = \left\{\left(\frac{d_o}{d_i}\right)\left(\frac{1}{d_i}\right) + \left(\frac{d_o}{d_i}\right) f_i + \left(\frac{d_o}{d_i}\frac{d_i}{2K_{wall}} ln\left(\frac{d_o}{d_i}\right)\right) + f_o + \left(\frac{1}{d_o}\right)\right\}^{-1} \tag{3.28}$$

where f_i and f_o are the fouling factors for the inside and outside surfaces of the tube, the value of which is assumed as 0.09 m^2 $K.kW^{-1}$[38],[115].

The heat from the condenser is transferred to the surrounding air (initially at ambient/dead state temperature, T_a) and raises its temperature to $T_{a,o}$ ($<T_k$) as shown in Fig.3.9. Therefore, the log mean temperature difference is given as,

$$\Delta T_{LM\,k} = \frac{(T_k - T_a) - (T_k - T_{a,o})}{ln\left(\frac{T_k - T_a}{T_k - T_{a,o}}\right)} \tag{3.29}$$

3.6.2 Economic Assessment

Economic assessment of SAC system is based on total cost rate (TCR) which comprised investment cost, C_{INV}, operating cost, C_{OP}, and environmental cost, C_{ENV} [116].

$$TCR = \frac{C_{INV} + C_{OP} + C_{ENV}}{N} \text{ (₹.h}^{-1}\text{)} \tag{3.30}$$

where 'N' is the number of operation hours in a year. C_{INV}, includes component capital cost (C_{CAP}), capital recovery factor (ζ), and the maintenance factor (φ). Thus, investment cost is computed as:

$$C_{INV} = \sum_j C_{CAP,j} \,.\, \zeta . \varphi \quad (₹.\ \text{year}^{-1}) \tag{3.31}$$

where $\zeta = \frac{i(1+i)^n}{(1+i)^n - 1}$

Component costs, are calculated according to Table 3.4.

Table 3.4 Component costs, $C_{CAP,j}$ [117]

Component	**Cost**	**Eq.**
Evaporator	$1397 \times {A_e}^{0.89}$	(3.32)
Condenser	$1397 \times {A_k}^{0.89}$	(3.33)
Compressor	$10167.5 \times \dot{P}^{0.46}$	(3.34)
Ex.valve	$114.5 \times \dot{m}_r$	(3.35)

Operating cost = Annual electricity consumption × Unit electricity cost

$$C_{OP} = W \times N \times C_{EL} (₹.\ \text{year}^{-1}) \tag{3.36}$$

where 'C_{EL}' is the electricity cost per kWh.

To assess the environmental consequences of selecting the systems (CSAC and DEC-SAC), an examination is undertaken to evaluate their impact on global warming. This analysis scrutinizes the indirect emissions stemming from the combustion of fossil fuels required to power the equipment.

The amount of CO_2 emission per kWh of electricity generated is given by,

$$m_{CO_2} = \mu_{CO_2} \times \text{ Annual electricity consumption (kWh)} \tag{3.37}$$

where CO_2, weighted average emission factor (μ_{CO_2}) for producing electricity, is about 0.82kg/kWh [118].

The annual penalty cost per annum, considering ₹7500 per ton of CO_2 produced [119], is estimated as:

$$C_{ENV} = (\mu_{CO_2}/1000) \times C_{CO_2} \text{ (₹.year}^{-1}\text{)} \quad (3.38)$$

Net Present Value (NPV) represents the difference between the present value of anticipated future cash inflows and the present value of the cash outflows. A positive *NPV* means that its rate of return will be higher than the discount rate and thus it is beneficial for the system. The *NPV* is calculated by (Eq. 3.39)[120].

$$NPV = -C_{CAP} + \sum_{j=1}^{n} \frac{CF_{net}}{(1+r)^j} \quad (3.39)$$

Here, *'j'* is the required return or discount rate and *'n'* is the number of time period. The net cash flow (CF_{net}) is obtained as,

$$CF_{net} = C_{ref}.Y_e - \varphi.C_{CAP} - C_{OP} \quad (3.40)$$

In the above expression, Y_e is the cooling produced in a year and cost of refrigeration, $C_{ref} = \frac{C_{EL}}{COP_{eq}}$, where COP_{eq} is the computed COP of DEC-SAC for cooling produced at T_e and heat rejection at T_k compared to CSAC for same temperatures.

The Internal Rate of Return (IRR) is the discount rate for which the net present value of future cash flows is equal to the initial investment, expressed as [121],

$$IRR = \frac{CF_{net}}{C_{CAP}}\left[1 - \frac{1}{(1+IRR)^n}\right] \quad (3.41)$$

The payback period is the duration it takes to recoup the initial costs, expenses, and investments made in the system until it reaches a point where it neither incurs

losses nor generates profits, known as the breakeven point. The simple payback period can be calculated by Eq. (3.42) [120].

$$SPP = \frac{C_{capital}}{CF_{net}} \tag{3.42}$$

Discount rate (r), maintenance factor (φ) and operating life (n) are taken as 3% [118], 1.06 of the capital cost , and 15 years [119], respectively.

3.7 Multi-Objective Optimization

While single-objective optimization proves advantageous when focusing on a singular aspect, the general requirements of thermal system design often demand the optimization of both thermodynamic performance and economics [122]. Multi-objective optimization becomes particularly suitable for addressing conflicting objectives within the constraints of various factors [123]. Thermo-economic assessment provides a means to identify cost-effective values for decision parameters in the overall system [124]. The application of Design of Experiment (DoE) serves as a technique to streamline the cost and time involved in experimentation, ensuring logical responses and acceptable products. Additionally, DoE aids in designing and developing robust processes capable of withstanding diverse environmental conditions and resource variations.

3.7.1 Objective functions, design variables and feasible limits

Objective functions

An assessment of a vapor compression refrigeration system (VCRS) revolves around its efficiency and total cost. The energy efficiency or coefficient of

performance (COP) is a key determinant of the system's thermodynamic performance and is thus selected as the primary objective function. The second objective function is the Total Cost Rate (TCR), encompassing the expenses associated with owning and operating the system, impacting its overall economic aspect. Recognizing the significance of exergy in determining a system's sustainability, it is chosen as the third objective function.

Design variables and feasible limits

Aligned with the prevailing outdoor environmental conditions, particularly in India, the decision variables for the optimization procedure include the ambient temperature (T_a) and relative humidity (RH) within the ranges of 30-45ºC and 20-80%, respectively. Additionally, in accordance with the system's specifications, the evaporator temperature (T_e) is chosen as the third decision variable, ranging from 3-12°C. The parameters maintained as constants in the optimization process are outlined in Table 3.5.

Table 3.5 Constants considered in the analyses

Parameter	**Life period[a]**	**Annual Operation hours[b]**	**Annual interest rate (r)[b]**	**Maintenance factor (∅)[b]**	**Unit electricity cost (C_E)[b]**
Value	15 years	1600 h	14%	1.06	₹7.5/kWh

[a][125],[b][119]

3.7.2 Box-Behnken Design Methodology

The Design of Experiment (DoE) serves as a technique aimed at reducing the cost and time associated with experimentation, ensuring logical responses and satisfactory product outcomes. It plays a crucial role in designing and developing robust processes capable of withstanding diverse environmental conditions and resource variations. In this study, the Numerical Optimization technique employing Box-Behnken design (BBD) and following the quadratic model is utilized to optimize the input parameters of the SAC system. This technique facilitates the exploration of interactions among individual factors in a polynomial relation, providing a means to project outcomes within defined limits. BBD proves advantageous not only in identifying individual factors and their correlations but also in optimizing the influential factors. The Design-Expert software integrates individual decision variables to generate an optimized solution. A computational design is executed for three levels and three factors, where Factors A, B, and C represent outdoor temperature, relative humidity, and evaporator temperature, respectively, with levels 1, 2, and 3 denoting low, medium, and high values of these factors.

3.7.3 Analysis of Variance (ANOVA)

The Analysis of Variance (ANOVA) is utilized to establish an empirical correlation between multiple inputs and outputs. ANOVA, a statistical technique, aims to estimate significant differences in the means of two or more groups. By comparing the means of various experiments, ANOVA assesses the impact of one or more factors. The numerical simulation data is fitted into a quadratic polynomial equation, as represented by Eq. (3.43), to encapsulate all the linear interactions of the factors.

Here, Y represents the response, β_0 is a constant, β_1 and β_2 denote the linear and second-order relationships of factor X_{i}, β_3 is the linear reaction of X_{ij}, and ε accounts for inaccuracies.

$$Y = \beta_0 + \beta_1 \sum_{i=1}^{3} X_i + \beta_2 \sum_{i=1}^{3} X_i^2 + \beta_3 \sum_{ij=1}^{3} X_i X_j + \varepsilon \quad (3.43)$$

CHAPTER 4

MODEL VALIDATION

This chapter compares the simulated values of theoretical model with the experimental results to ensure the applicability of the model for further work. The analysis of variance is carried out for the model fitness.

4.1 Model Verification

The responses of the DEC-SAC system are gathered with experimental results (Fig.4.1). A fair accuracy is observed in the present model compared to experimental findings with maximum variation of 4.09% in the DEC outlet temperature.

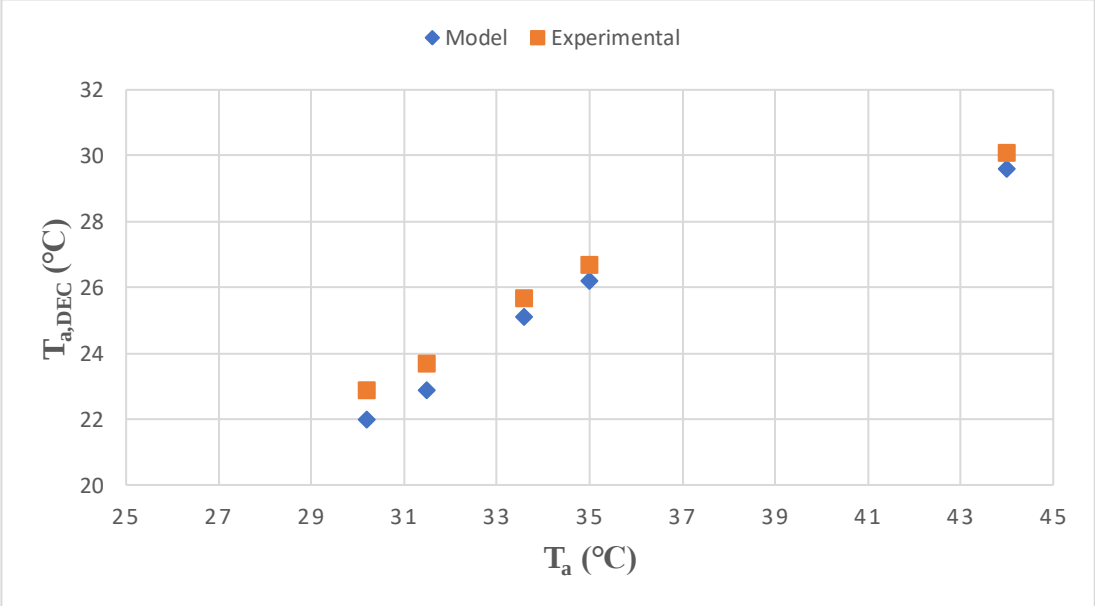

Fig.4.1 Model validation of present work with experimental outcomes

In addition to above, the outputs of the current model are met with experimental findings. The variations in ΔT_a and COP in accordance with Table 4.1 are noted to be 3.33% and 4.08%, respectively. With these small deviations, the proposed model is implemented for additional study.

Table 4.1 Comparison of model and experimental values

	Input parameters			**Output parameters**		
Model	T_a **(°C)**	RH **(%)**	ΔT_a **(°C)**	**Variation in** ΔT_a **(%)**	COP	**Variation in** COP **(%)**
Model	37.1	20.6	12.0	-	4.9	-
Experimental	37.1	20.6	11.6	3.33	4.7	(-) 4.08

4.2 Model Analysis

Analyzing variance involves the systematic allocation of variability into distinct sources of variation, along with their corresponding degrees of freedom within an experimental setting. The F-test, employed in statistics, is used to examine the significance of the parameters that constitute the quality characteristics of three or more groups. In the context of ANOVA, a larger F-statistic indicates a larger difference between the group means. The F-statistic is used to calculate the p-value, which determines whether the observed differences in means are statistically significant. Similar to the t-test, if the p-value is below a certain threshold (often 0.05), it suggests significant differences among the groups. ANOVA tests are conducted to determine the significant terms and the results attained are presented in Table 4.2. This

analysis was conducted at a significance level of 5%, indicating a confidence level of 95%. Upon examining Table 4.2, it is evident that the large F-values for Large F-values of 44.45, 52.55, and 44.67 conforming to enhancement in cooling effect, work spent, and coefficient of performance accompanied by extremely small p-values signify their statistical and physical significance in influencing the performance. The tests approve the good fitness of DEC-SAC model.

Table 4.2 ANOVA model analysis

	Δq		Δw		ΔCOP	
Source	**F-value**	**p-value**	**F-value**	**p-value**	**F-value**	**p-value**
Model	44.45	< 0.0001	52.55	< 0.0001	44.67	< 0.0001
A (T_a)	35.14	< 0.0001	40.85	< 0.0001	35.47	< 0.0001
B (RH)	53.75	< 0.0001	64.24	< 0.0001	53.88	< 0.0001
Lack of Fit	1.63		0.9352		1.63	
R^2	0.8811		0.8811		0.8816	
R_a^2	0.8612		0.8612		0.8619	
R_p^2	0.7831		0.7831		0.7841	
Adq.Pres.(S/N)	20.9655		20.9655		21.0223	
SD (σ^2)	1.16		0.8828		1.16	
Mean	9.57		8.68		9.58	
C.V.	12.12		10.17		12.10	

The accuracy of the fit was assessed using the determination coefficient (R^2). Model terms with p-values less than 0.0500 were deemed significant, and in this instance, A(T_a) and B*(RH)* were identified as such. The results indicate a high confidence level (exceeding 95%) for both R^2 and R_a^2 values, supporting the

acceptance of the model [126]. The predicted R^2 (0.7841) aligns reasonably well with the Adjusted R^2 (0.8619) values for the COP, and a similar trend is observed for other responses. The model is deemed acceptable, as the differences between R_a^2 and R_p^2 are less than 0.1% [127]. Adequacy Precision, measuring the signal-to-noise (S/N) ratio (>4), demonstrates satisfactory results for the current analysis, confirming the validity of the fit [73]. Additionally, the low values of the standard deviation (SD) and mean ratio, i.e., coefficient of variation (C.V.) suggest that the model is accurate.

Diagnostic plots (depicted in Fig. 4.2 (a) to (c)) indicate a favorable fit of the model. The normal probability plot for residuals, showcasing the accumulation of residuals around the central line, serves as an indicator of the suitability of the analysis. These findings affirm the effective application of the BBD to the current model. With the objective of exploring the parameters influencing the cooling effect, work input, and coefficient of performance of the DEC-SAC system, simulations conducted based on the Box-Behnken design contribute to enhance the cycle performance under varying conditions of outside temperature, relative humidity, and evaporator temperature.

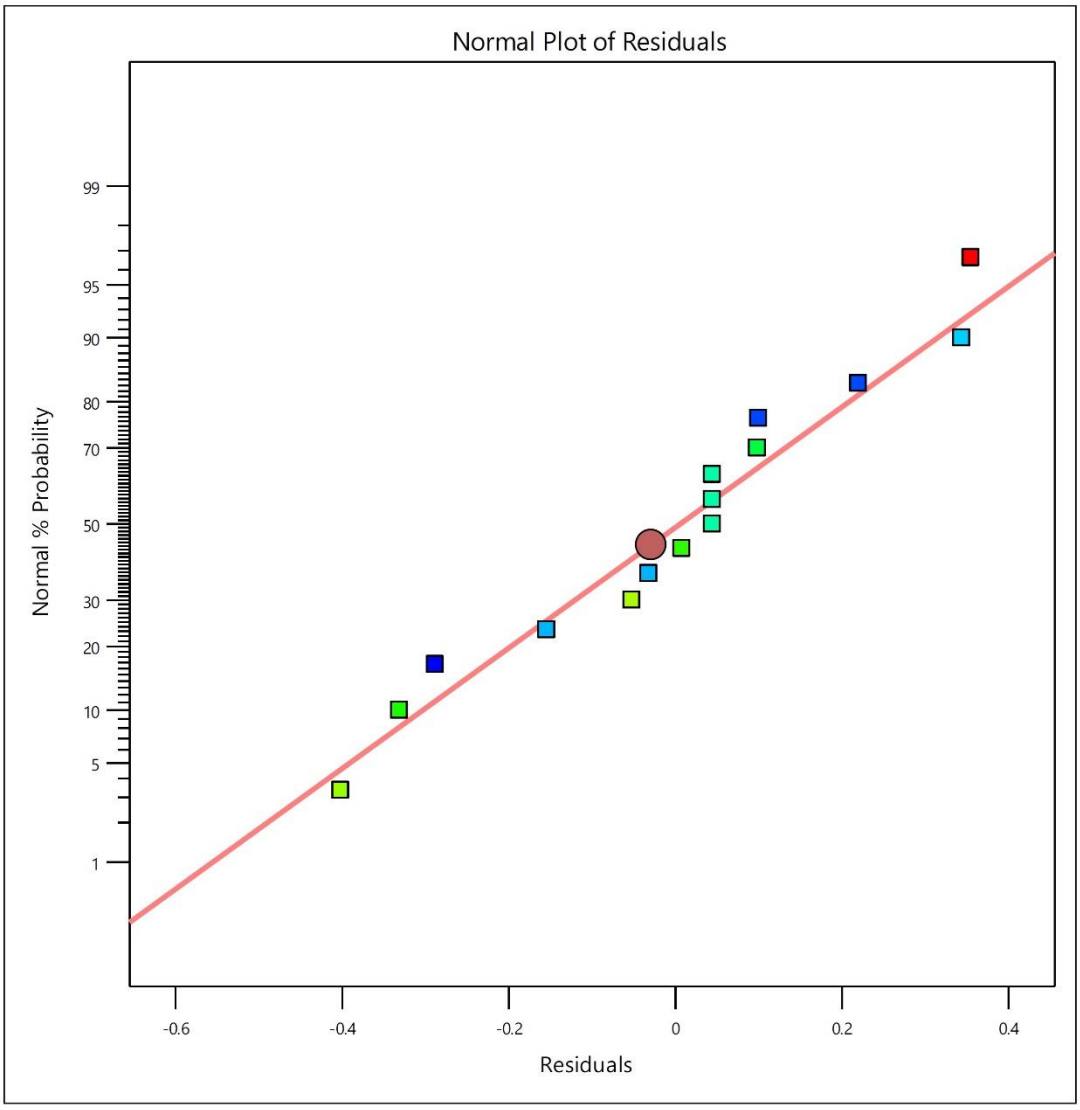
Normal Plot of Residuals
Normal % Probability
99
95
90
80
70
50
30
20
10
5
1
-0.6
-0.4
-0.2
0
0.2
0.4
Residuals

(a)

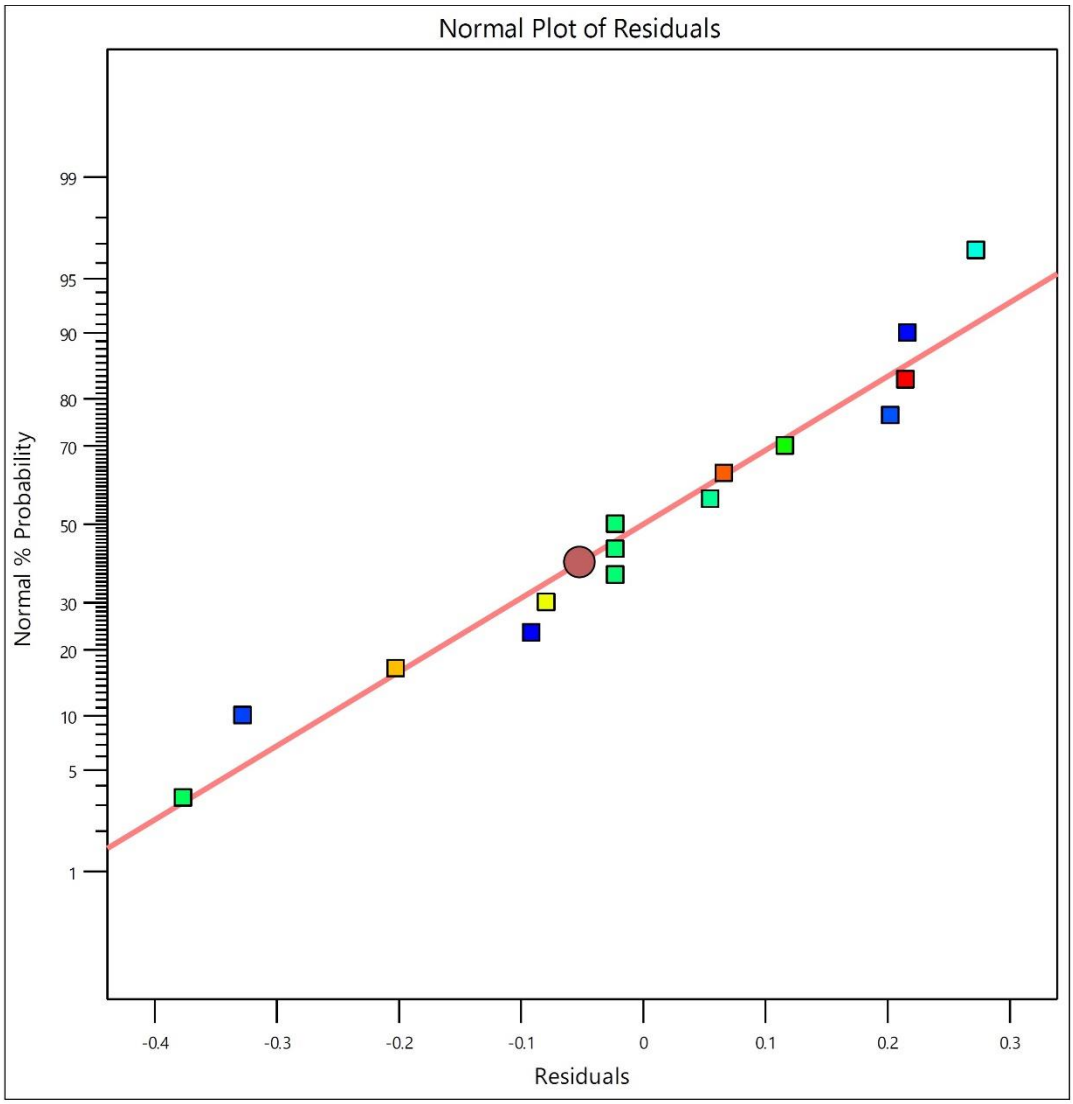
Normal Plot of Residuals
Normal % Probability
99
95
90
80
70
50
30
20
10
5
1
-0.4
-0.3
-0.2
-0.1
0
0.1
0.2
0.3
Residuals

(b)

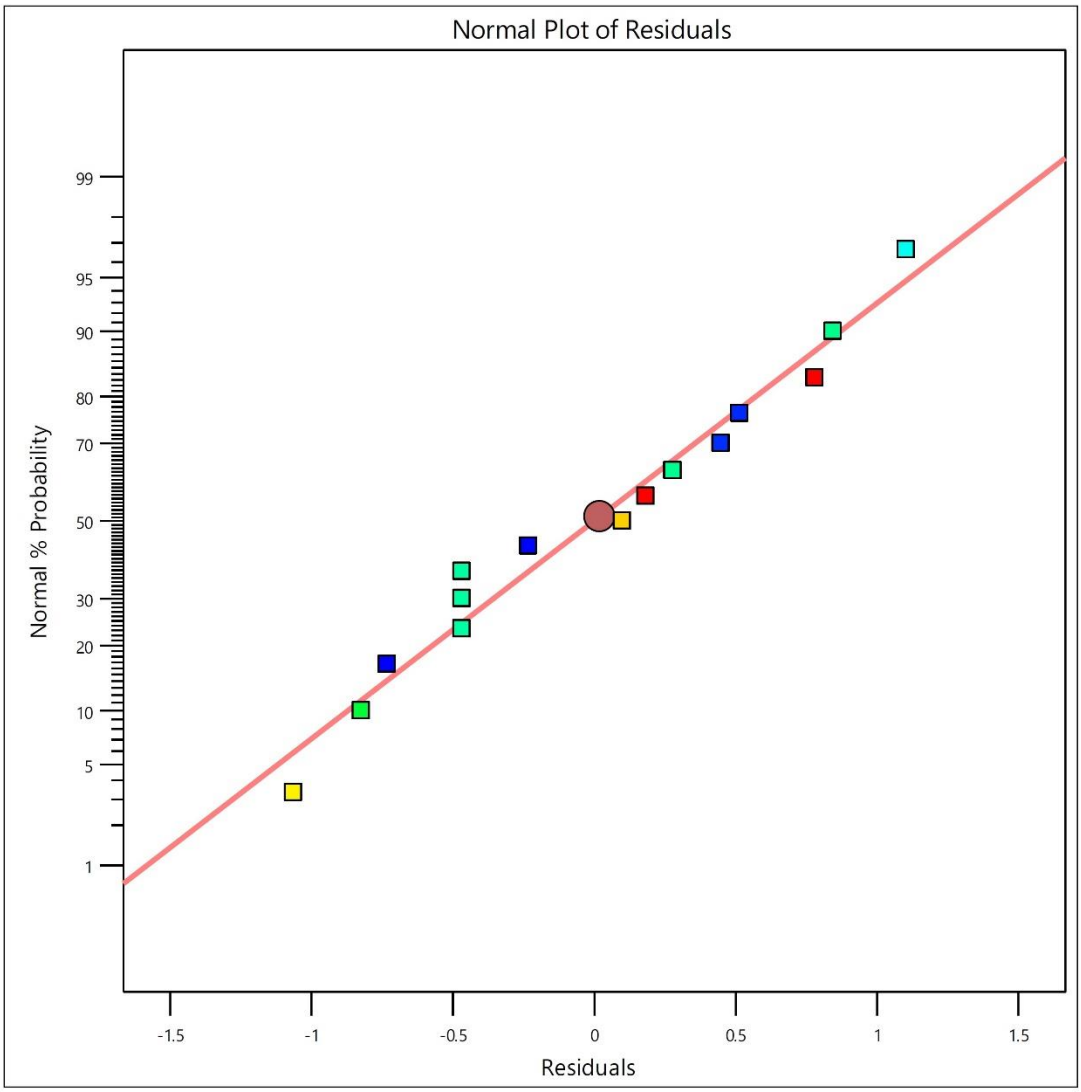

(c)

Fig. 4.2 Residuals of (a) Δq, (b) Δw, and (c) ΔCOP

4.3 Statistical Analysis

Statistical analysis is carried out to ensure that the model has a good fit.

4.3.1 Box-Behnken Design (BBD) Simulated Responses

The outcomes derived from the Box-Behnken Design (BBD) specified combinations of design variables are outlined below. Table 4.3 showcases the factor

combinations according to the Box-Behnken Design, and the analysis is carried out utilizing Design Expert software.

Table 4.3 Three variable three levels of design

Variables	**Unit**	**Levels**		
Level code		-1	0	1
Ambient Temperature, T_a	℃	30	37.5	45
Relative Humidity, RH	%	20	50	80
Evaporator Temperature, T_e	℃	3	7.5	12

The following are the abridged prediction correlations taking only the significant terms where variables $A, B\ and\ C$ represent T_a, RH and T_e, respectively.

$$\Delta COP = 2.6607 - 0.05585 \times A - 0.02931 \times B + 0.050414 \times C + 0.00017 \times A \times B + 0.0005 \times A \times C - 0.00013 \times B \times C + 0.000549 \times A^2 + 0.000093 \times B^2 - 0.00344 \times C^2 \quad (4.1)$$

$$\Delta TCR = 32.38 - 0.95463 \times A - 0.04584 \times B + 0.035431 \times C - 0.01449 \times A \times B - 0.0244 \times A \times C + 0.011766 \times B \times C + 0.041344 \times A^2 + 0.000861 \times B^2 - 0.01991 \times C^2 \quad (4.2)$$

$$\Delta E_{D,t} = 0.507831 - 0.01911 \times A + 0.002748 \times B + 0.002232 \times C - 0.00039 \times A \times B - 0.00105 \times A \times C + 0.000349 \times B \times C + 0.001067 \times A^2 + 0.0000055 \times B^2 + 0.000037 \times C^2 \quad (4.3)$$

Equations (4.1) to (4.3) examine the comparative implication of regulating variables and their constants. A positive regression coefficient indicates a hike in the outcome with a rise in the specific parameter, while a negative regression constant specifies a reduction in outcome for a rise in the particular parameter. For instance, if the parameter B (relative humidity) has a negative constant and changes to an upper value (e.g., 20% to 80℃), the response (exergy destruction) also increases.

Table 4.4 depicts the contrasts between prediction and experimental values for response enhancement. The variation between prediction and experimental data is moderately trivial except for a very few values and the ambiguity in the experimental values of the response variations lie below 9.02%.

Table 4.4 Error between prediction data and experimental results

Input parameters			**BBD prediction data**			**Experimental results**			**Error (%)**		
T_a(℃)	RH (%)	T_e(℃)	ΔCOP	ΔTCR	$\Delta E_{D,t}$	ΔCOP	ΔTCR	$\Delta E_{D,t}$	ΔCOP	ΔTCR	$\Delta E_{D,t}$
37.5	50	7.5	0.66	26.03	0.62	0.66	26.04	0.62	0.38	-0.03	0.81
45	20	7.5	1.13	51.79	1.23	1.14	52.47	1.25	-0.89	-1.30	-1.63
37.5	80	12	0.31	14.35	0.37	0.33	14.81	0.37	-9.02	-3.21	1.35
45	50	12	0.71	31.84	0.75	0.71	31.42	0.74	0	1.32	1.33
30	20	7.5	1.24	26.70	0.54	1.22	26.96	0.56	1.61	-0.95	-4.67
45	50	3	0.57	38.79	0.99	0.59	39.15	1.00	-3.51	-0.93	-1.01
30	50	3	0.65	18.57	0.42	0.64	19	0.42	1.54	-2.32	0
45	80	7.5	0.33	20.38	0.54	0.34	20.75	0.53	-3.08	-1.82	1.87
30	80	7.5	0.29	8.33	0.21	0.31	8.88	0.21	-8.77	-6.61	0
37.5	20	12	1.25	35.01	0.76	1.28	35.88	0.78	-2.40	-2.48	-3.31
30	50	12	0.71	14.91	0.32	0.69	14.57	0.30	2.82	2.28	6.25
37.5	20	3	1.12	43.49	1.01	1.08	43.55	1.03	3.59	-0.14	-1.98
37.5	80	3	0.32	13.53	0.35	0.35	14.25	0.34	-7.81	-5.28	-1.49

The outcomes of response improvement from ANOVA are presented in Table 4.5 showing parameter of significance. Regression examination is utilized to reject insignificant parameters, as they are improbable to affect the response. The Model F-values suggest the model's significance. Significantly large F-values of 135.16, 826.59, and 793.58 conforming to improvements in *COP*, and reductions in *TCR* and $E_{D,t}$ with quite small p-values approve the good fitness of the DEC-SAC model. A large F-value of the relative humidity indicates its greatest substantial impact on exergy destruction and least effect on *TCR*.

P-values below 0.0500 specify significant model parameters. The prediction error sum of squares (PRESS) is a measure of the deviation between the fitted values and the observed values. The outputs indicate an assurance level higher than 95% for R^2 and R_a^2 values, supporting the acceptance of the model [126]. Predicted R^2 (0.9345) align well with Adjusted R^2 (0.9885) values for *COP*, and similar results are observed for other outcomes. The model is considered suitable, as the differences between R_a^2 and R_p^2 are below 0.1% [127]. Adequate Precision computes the signal-to-noise (S/N) ratio (>4), which is reasonable for the current study, validating the fit [73]. The small values of SD and Mean ratio, i.e., coefficient of variation (C.V.) recommend that the model is correct.

Table 4.5 ANOVA model for improvement in COP, decrease in TCR, and decrease in $E_{D,t}$ of DEC-SAC in comparison to CSAC

	ΔCOP		ΔTCR		$\Delta E_{D,t}$	
Source	**F-value**	**p-value**	**F-value**	**p-value**	**F-value**	**p-value**
Model	135.16	< 0.0001	826.59	< 0.0001	793.58	< 0.0001
A-T_a	2.02	0.2145	3150.77	< 0.0001	2389.49	< 0.0001
B-RH	1156.12	< 0.0001	3550.17	< 0.0001	4287.62	< 0.0001
C-T_e	14.62	0.0123	369.59	< 0.0001	194.97	< 0.0001
AB	4.34	0.0917	197.48	< 0.0001	147.10	< 0.0001
AC	0.8469	0.3997	31.44	0.0025	9.38	0.0280
BC	0.9446	0.3757	55.85	0.0007	34.92	0.0020
A^2	2.62	0.1664	83.62	0.0003	69.10	0.0004
B^2	19.08	0.0072	0.5654	0.4859	7.67	0.0394
C^2	13.32	0.0148	0.0130	0.9135	2.08	0.2091
Residual	0.0013		0.0002		0.2890	
Lack of Fit	0.0022		0.0003		0.4817	
R^2	0.9959		0.9993		0.9993	
Ra^2	0.9885		0.9981		0.9980	
Rp^2	0.9345		0.9893		0.9888	
PRESS	35.7558		0.0127		23.12	
Adq.Pres.	0.1074		100.21		99.04	
SD (σ^2)	0.0366		0.0126		0.5376	
Mean	0.7222		0.5946		25.56	
C.V.	5.07		2.12		2.10	

The diagnostic plots (depicted in Fig. 4.3 (a) to (c)) indicate a well-fitted model. The normal probability plot for residuals, displaying the accumulation of residuals around the central line, signifies the relevance of the analysis. These findings imply the effective application of the Box-Behnken design to the current model. With the

aim of exploring the parameters influencing variations in *COP*, *TCR*, and $E_{D,t}$ between DEC-SAC and CSAC, simulations specified by the BBD contribute to enhancing the cycle under changing situations of outdoor temperature, relative humidity, and evaporation temperature.

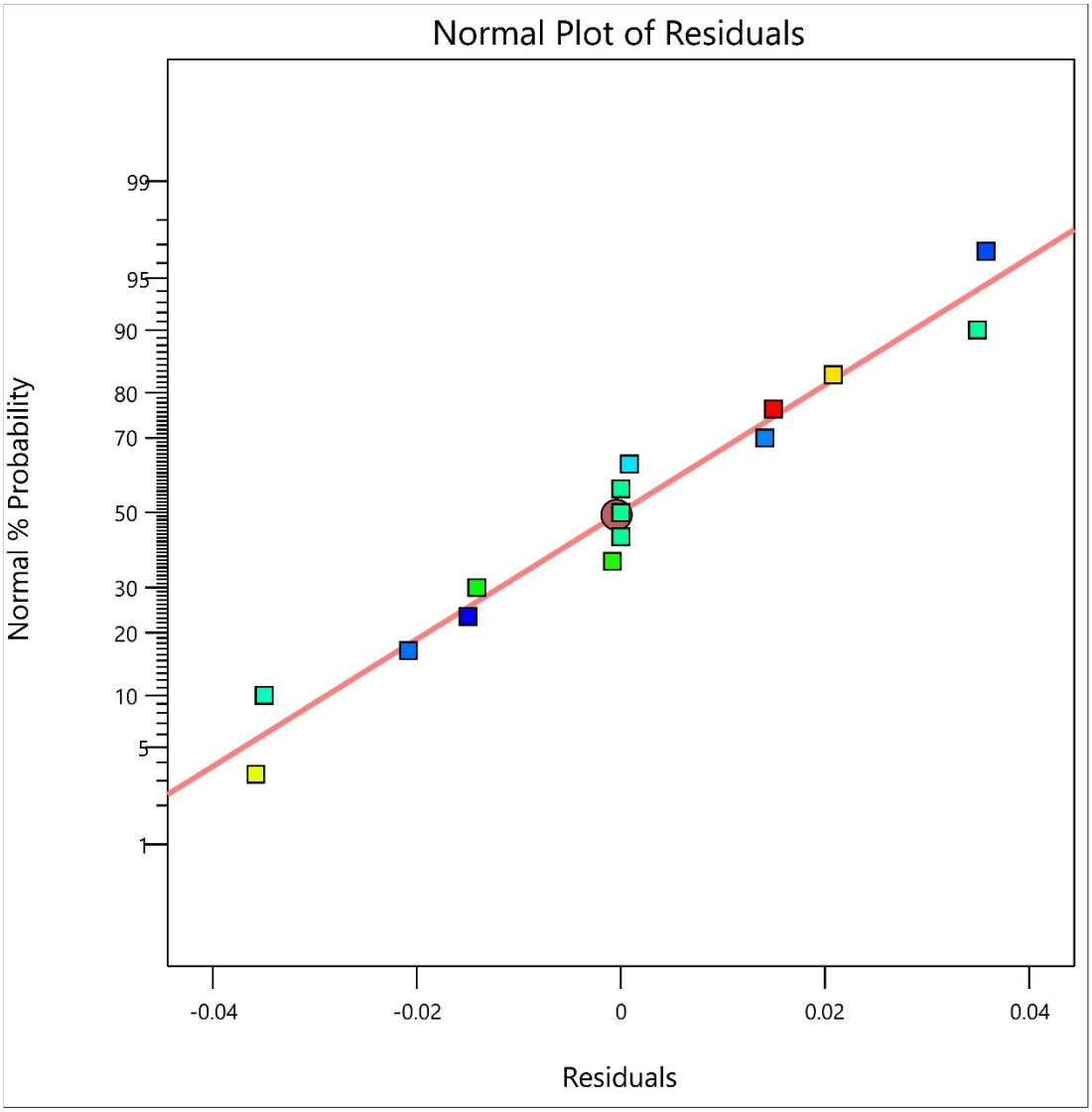

(a)

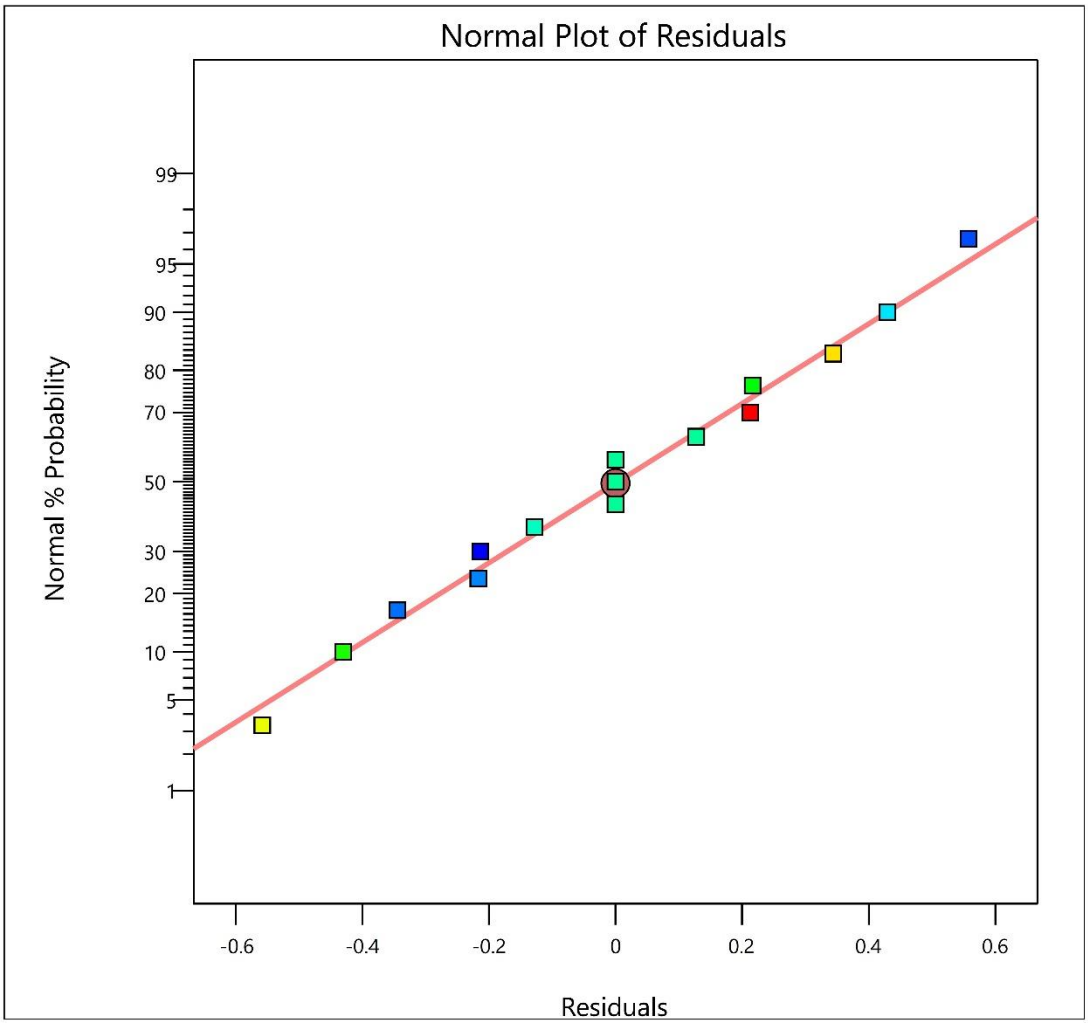
Normal Plot of Residuals
Normal % Probability
99
95
90
80
70
50
30
20
10
5
1
-0.6
-0.4
-0.2
0
0.2
0.4
0.6
Residuals

(b)

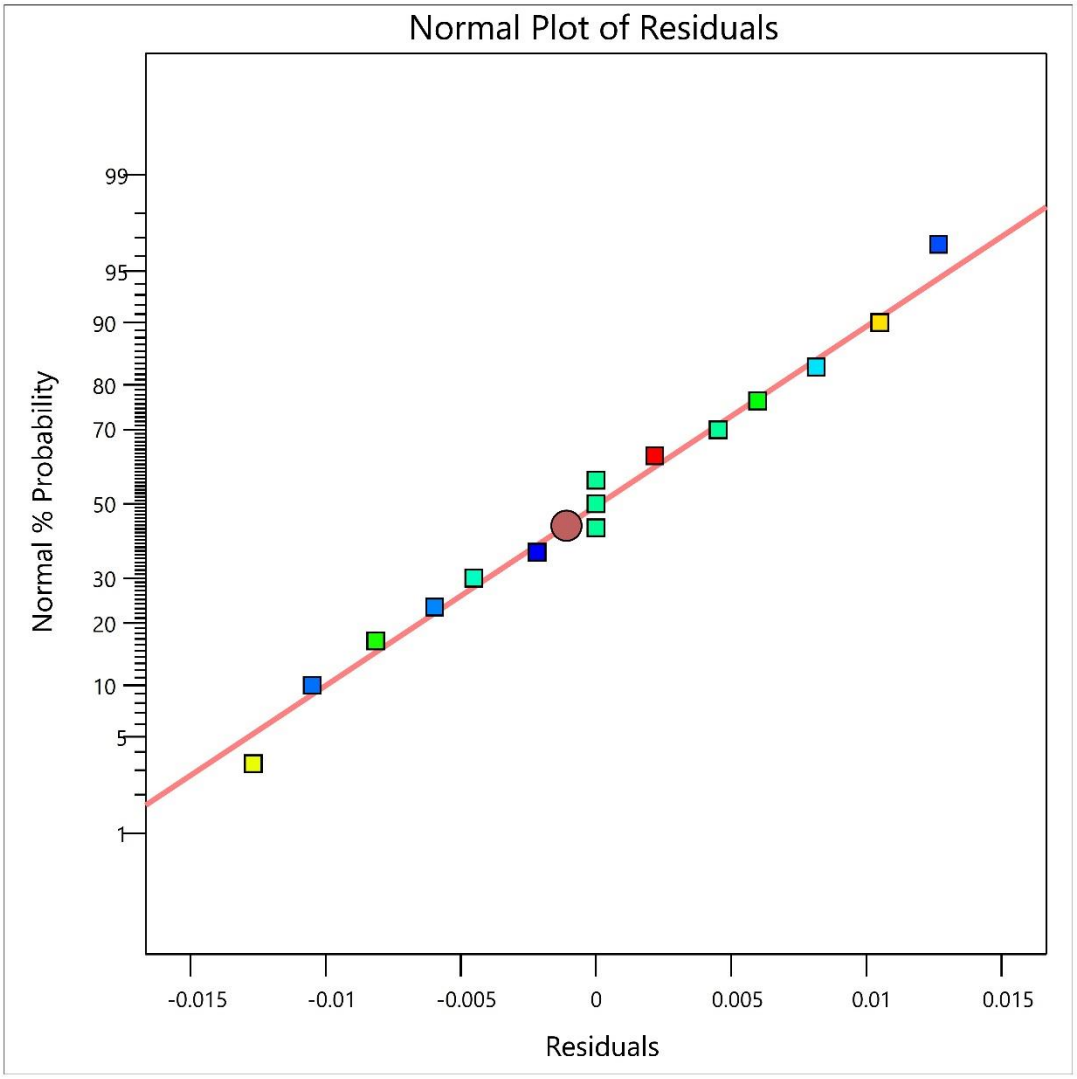

(c)

Fig. 4.3 Residuals of **a.**ΔCOP; **b.**ΔTCR; **c.** $\Delta E_{D,t}$

CHAPTER 5

RESULTS & DISCUSSION

This chapter presents the obtained results. The system is described in detail with its specifications and assumptions. Parametric investigation is carried out to find out the impact of different input parameters on the outcomes. The thermodynamic performances of conventional SAC and DEC-SAC are compared in terms of their COP, TCR, and $E_{D.t}$. The comparisons of energy expenditure, economics and environmental responses are also discussed. Finally, the decision variables are optimized to get the optimum output from DEC-SAC. Payback period is also computed for the DEC-SAC system.

5.1 Model Description

In this study a 1.5 Ton refrigerating capacity split air conditioning system (SAC) is employed.

The operational parameters for the SAC system are outlined in Table 5.1. The Bureau of Energy Efficiency, Government of India [125] prescribes the guidelines for conducting performance testing of domestic split air conditioners . Following these guidelines, the investigations are conducted within the evaporating temperature range of 3°C to 12°C. The outdoor temperature and relative humidity are taken in the limits 30°C to 45°C and 20% to 80%, respectively, as indicated by [35]. The difference between ambient air temperature with the evaporating and condensing temperature is supposed to exhibit a 15°C difference each, as suggested by [128]. The density and

specific heat values of air are assumed constant at 1.3 kg m^{-3} and 1.0 kJ $kg^{-1}°C^{-1}$, respectively. To assess the impact of evaporative cooling on COP, knowledge of the authentic air temperature reduction ($\Delta T_{a,dec}$) at the condenser entry point under various ambient conditions is essential. Eq. (3.6) from the proposed model is utilized for this purpose.

5.1.1 System Specifications

The specifications of the SAC system are appended below:

Split type air conditioner Daikin make, model no. RL50TV16U3

Rated cooling capacity = 5200 W,

Rated power input 1425W, supply-50 Hz, 230V,

Outdoor conditions: 35°C (DBT) and 24°C (WBT),

Refrigerant R32.

Outside (d_o) and inside (d_i) tube diameters for condenser and evaporator = 14.97mm and 13.57mm, respectively.

Other standard conditions of operation are taken as under:

Refrigerant superheat at the evaporator exit = 5°C [92]

The mean air temperature difference in both the heat exchangers = 5ºC [119]

Condensing temperature = 15°C greater than T_a [92][128].

Cooling space temperature, T_R = 15°C greater than T_e [128].

Pressure drop = 20kPa and 10kPa for evaporation and condensation, respectively [52].

The system is analyzed under the following conditions:

1. SAC operates on a vapor-compression refrigeration cycle

2. The system operates in steady-state condition.

2. The energies due to motion and position are neglected.

3. The heat losses to or from the environment that surrounds the system are negligible.

Genetron Properties software [110] utilizes the NIST Refprop database to calculate the thermodynamic and transport features of the fluid medium (R32).

Table 5.1 Design variables for SAC

Room temperature, T_R[a]	18-27℃
Superheat at the evaporator outlet[b]	5℃
Compressor isentropic efficiency[b]	70%
Compressor volumetric efficiency[b]	95%
$(T_R - T_e)$[c]	15℃
$(T_k - T_a)$[c]	15℃

[a][125], [b]as per product catalogue, [c][128]

5.2 Investigation of Isentropic and Volumetric Efficiencies

The variation in input parameters affect the isentropic and volumetric efficiencies of the compressor. Hereunder, the influence of condensing and evaporating temperature on the isentropic and volumetric efficiencies and the system responses is examined.

5.2.1 Effect of T_k and T_e on Isentropic and Volumetric Efficiencies

Figures 5.1 (a) and (b) represent the influence of ambient temperature on the compressor isentropic efficiency (η_s) and volumetric efficiency (η_{vol}) for the conventional split air conditioner (CSAC) at 3℃ and 12℃ evaporator temperature

(T_e), respectively. Both the efficiencies decrease with the increase in ambient temperature when relative humidity is kept constant (50%). The reason is that the rise in T_a increases the condenser temperature and also the compression ratio which decreases the volumetric efficiency. The flatter curve at higher condenser temperature stipulates more compressor work. Thus, the isentropic efficiency decreases by 8.76% and volumetric efficiency decreases by 9.21% ($T_e = 3$℃) when T_a rises from 30℃ to 45℃. The corresponding decreases at $T_e = 12$℃ are 6.33% and 6.64%. Higher isentropic and volumetric efficiencies are obtained at elevated evaporating temperature, obviously due to lower compression ratio.

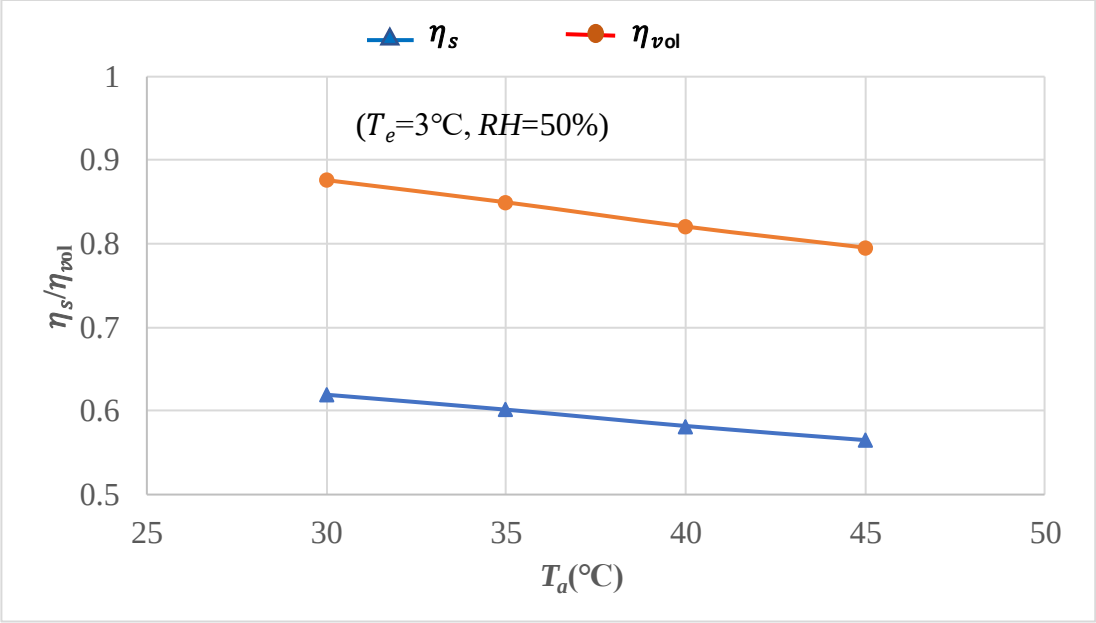

(a)

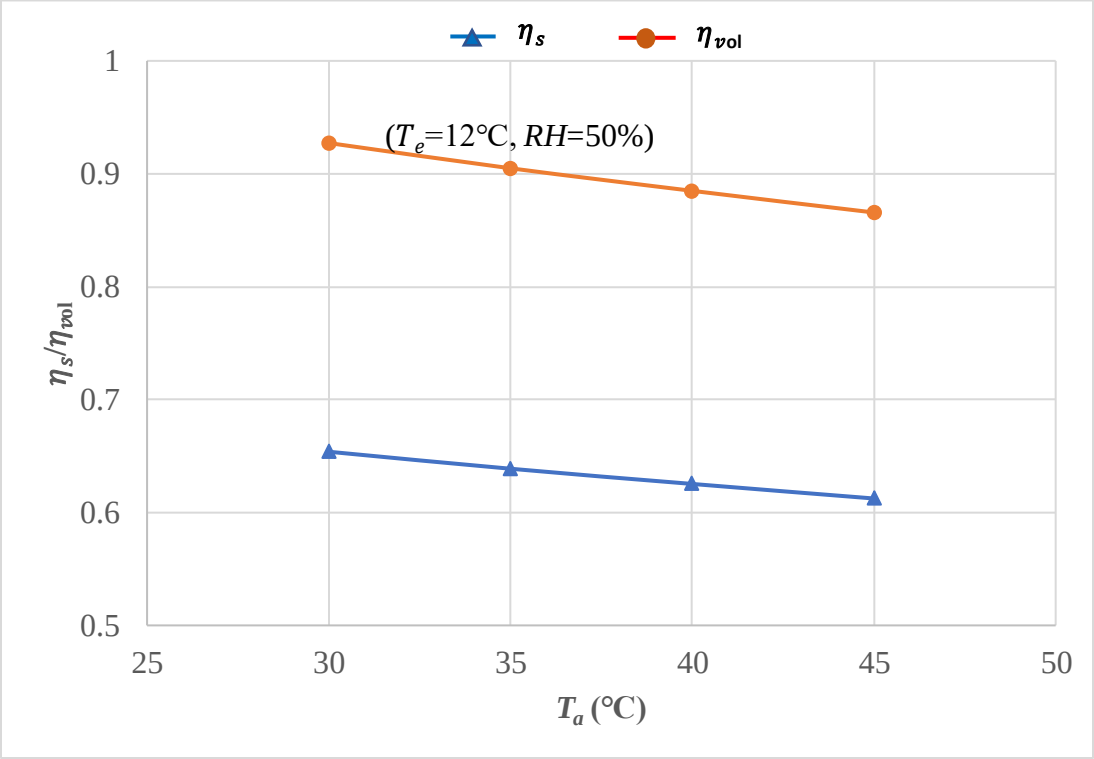

(b)

Fig. 5.1 Effect of ambient temperature on η_s and η_{vol} at (a) $T_e = 3$℃; (b) $T_e = 12$℃

5.2.2 Effect of variable Isentropic and Volumetric efficiencies on specific refrigerating effect and specific compressor work

The effects of variations in isentropic and volumetric efficiencies on specific refrigerating effect as well as specific compressor work for CSAC (T_e=7.5C) are shown in Fig.5.2 (a) and (b). As shown in the figures, higher refrigerating effect is realized for higher η_s and η_{vol}. Obviously, the specific work decreases with increase in η_s and η_{vol}.

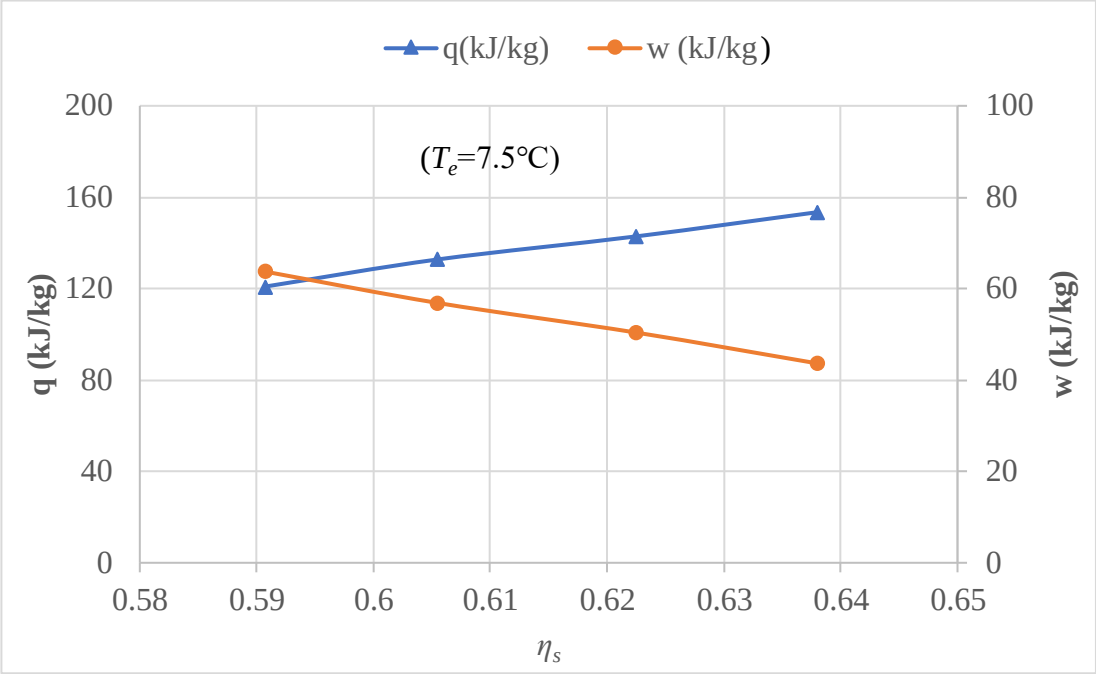

(a)

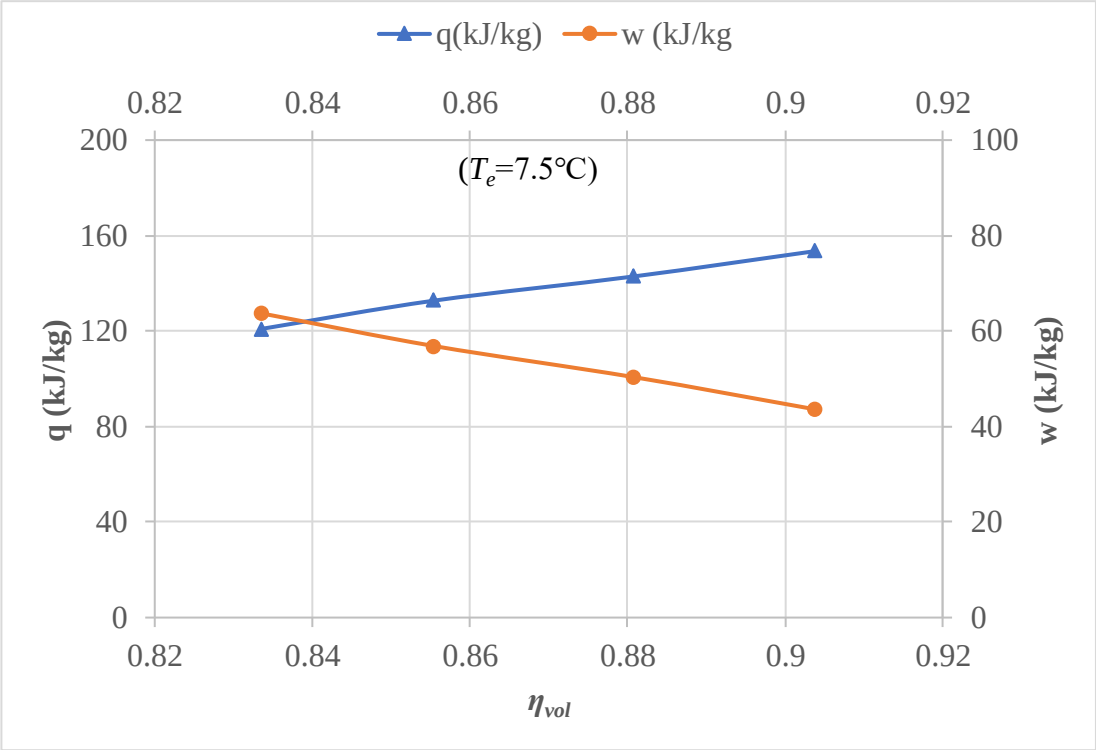

(b)

Fig.5.2 Effect of (a) η_s and (b) η_{vol} on specific refrigerating effect and specific compression work

5.3 Performance Comparison of CSAC and DEC-SAC

This section presents the comparative analysis of responses obtained with conventional and DEC-SAC systems.

5.3.1 Effect of T_a and RH on evaporative cooling degree

Figure 5.3 shows the reduction in condenser inlet air temperature as a function of ambient temperature and relative humidity. A higher drop in ambient temperature (ΔT_a) is noted at 45°C than at 30°C. However, ΔT_a reduces with the increase in RH.

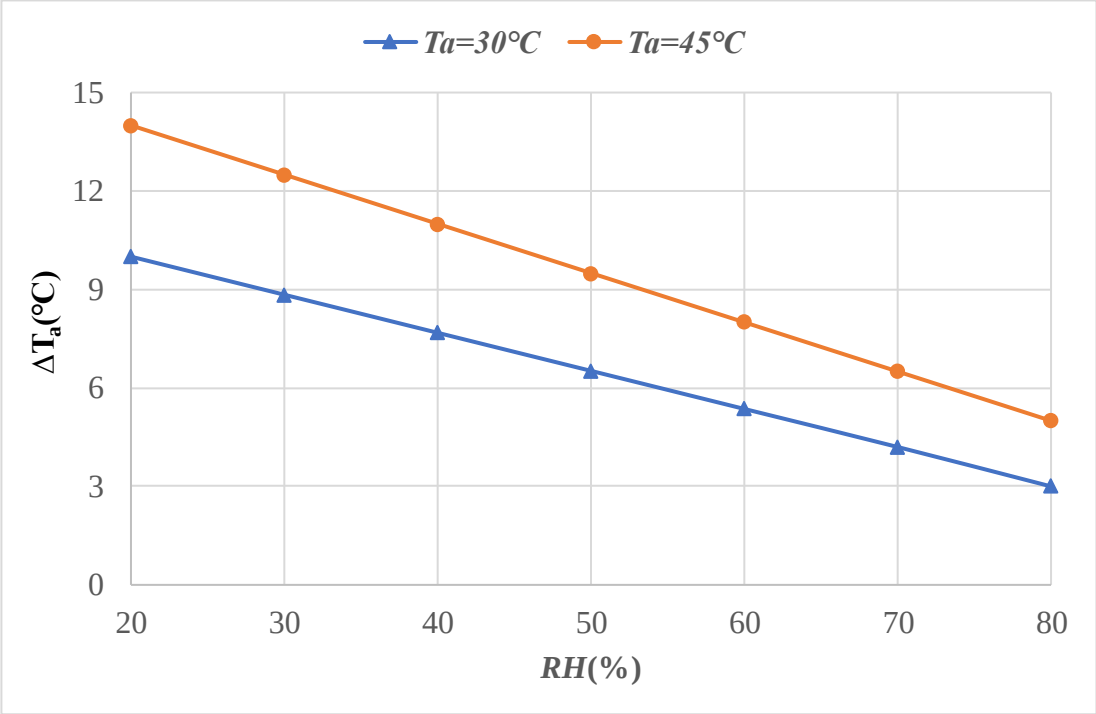

Fig. 5.3 Reduction in ambient temperature due to evaporative cooling

5.3.2 Effect of evaporative cooing on the performance parameters of DEC-SAC

The effect of evaporative cooling on the outputs of DEC-SAC is as follows.

Specific refrigerating effect

The introduction of liquid at reduced condenser temperature with lower enthalpy into the evaporator enhances the refrigerating effect per unit mass. As a result, the refrigerant mass velocity decreases per unit capacity in the evaporatively cooled cycle. Illustrated in Figure 5.4 are the increased refrigerating effect, reduced work consumption, and improved COP achieved through evaporative cooling. A noticeable elevation in the refrigerating effect occurs with an increase in the degree of evaporative cooling. The behavior of the refrigerating effect serves as an indicator for the mass flow rate volume and, consequently, the size of the air conditioner. A higher refrigerating effect leads to a reduction in the mass flow rate, resulting in a smaller system for the same cooling capacity compared to a system without evaporative cooling.

Compression work

The specific volume of the gaseous refrigerant at the compressor entry remains consistent for individual cycles, whether employing conventional (non-evaporative cooling) or DEC (with evaporative cooling). Nevertheless, the subcooled cycle experiences a lower mass flow compared to that without subcooled process. As a result, the compressor deals with a smaller vapor volume for a given capacity. Due to this reduced vapor volume, the subcooled cycle requires a lesser compressor

movement than what is needed for non-evaporative cooled process. The reduction in specific work input attributed to evaporative cooling is depicted in Fig. 5.4.

The incorporation of enhanced evaporative cooling results in a reduction in the saturation condenser temperature. This, in turn, leads to a decrease in compression work due to the lower compression ratio, assuming a constant evaporator temperature. This decline becomes more noticeable at elevated levels of evaporative cooling. The decrease in input work for DEC-SAC, in comparison to traditional SAC, is particularly noteworthy under the conditions of the highest ambient temperature (45°C) and lowest relative humidity (20%).

Coefficient of performance (COP)

In Fig. 5.4, the COP improvement is presented in relation to the escalating evaporatively cooled process. The cooling capacity is held constant at 5.25 kW, focusing solely on enhancing the COP. As evaporative cooling increases, the two-phase area decreases to accommodate the subcooled liquid formed in the condenser. In the subcooled zone, the temperature differential between air and refrigerant, along with the coefficient of heat transfer, is smaller compared to the liquid-vapor zone. The increase in saturation temperature intensifies the temperature difference in the two-phase area, offsetting the decrease in condenser heat transfer effectiveness. This results in a relative reduction in specific compressor work, as mentioned earlier. Concurrently, the decrease in condenser outlet temperature enhances the refrigerating effect with a greater enthalpy variation in the evaporator.

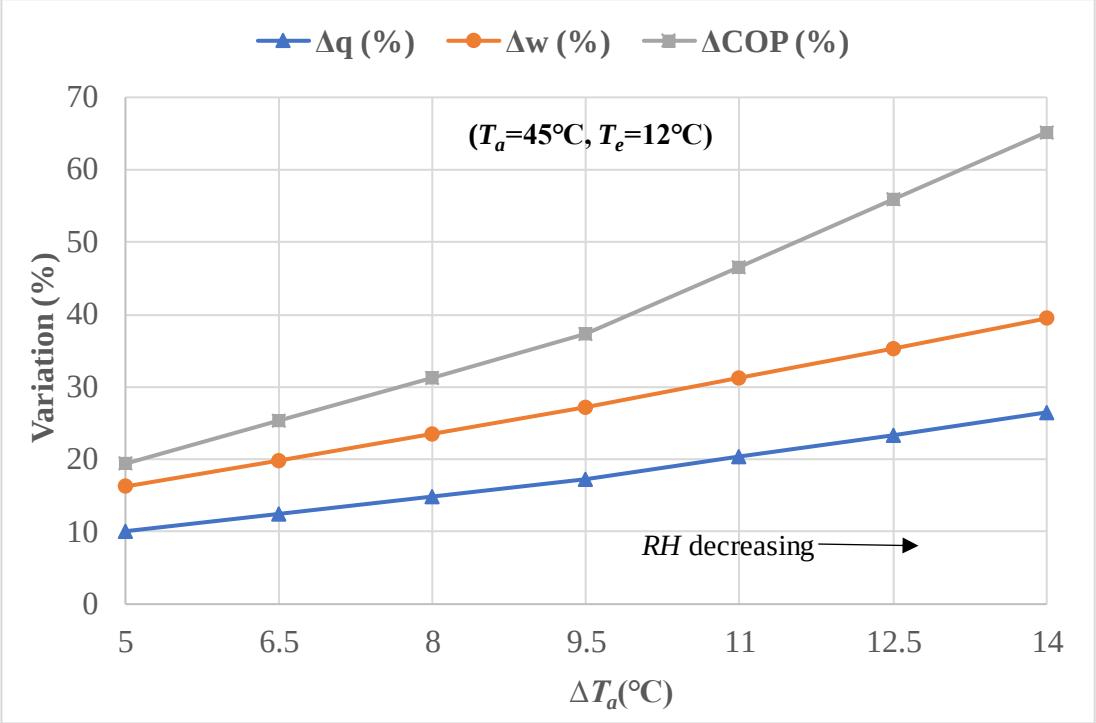

Fig. 5.4 Effect of Evaporative cooling on specific refrigerating effect, specific work consumption and COP

The calculated amount for the rise in specific cooling effect (Δq), lowering of specific work (Δw), and increase in COP at T_a=37.5℃ and T_e=7.5℃ for variable relative humidity are detailed in Table 5.2.

The most substantial improvement in cooling effect (17.80%) happens at 20% relative humidity, accompanied by a 34.55% reduction in input work. Conversely, the least improvement in cooling effect is observed as 6.17% under the maximum relative humidity considered (80%), attributed to the minimal temperature reduction in environmental air and as a result, lower temperature drop occurs during condensation. The consumption of work reduces correspondingly by 12.78%. For average operating conditions, the maximum and the minimum enhancements in COP are 52.93% (20%

relative humidity) and 14.66% (80% relative humidity), conclusively demonstrating the beneficial impact of evaporative cooling on COP.

These findings collectively affirm that evaporative cooling enhances the system's performance.

Table 5.2 Calculated values of the performance parameters for average condenser inlet air temperature, T_a=37.5℃ and average evaporator temperature, T_e=7.5℃

$\boldsymbol{RH}$ (%)	20	30	40	50	60	70	80
$\boldsymbol{\Delta T_{a,dec}}$**(°C)**	14	10.7	9.4	8.1	6.8	5.4	4
$\boldsymbol{\Delta q}$ **(%)**	17.80	15.73	13.66	11.59	9.78	7.97	6.17
$\boldsymbol{\Delta w}$ **(%)**	34.55	30.88	27.20	23.53	19.94	16.36	12.78
$\boldsymbol{\Delta COP}$ **(%)**	52.93	45.53	38.15	30.77	25.40	20.03	14.66

5.3.3 Performance Analysis of DEC-SAC

Figure 5.5 shows the improvements in performance parameters of DEC-SAC over CSAC with varying degree of evaporative cooling. The *COP* enhancement lies between 3.53% ($\Delta T_a = 2$℃) to 65.21% ($\Delta T_a = 14$℃), while *TCR* reduces by 2.23% to 23.2%. The total exergy destruction also decreases by 7.83% to 55.1%, when the evaporative cooling increases from 2℃ to 14℃.

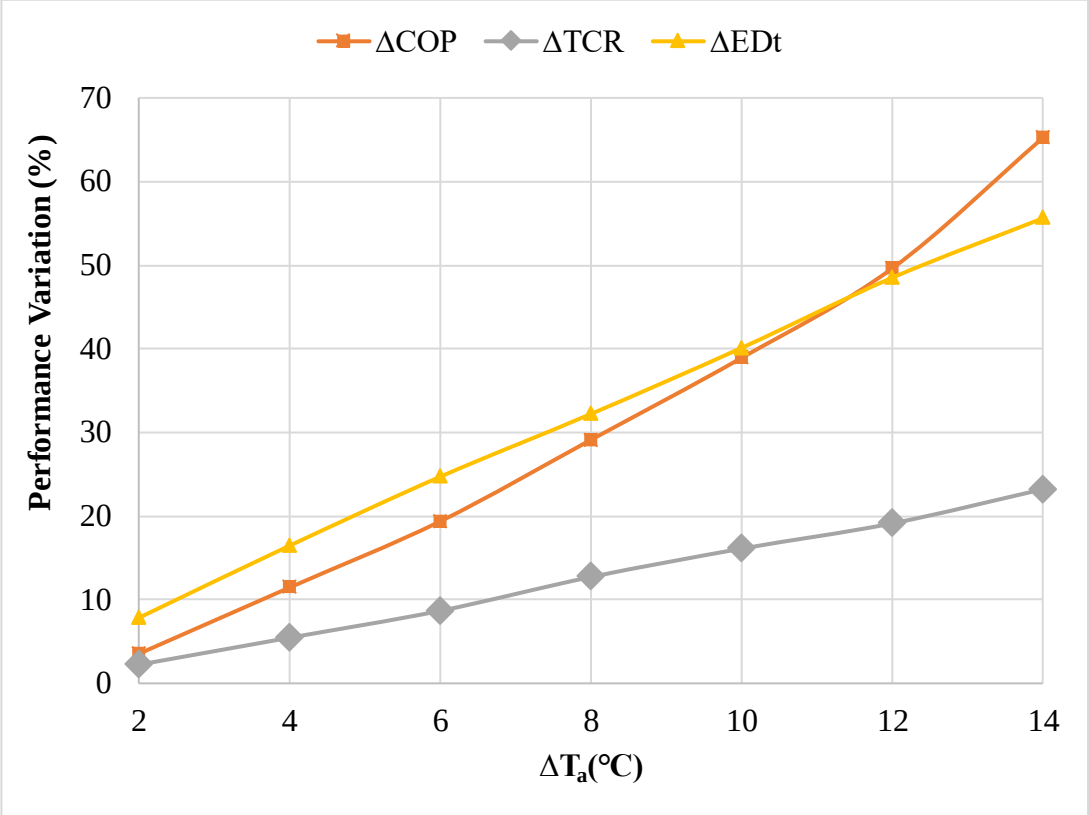

Fig.5.5 Effect of reduction in condenser inlet air temperature due to evaporative cooling on DEC-SAC performance

5.3.4 Parametric investigation of the response improvements for DEC-SAC

Figures 5.6 (a, c & e) illustrate the impact of environmental temperature (T_a), and relative humidity (RH) on the improvement in COP and declines in TCR and $E_{D.t}$, respectively. While an increase in T_a results in more significant reductions in TCR and $E_{D.t}$, an adverse impact is observed on the improvement in COP. Moreover, an increase in RH diminishes the benefits in COP, TCR, and $E_{D.t}$. Nevertheless, for the presumed parameter range, beneficial enhancements are consistently achieved for all outputs using DEC-SAC.

An elevated condenser temperature (T_k) results in an increased compression ratio, leading to higher costs in terms of investment, operation, and penalties. Conversely, a decrease in ambient temperature (T_a) creates a significant temperature gradient (ΔT_{LM_k}) between the condenser temperature and ambient air. This heightened heat transfer rate allows for a smaller condenser area, thereby reducing the investment cost. However, a higher-pressure ratio amplifies the compressor's power input, resulting in increased costs in terms of investment, operation, and penalties. Notably, the operating cost has a more pronounced impact than the investment cost. Additionally, a higher compression ratio and power for the same cooling capacity contribute to a decrease in COP with a rise in ambient temperature (T_a).

The combined effect of T_a, and T_e variations on COP, TCR, and $E_{D.t}$ is presented in Fig. 5.6(b, d & f). A higher (T_a), and T_e slightly improve COP, while significant reductions are observed in TCR, and $E_{D.t}$.

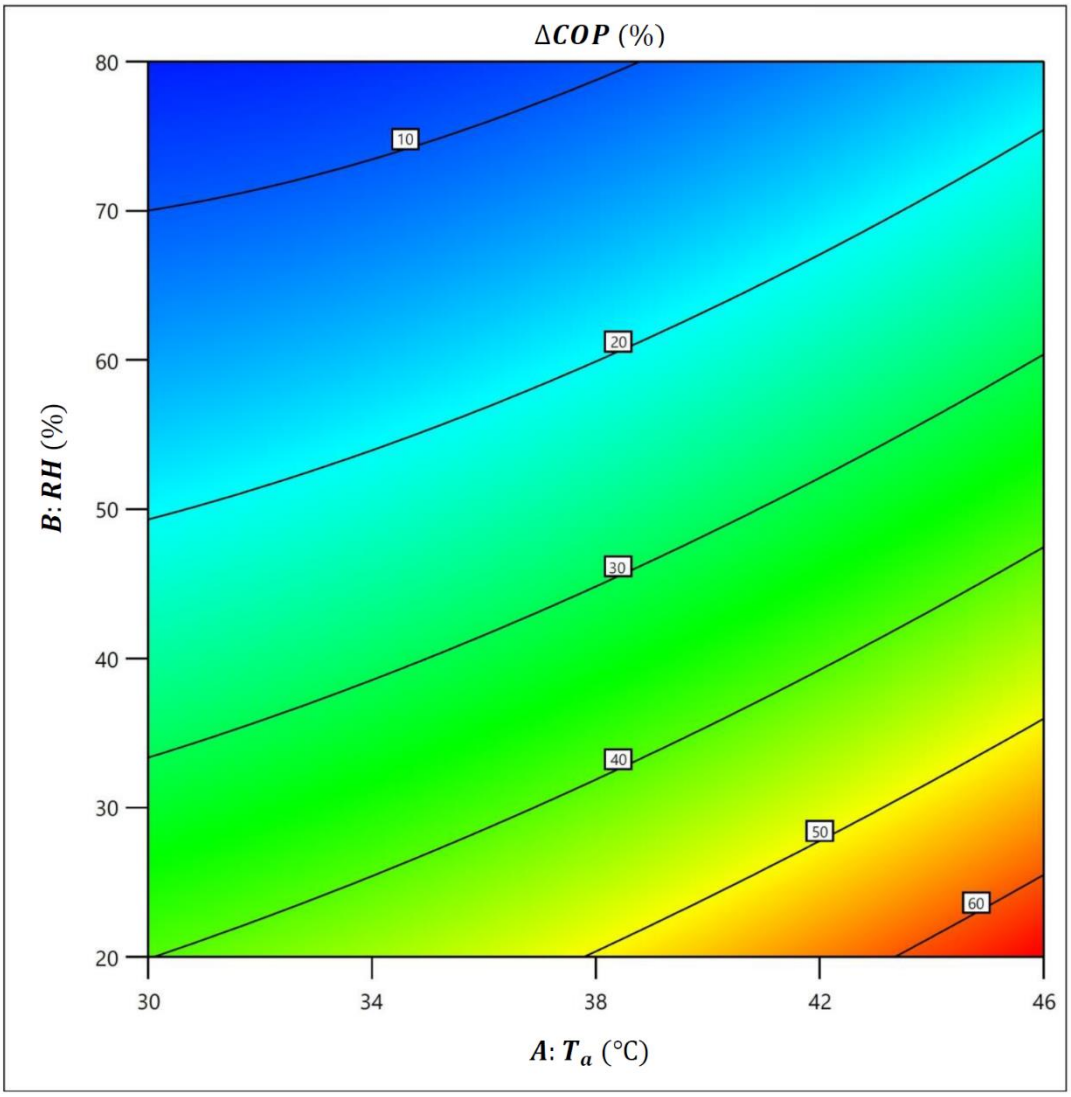

Fig. 5.6 (a) Effect of operating parameters T_a and *RH* on *COP*

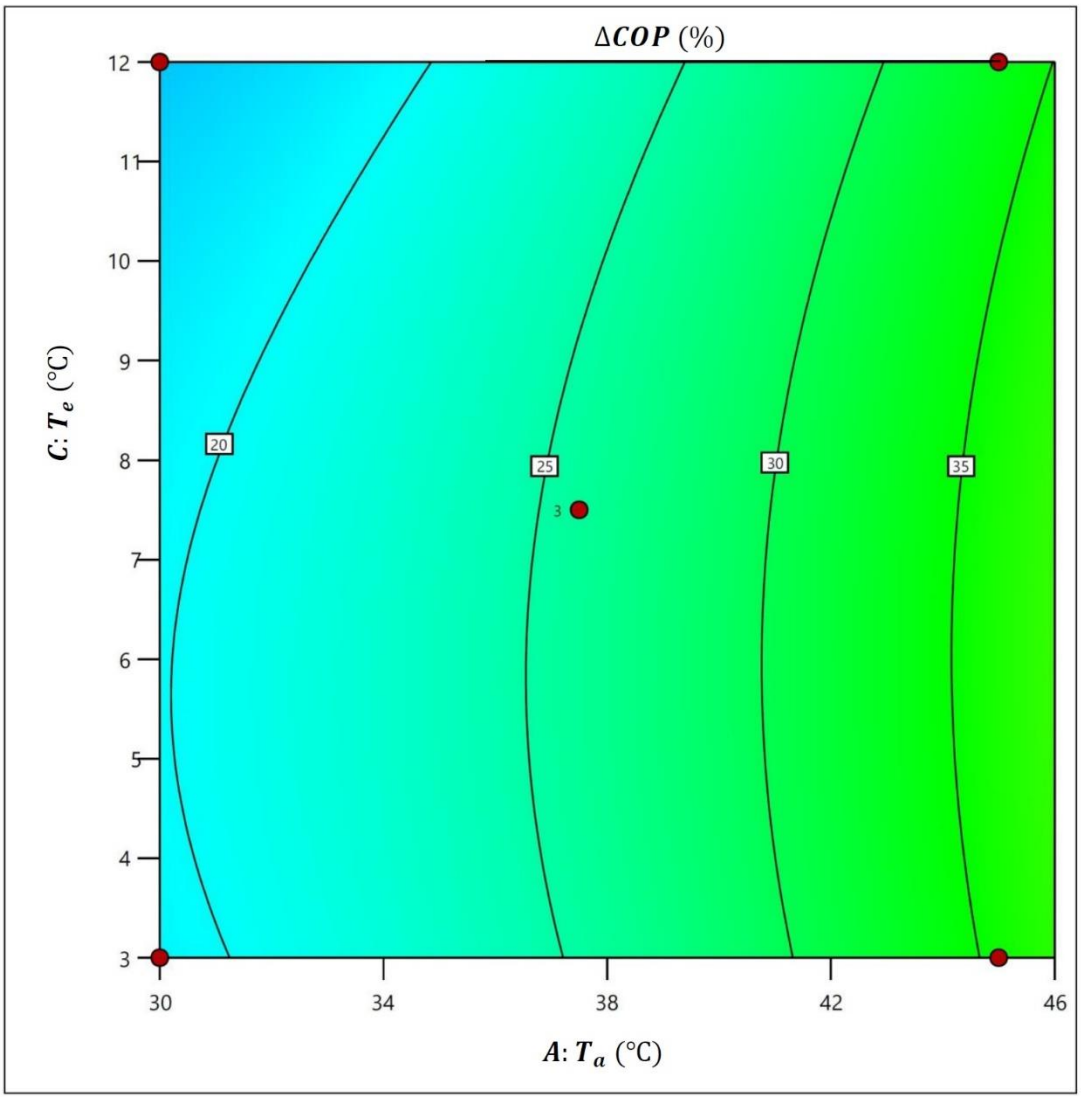

Fig. 5.6 (b) Effect of operating parameters T_a and T_e on *COP*

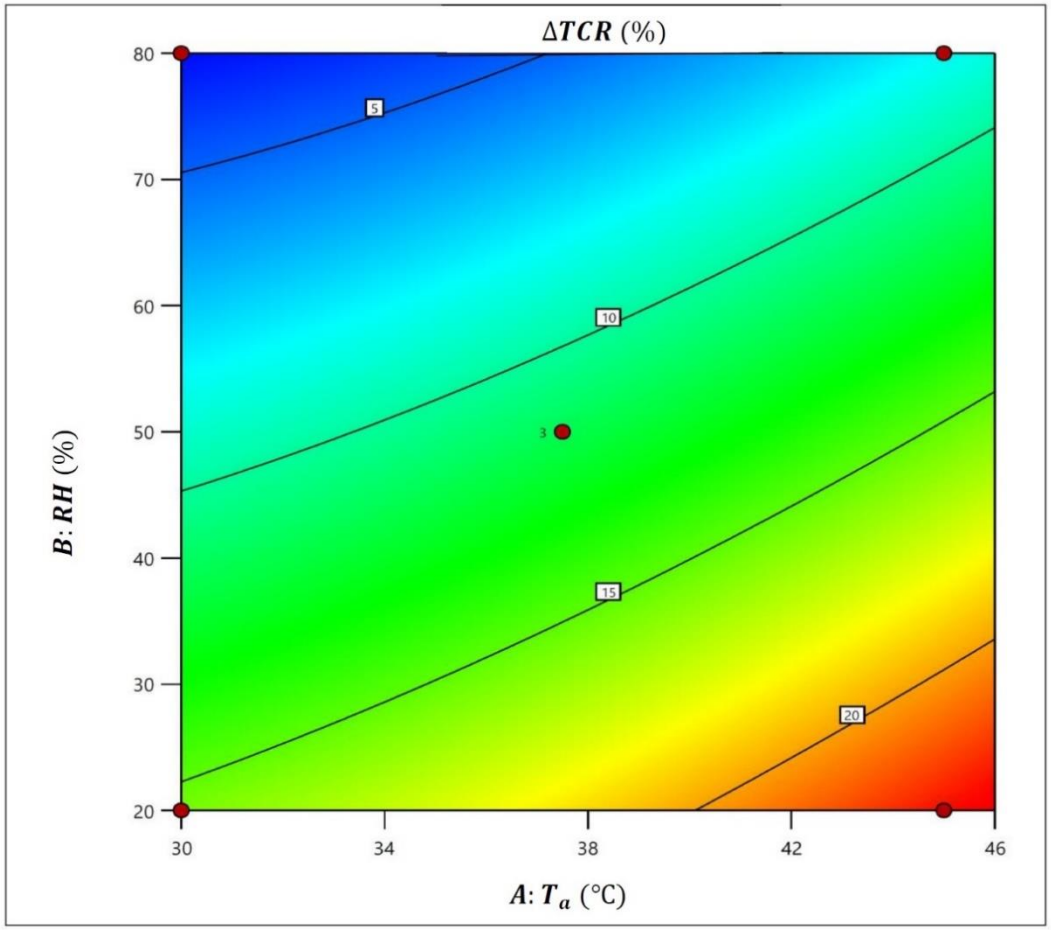

Fig. 5.6 (c) Effect of operating parameters T_a and RH on TCR

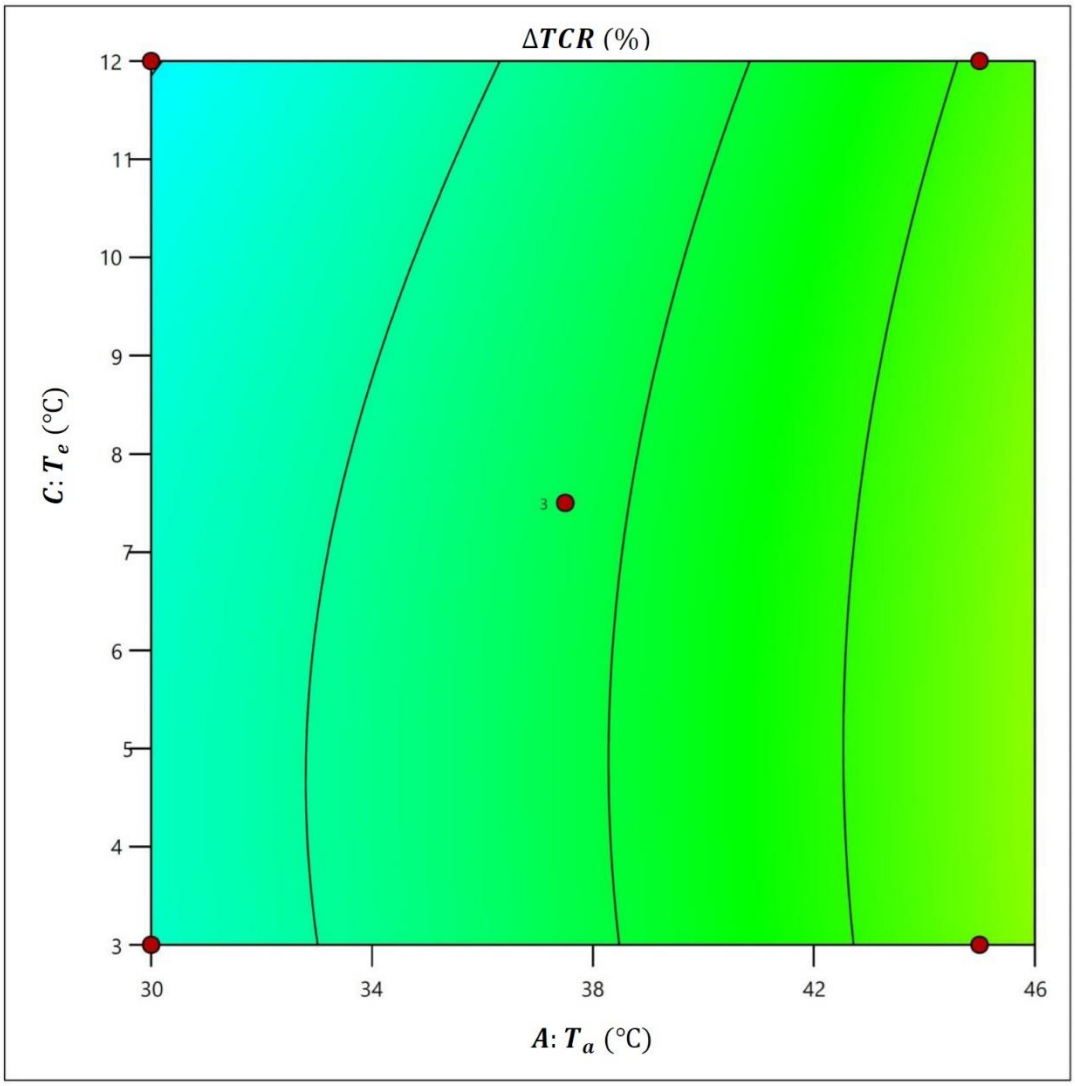

Fig. 5.6 (d) Effect of operating parameters T_a and T_e on *TCR*

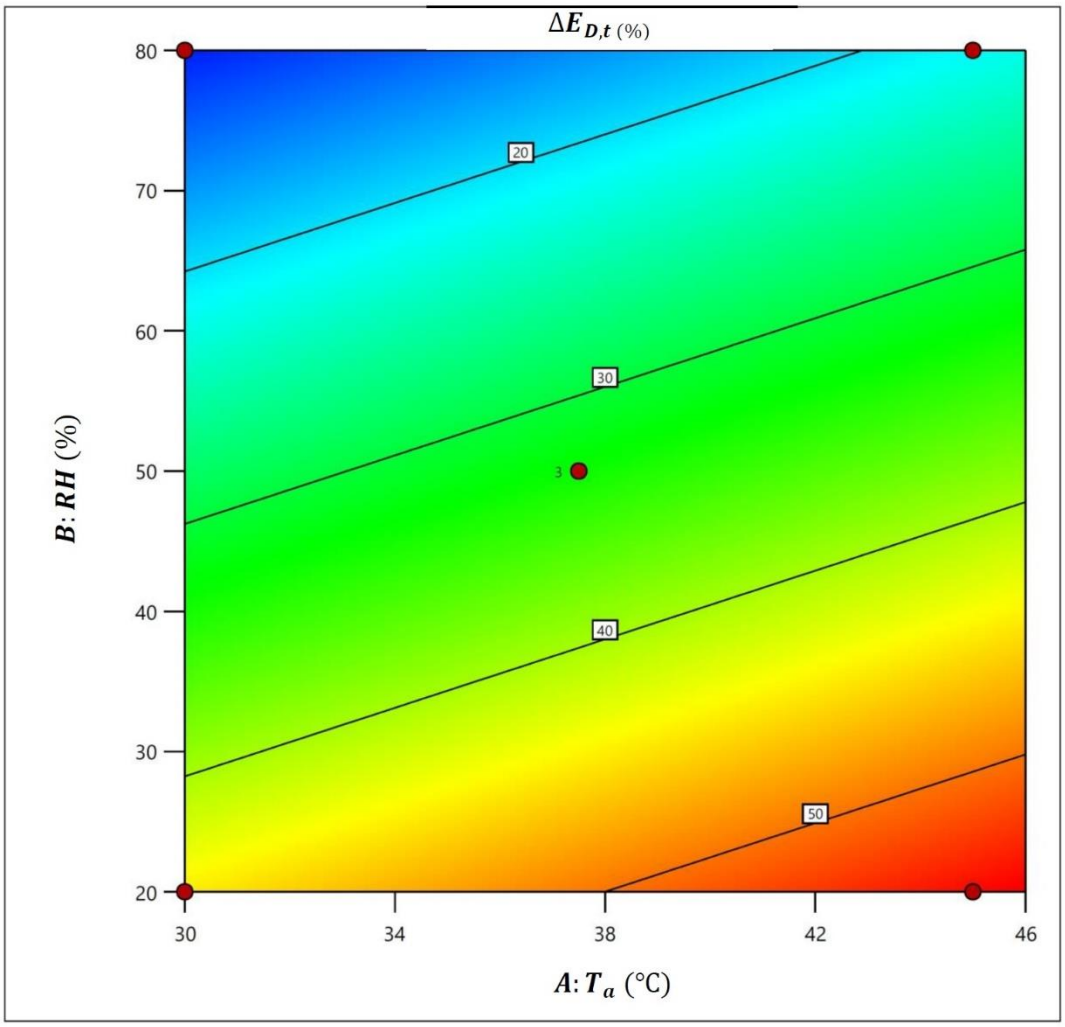

Fig. 5.6 (e) Effect of operating parameters T_a and *RH* on $\Delta E_{D,t}$

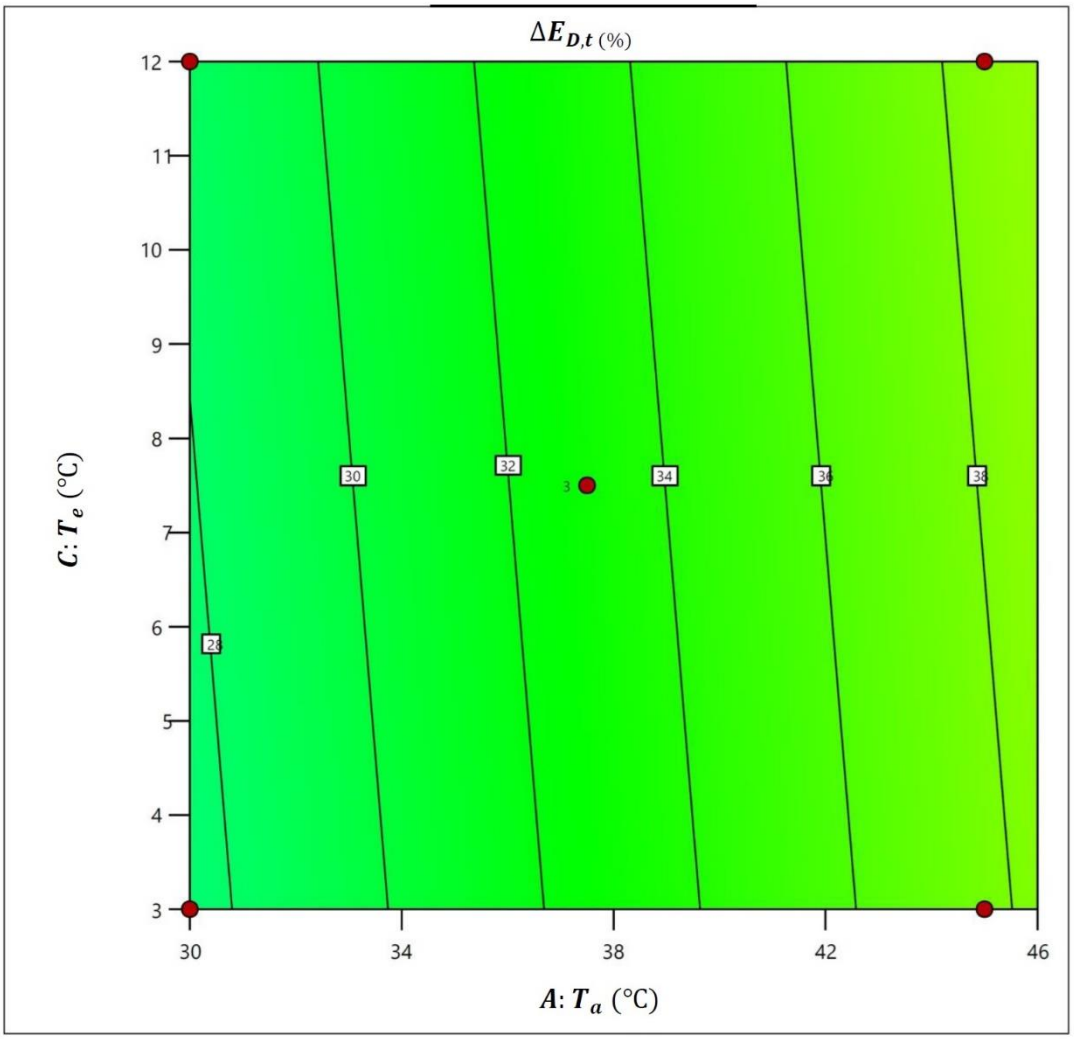

Fig.5.6 (f) Effect of operating parameters T_a and T_e on $\Delta E_{D,t}$

Table 5.3 presents the combination of factors for reduction in TCR and $E_{D,t}$ and enhancement in *COP* of DEC SAC compared to CSAC.

A maximum COP enhancement (65.21%) is obtained for hot-dry condition when T_a = 45°C, RH is 20%, and T_e=12°C. The corresponding reduction in TCR and $E_{D,t}$ are also maximum (23.2% and 55.1%, respectively) for the stated combination of input parameters. A minimum COP enhancement (3.53%) is revealed under high

humidity and low ambient temperature conditions (T_a = 30℃, RH is 80%, and T_e=3℃). The corresponding reductions in TCR and $E_{D,t}$ are also minimum (2.23% and 7.83%, respectively). Measured data for CSAC and DEC-SAC is given in Appendix-A. Corresponding refrigerant properties (at T_e=3℃ & 12℃) are given in Appendix-B.

Table 5.3 Results obtained for variations in responses of CSAC and DEC-SAC

T_a(℃)	RH(%)	T_e(℃)	ΔCOP(%)	ΔTCR(%)	$\Delta E_{D,t}$(%)
30	20	3	36.11	15.12	40.04
30	80	3	3.53	2.23	7.83
30	50	7.5	15.92	8.21	23.69
30	20	12	34.62	14.33	42.71
30	80	12	4.14	2.91	11.22
37.5	20	3	46.48	18.56	45.15
37.5	80	3	5.73	4.45	11.92
37.5	50	7.5	23.37	11.24	29.41
37.5	20	12	41.95	16.87	46.32
37.5	80	12	6.39	4.58	14.31
45	20	3	62.74	22.9	50.82
45	80	3	13.51	8.04	18.18
45	50	7.5	32.48	14.7	34.15
45	20	12	65.21	23.2	55.1
45	80	12	12.01	7.18	18.54

5.3.5 Exergy Destruction Analysis

Figure 5.7(a) delineates the exergy destruction in various components of the refrigeration system, and Fig.5.7(b) presents the total exergy destruction.

The compressor displays the highest exergy destruction, while the condenser of DEC-SAC exhibits the lowest exergy destruction (Fig. 5.7(a)). Increases in both ambient temperature (T_a) and relative humidity (RH) contribute to the rise in exergy destruction, as depicted in Fig. 5.7(b). The difference in exergy destruction between CSAC and DEC-SAC becomes more apparent at elevated T_a levels across different *RH* levels. At an ambient temperature of 30°C, these variances range from 7.83% (80% *RH*) to 47.32% (20% *RH*), and the corresponding differences at T_a=45°C increase to 18.57% and 55.1%, respectively.

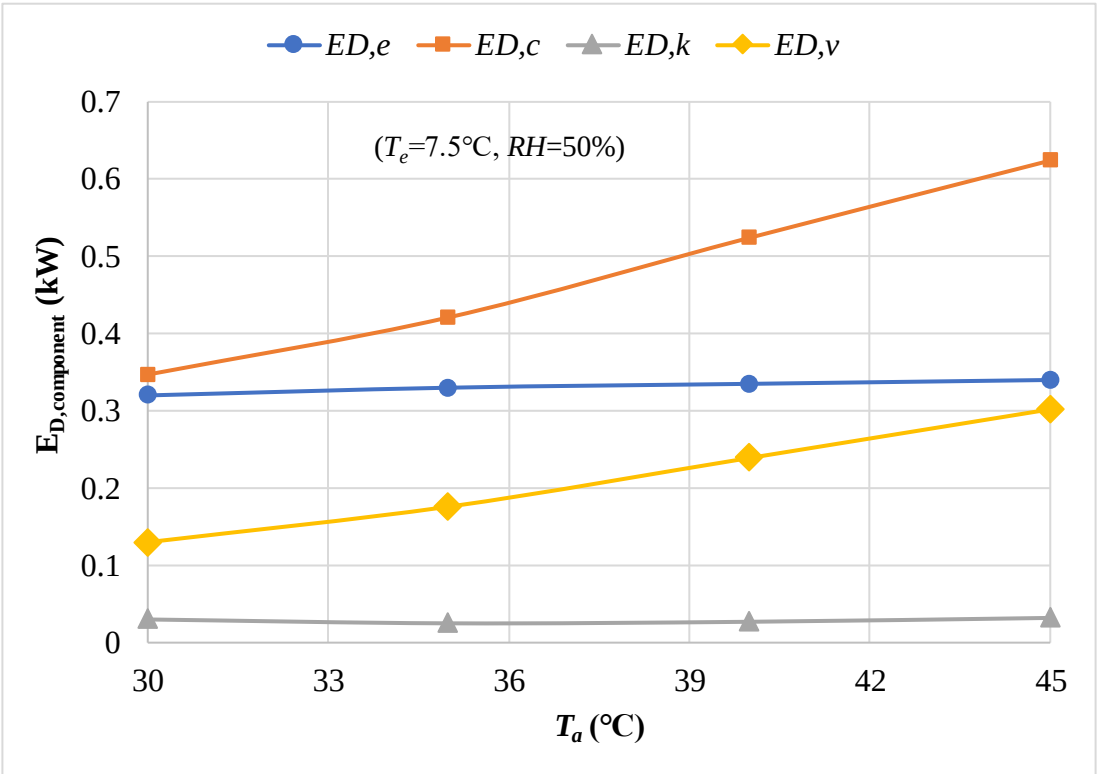

(a)

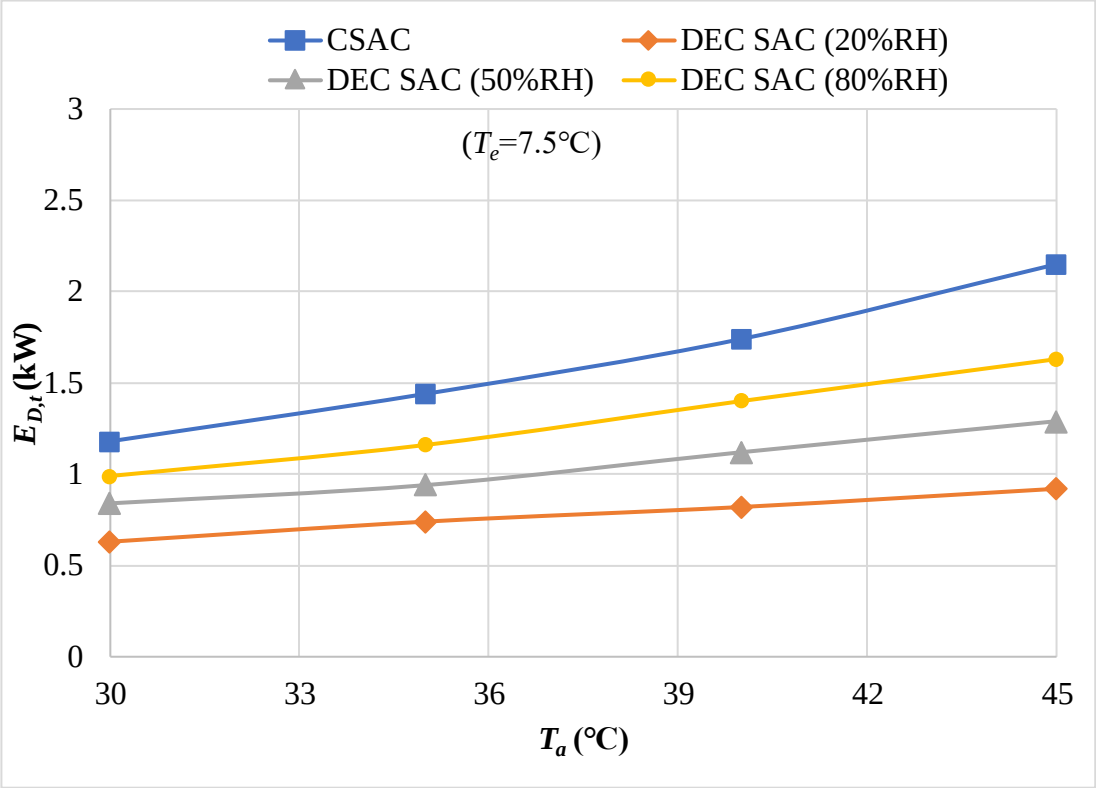

(b)

Fig.5.7 Variations in (a) $E_{D,component}$; (b) $E_{D,t}$, as a function of T_a

Table 5.4(a) displays the total exergy destruction in conventional and modified DEC-SAC. The total exergy destruction in DEC-SAC increases with RH. Accordingly, there is minimum decrease in $E_{D,t}$ (7.83%) at 80% RH, when T_a =30℃ and T_e = 3℃, while a maximum decrease in $E_{D,t}$ (55.1%) occurs at 20% RH, when T_a = 45℃ and T_e = 12℃.

Table 5.4(b) displays exergy destruction amount in different elements of the air conditioning system. The condenser of DEC-SAC shows highest reduction in exergy destruction (87.75%) compared to CSAC while expansion valve and compressor follow. The evaporator exhibits the minimum reduction (0.82%). However, all the components present minimum reductions in exergy destruction at

$T_e = 3$℃ and 80% RH, and the maximum reductions in exergy destruction are seen at $T_e = 12$℃ and 20% RH.

Table 5.4(a) Total exergy destruction (kW)

			($T_e = 3$℃)				($T_e = 12$℃)	
	CSAC		**DEC-SAC**		**CSAC**		**DEC-SAC**	
T_a(℃)		**20% RH**	**50% RH**	**80% RH**		**20% RH**	**50% RH**	**80% RH**
30	1.37	0.74	0.95	1.14	1.02	0.61	0.71	0.84
35	1.68	0.85	1.11	1.38	1.24	0.69	0.80	0.99
40	2.04	0.98	1.32	1.64	1.48	0.71	0.94	1.19
45	2.53	1.10	1.53	1.93	1.81	0.81	1.09	1.39

Table 5.4(b) Component wise exergy destruction (kW)

($T_e = 3$℃, $RH = 80$%)								
	CSAC				**DEC-SAC**			
T_a(℃)	$E_{D,e}$	$E_{D,c}$	$E_{D,k}$	$E_{D,v}$	$E_{D,e}$	$E_{D,c}$	$E_{D,k}$	$E_{D,v}$
30	0.357	0.589	0.176	0.255	0.354	0.496	0.085	0.202
35	0.362	0.754	0.218	0.353	0.358	0.648	0.125	0.289
40	0.366	0.953	0.253	0.471	0.363	0.784	0.130	0.369
45	0.371	1.208	0.313	0.645	0.366	0.942	0.157	0.465

Table 5.4(b) Continued….

				$(\boldsymbol{T_e = 12}$℃$\boldsymbol{, RH = 20}\%)$				
30	0.340	0.379	0.136	0.166	0.311	0.201	0.045	0.063
35	0.344	0.494	0.165	0.241	0.321	0.232	0.038	0.102
40	0.349	0.622	0.185	0.332	0.323	0.254	0.031	0.113
45	0.352	0.792	0.196	0.468	0.328	0.338	0.024	0.126

5.4 Sustainability Index

The higher sustainability indices signify lower levels of environmental degradation. Figures 5.8 (a) and (b) illustrate the impact of outdoor environment temperature and *RH* (with fixed T_e) on the sustainability indices of CSAC and DEC-SAC, respectively. The sustainability index clearly rises for DEC with an increase in ambient temperature. The index of DEC-SAC surpasses that of CSAC (Fig. 5.8(a)) at higher T_a (>37.5℃), possibly due to the enhanced evaporative cooling degree accompanying the rise in ambient temperature, leading to a greater temperature differential between the condenser and inlet air.

From Figure 5.8 (b), it is evident that the index of DEC-SAC increases with RH at high T_e (12℃), but the opposite trend is observed when T_e is low (3℃). However, a higher sustainability index is observed at T_e=3℃ compared to T_e=12℃ for both CSAC and DEC-SAC. The sustainability index of DEC-SAC increases by 6.01% to 44.18% compared to CSAC at different operating conditions.

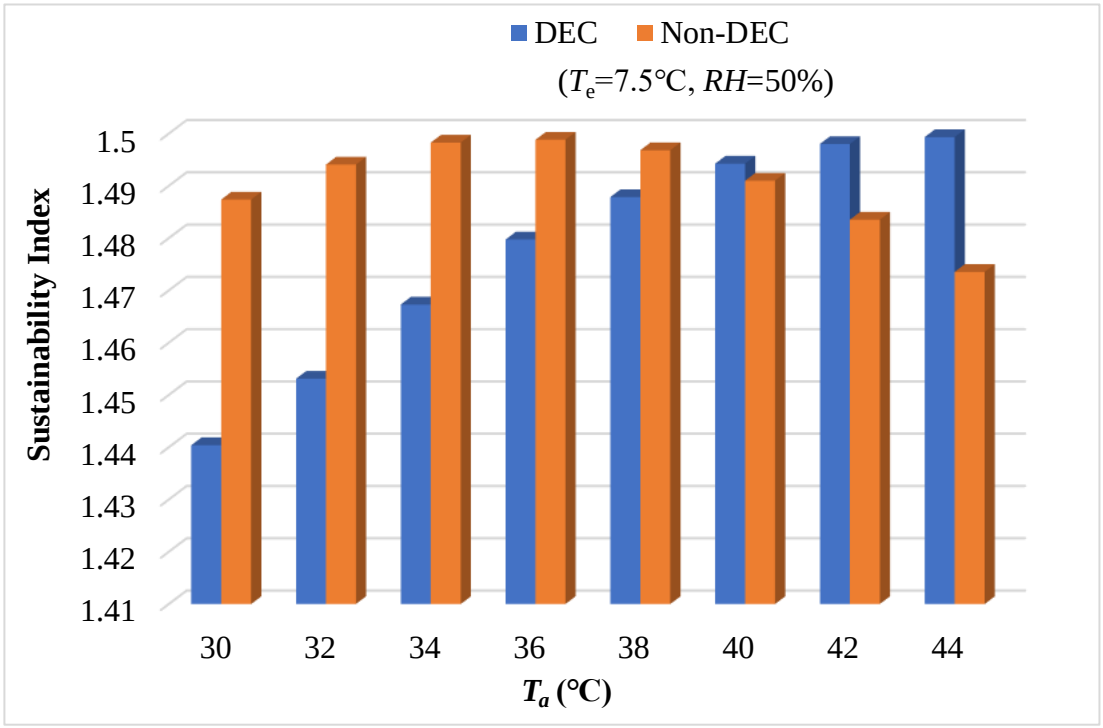

(a)

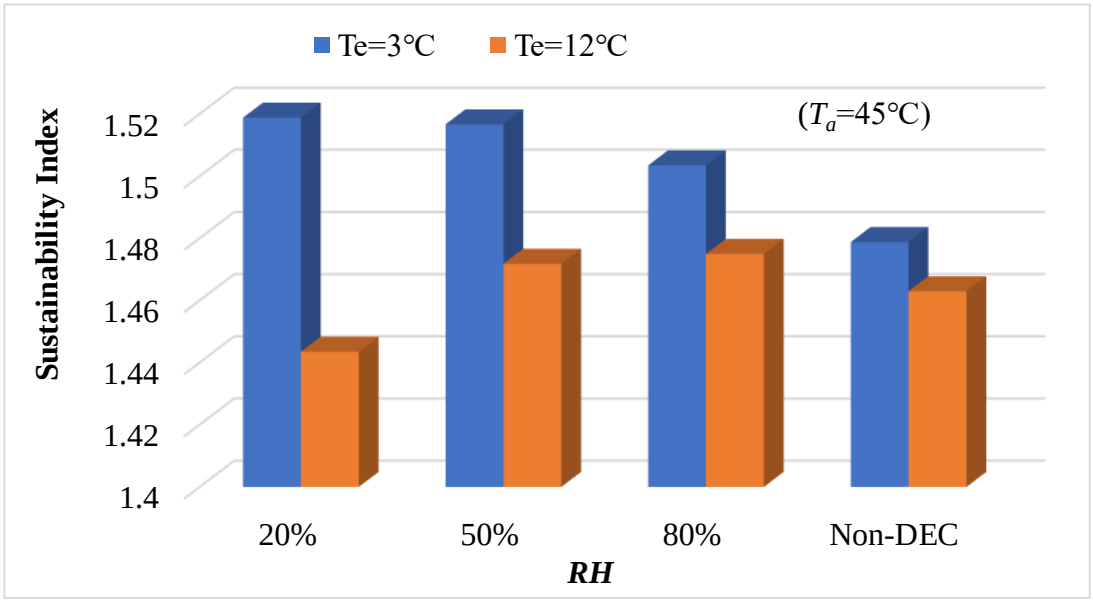

(b)

Fig. 5.8 Comparative sustainability index with and without evaporative cooling: (**a)** T_a varying, **(b)** RH varying

5.5 Daily and Monthly Analysis

The following sub section investigates the daily and monthly variation in various outputs of DEC-SAC with that of CSAC for New Delhi, India in particular. The climatic conditions of New Delhi with mean outdoor situations during various cooling periods are as illustrated in Fig. 5.9 [129].

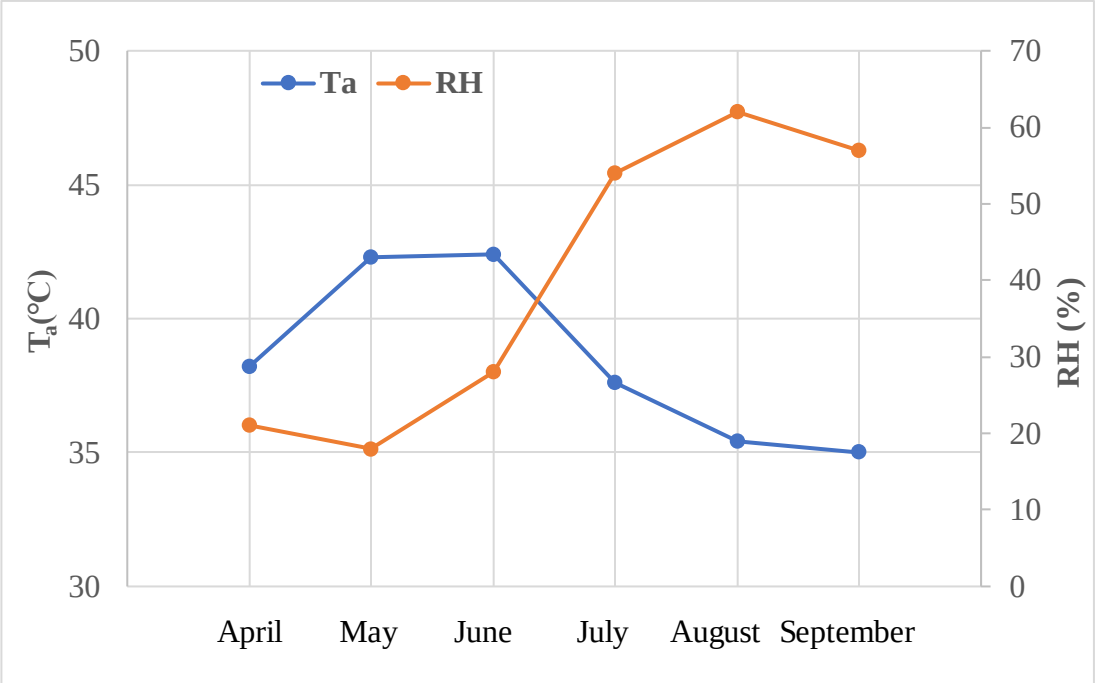

Fig.5.9 Monthly average ambient conditions for New Delhi, India [130]

Figures 5.10 (a) to (c) illustrate the hourly variations in COP, TCR, and $E_{D,t}$ employing the DEC-SAC system against conventional SAC for the 20th day of each month of the cooling period. The lower hourly variation in ΔCOP is in the month of April and higher variations are seen for the months of May and September. In April, the average temperature and relative humidity variations during the day are small. Large temperature variations are seen for the month of May while large relative humidity variations are present in the month of September.

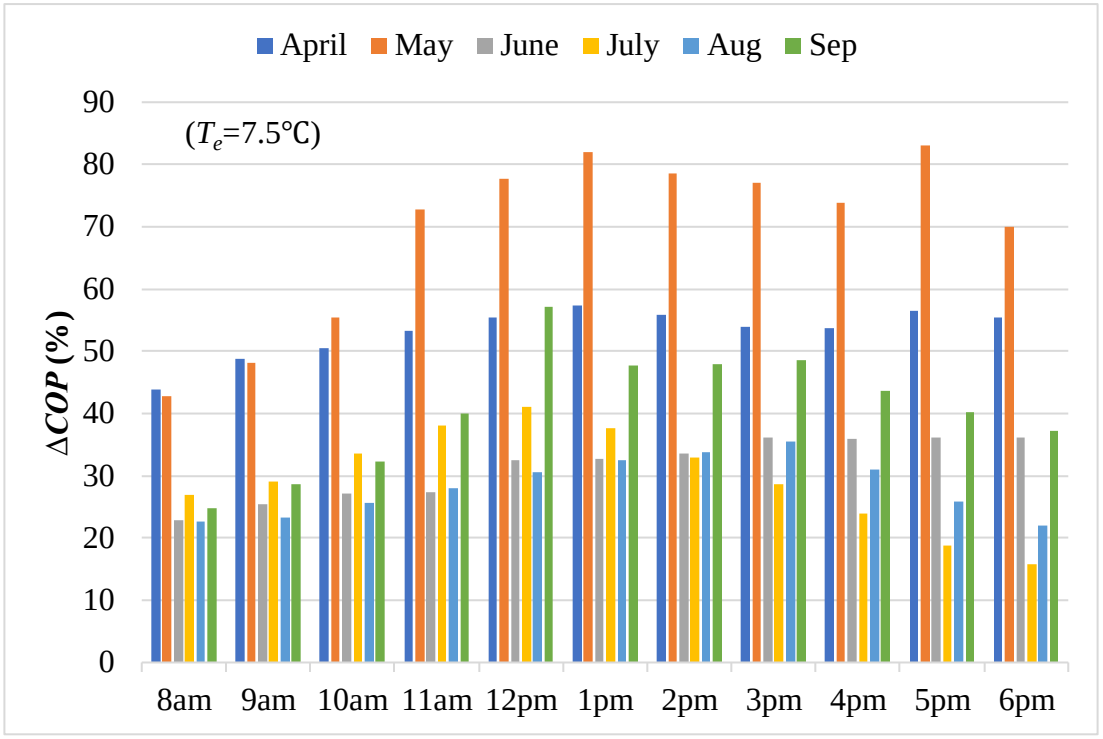
April
May
June
July
Aug
Sep
(T_e=7.5℃)
ΔCOP (%)
90
80
70
60
50
40
30
20
10
0
8am
9am
10am
11am
12pm
1pm
2pm
3pm
4pm
5pm
6pm

(a)

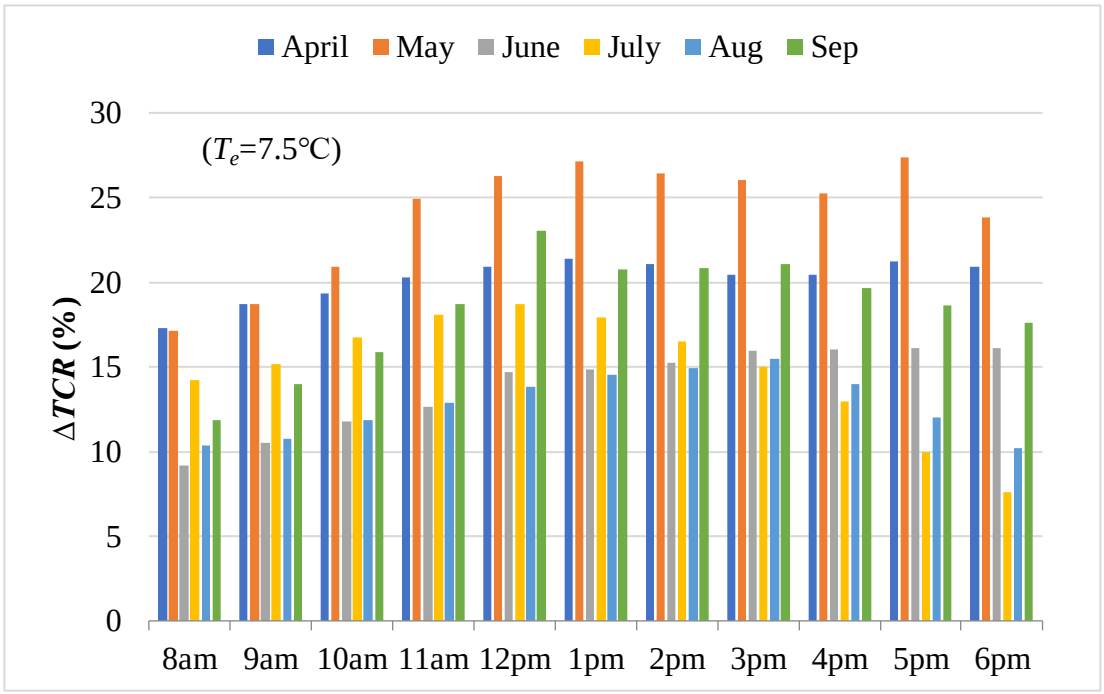
April
May
June
July
Aug
Sep
(T_e=7.5℃)
ΔTCR (%)
30
25
20
15
10
5
0
8am
9am
10am
11am
12pm
1pm
2pm
3pm
4pm
5pm
6pm

(b)

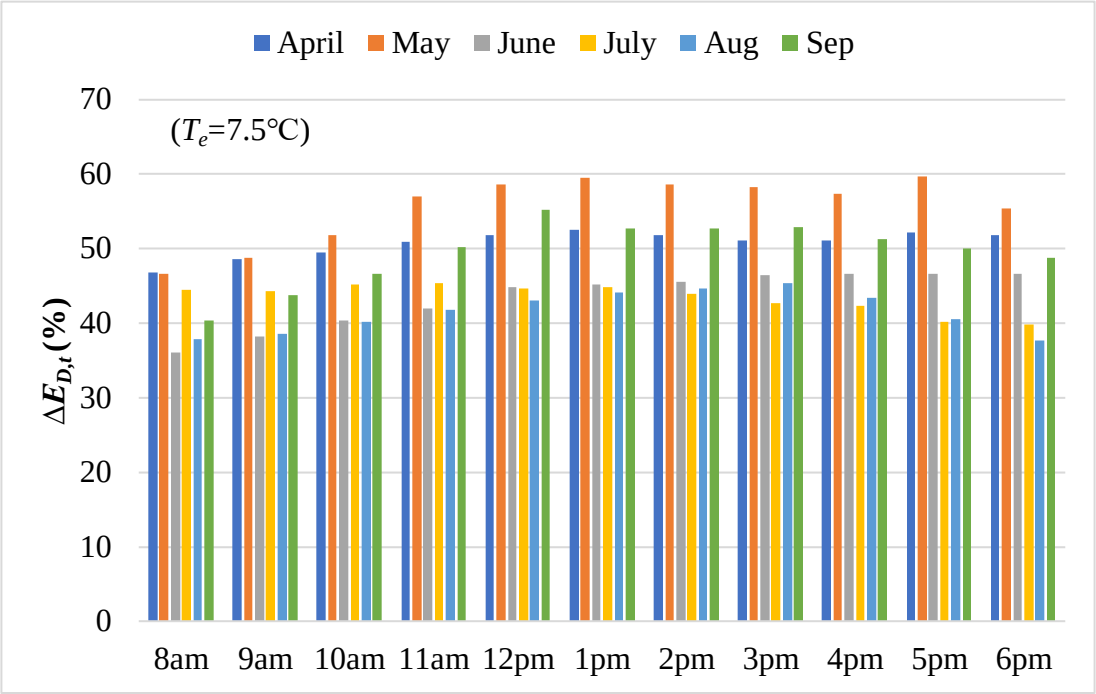

(c)

Fig.5.10 Hourly variations in **(a)** COP, **(b)** TCR, and **(c)** $E_{D,t}$, respectively on 20th day of each month

Figure 5.11 presents the monthly fluctuations in ΔCOP, ΔTCR, and $\Delta E_{D,t}$ using the DEC-SAC for each month of the cooling period. The highest improvement in COP (65.21%) is achieved in hot-dry month of May and the minimum COP enhancement (3.53%) is observed in the most warm and humid month of August. In May, the average ambient temperature within New Delhi approaches 42.3°C with a mean RH of 18%, while in August, the average temperature is 35.4°C with an RH of 62%. Consequently, the COP improvement is more significant in May compared to August, as explained above. At mean evaporator temperature ($T_e = 7.5$°C), the highest saving in TCR is 21.41% and the minimum is 9.11% in the months of May and August,

respectively. Similarly, maximum decrease (49.65%) in $E_{D,t}$ is in May and the minimum drop (24.12%) is in August.

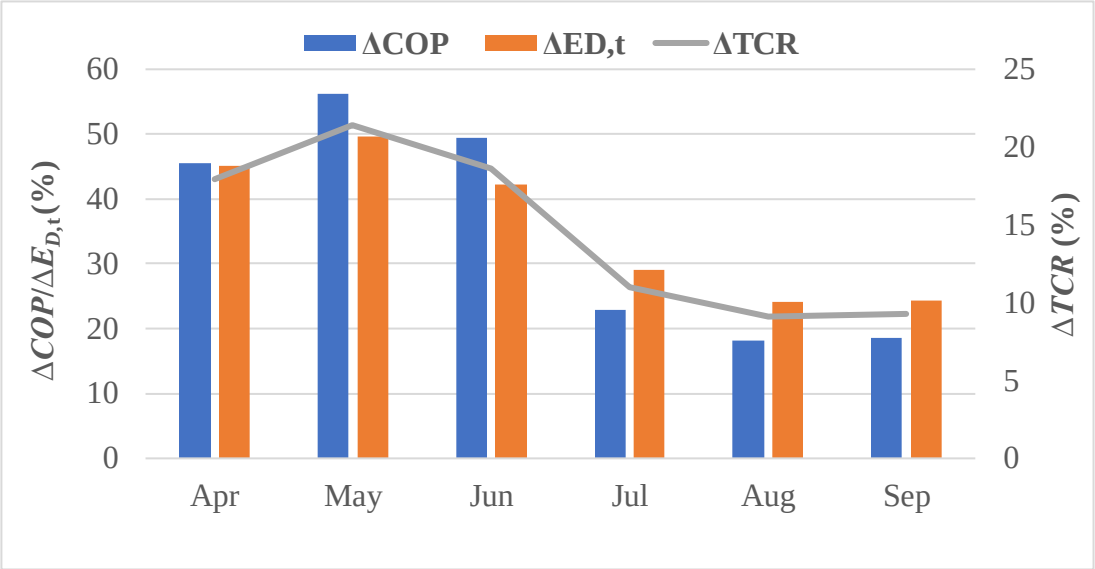

Fig.5.11 Monthly variations in COP, TCR, and $E_{D,t}$ during the cooling season

5.6 Economic Analysis

This segment discusses the economic audit of the proposed system with input parameters ranging from $T_e = 3℃\ to\ 12℃$, T_a=30℃ to 45℃, and RH=20% to 80%.

5.6.1 Operating Cost Analysis

The results of parametric variations on operating cost are analyzed in this section.

With a constant condenser temperature, an elevated evaporator temperature (T_e) brings about a reduction in the compression ratio. This consequent decrease in $\Delta T_{LM\,e}$ leads to an expanded evaporator area. The decrease in compressor input lowers the operating cost, while the enlargement of the evaporator area raises the investment

cost. Nonetheless, the impact of the investment cost is less pronounced compared to that of the operating cost, resulting in an overall cost reduction. A lower ambient temperature is advantageous both from a thermodynamic and economic standpoint. However, considering climate conditions, striking a balance is essential to determine the optimal value.

Fig. 5.12 (a) and (b) show the variations in operating cost savings for DEC-SAC over CSAC under different temperature and humidity. As depicted by Figures, more savings are obtained with the increase in T_a, while drastic reduction is seen in the savings when relative humidity increases. The reason being the increased outside temperature, the compressor works for increased duration so as to make the system achieve the set temperature desired in the cooling room. This is because of the higher temperature differential between the cooling room and outside environment. The lowest saving in the operating cost is 12.12% when T_a=30℃, *RH*=80% and T_e=3℃. The highest saving of 47.17% in operating cost is achieved at T_a=45℃, *RH*=20% and T_e=12℃.

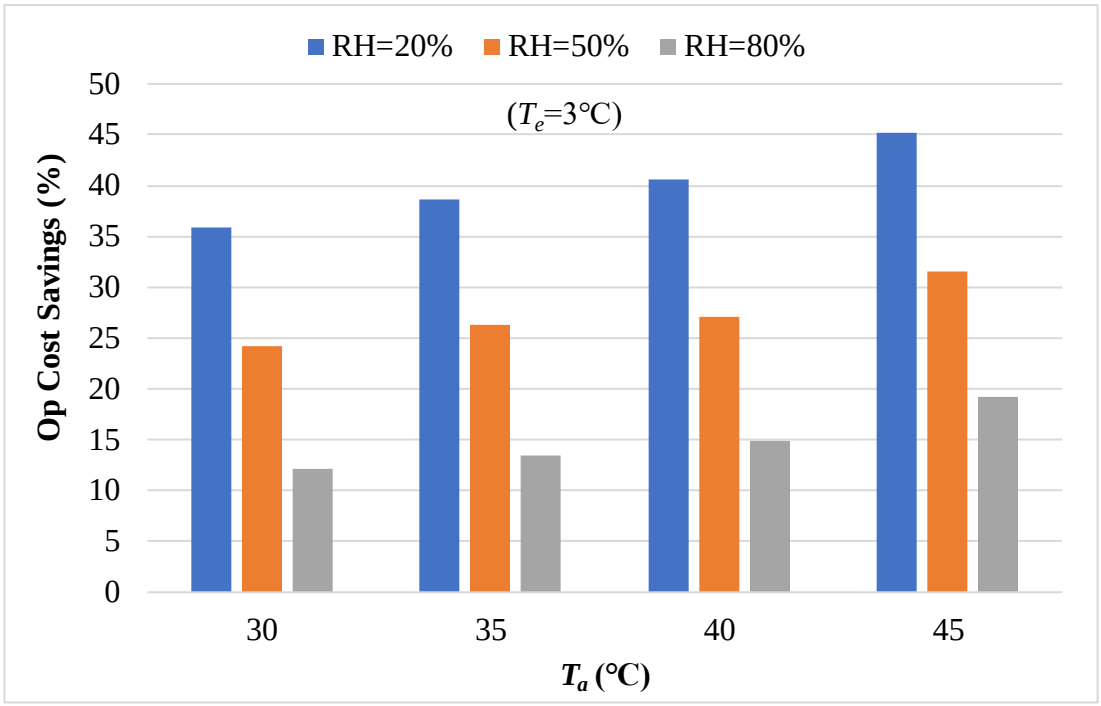

(a)

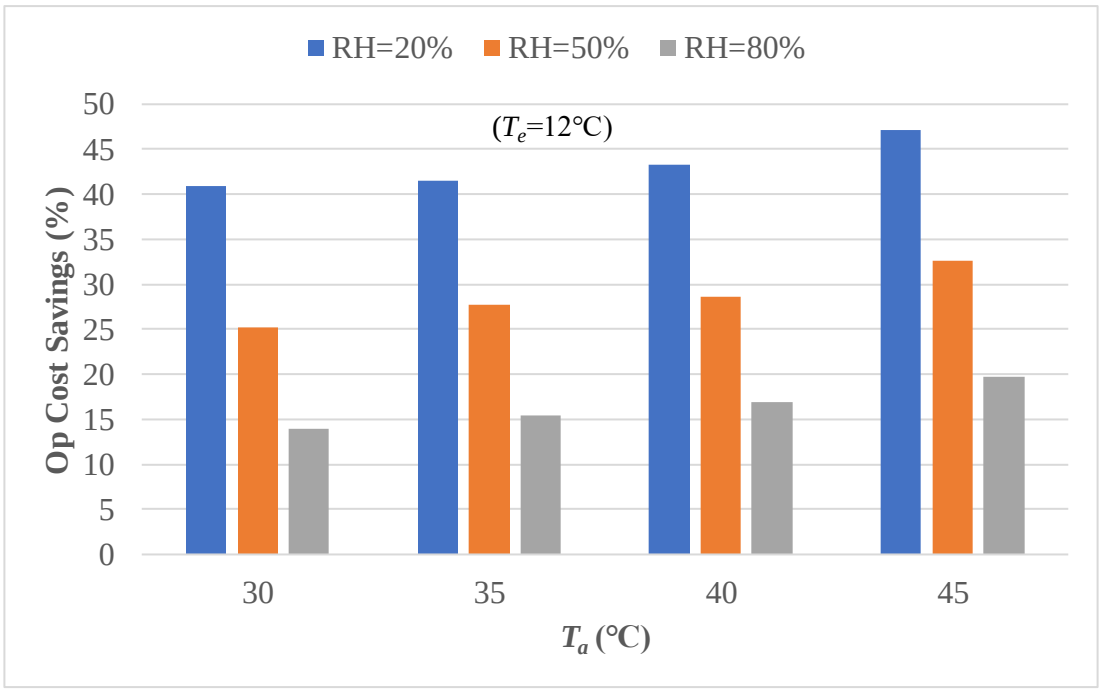

(b)

Fig.5.12 Operational cost savings corresponding to ambient temperature at (a) T_e = 3℃, (b) T_e = 12℃

Operational costs are influenced by ambient conditions, specifically the air temperature and relative humidity (*RH*), calculated with electric energy costing ₹7.5/kWh per kWh. The annual operational cost ranges from ₹11,469 to ₹28,790, with notable effects resulting from changes in operating parameters. An uptick in ambient temperature from 30°C to 45°C (*RH*=20%) raises the operating cost from ₹11,469 to ₹20,459, while an increase in *RH* from 20% to 80% (T_a=45°C) results in an operating cost hike from ₹16,485 to ₹28,790. Elevations in both T_a and *RH* lead to an increase in the operating cost, whereas a rise in T_e reduces the operating cost of the DEC-SAC.

5.6.2 Cost Benefit Analysis

The DEC-SAC system's investment cost varies between ₹68,223 and ₹1,02,209, depending on the heat exchanger area. The net present value (NPV) spans from ₹2,39,265 to ₹4,09,675 for average environmental situations (T_a=37.5°C, *RH* =50%). It is minimum for $T_e = 12$°C, and largest for $T_e = 3$°C. As far as the internal rate of return (IRR) is concerned, the range is from 27% ($T_e = 12$°C) to 59% ($T_e = 3$°C), and the simple payback period (SPP) ranges between 1.21 years ($T_e = 3$°C) to 2.99 years ($T_e = 12$°C). Table 5.5 presents the NPV, IRR, and SPP at T_a=37.5°C.

Table 5.5 Cost benefits of the proposed system at T_a=*37.5℃*

T_e (℃)	RH (%)	NPV (₹)	IRR (%)	SPP (Years)
3	20	512395	59	1.21
3	50	409676	47	1.55
3	80	302335	36	2.06
12	20	318273	44	1.66
12	50	239265	35	2.18
12	80	160260	27	2.99

5.7 Environmental Consideration

Table 5.6 presents the monthly energy cuts for cooling period at T_e=3℃ and 12℃. The highest amount of energy saved is 41.23% which is achieved at ambient conditions (T_a=45℃, RH=20%, T_e=3℃), while the minimum savings of energy is observed as 9.54% at (T_a=30℃, RH=80%, T_e=12℃). It may be noted that the months of April to June are very hot and dry, hence high temperature drop is achieved leading to more effective evaporative cooling than the months of more humid climate, i.e., July to September. Consequently, compressor work duration is decreased for lower condenser inlet temperature and hence maximum energy savings (46.59%) are accounted for the hot and dry month of April when T_e is maintained at 12℃. The reason for the energy-saving effect by altering the condenser temperature can also be described by the compression ratio. Lower average compression ratio of the SAC is observed during the hot-dry months when the DEC process is performed. Therefore, the energy is saved during DEC operation because the reduction in the SAC

compression ratio directly affects the input air. This indicates that under high relative humidity conditions, energy savings declined. For the above stated reason, the lowest energy savings of 19.54% are accumulated in the most humid month of August.

Table 5.6 Month wise energy consumption in kWh for conventional and DEC SAC in the climate of New Delhi, India

T_e	System	April	May	June	July	August	September
3℃	CSAC	708.62	772.56	775.22	642.02	583.41	578.08
3℃	DEC SAC	404.92	447.55	451.21	489.11	469.39	447.55
Monthly Savings		**303.7**	**325.01**	**324.01**	**152.91**	**114.02**	**130.53**
12℃	CSAC	508.82	566.10	566.63	460.33	415.05	413.18
12℃	DEC SAC	271.72	307.95	308.22	333	320.47	307.95
Monthly Savings		**237.1**	**258.15**	**258.41**	**127.33**	**94.58**	**105.23**

Under average ambient conditions (T_a=37.5℃, RH=50%), increasing the evaporator temperature from 3℃ to 12℃ results in a reduction in annual energy savings from 1014.4kWh to 770.4kWh. The CO_2 emission factor is 0.82kg/kWh in Indian context, leading to a decrease in equivalent CO_2 emissions from 831.8kg/year to 631.7kg/year.

One unit of DEC-SAC running at evaporator temperature, T_e=7.5℃, is projected to deliver an average of 892.4kWh electric energy savings in a year and lower CO_2 emissions by approximately 731.7kg/year, assuming it operates for 1600

hours during the cooling period. The quantity of CO_2 emissions is remarkably influenced by operational variables.

According to a report, approximately 2.2×10^7 air conditioning units are estimated to be put in for residential sector in India [7]. Therefore, for mean environmental conditions and T_e=7.5℃, the proposed system could potentially result in an annual energy saving of around 19.6TWh. These substantial energy savings have the potential to mitigate approximately 16.1×10^9kg of CO_2 emissions, contributing to environmental preservation.

5.8 Impact on Water Usage by the Proposed System

Based on the preceding discourse, it is clear that DEC-SAC is most suitable for high temperature and low relative humidity (hot-dry) situations. Assessing water accessibility in such situations is crucial. Water consumption is directly proportional to the water vaporization rate, and computed as follows:

$$d\dot{m}_w = \frac{h_m.\xi.B.H.\delta.(T_a - T_w)}{L_w} \times 3600 \text{kg h}^{-1} \quad (5.1)$$

At environment temperatures of 30℃, 35℃, 40℃, and 45℃ (with *RH* at 20%), the hourly water consumptions are estimated as 6150ml, 6920ml, 7740ml, and 8510ml, respectively. Simultaneously, the hourly power savings at T_e=3℃, are found to be 625W, 835W, 1065W, and 1460W, respectively. The corresponding power savings at T_e=12℃ are 490W, 617W, 807W, and 1093W, respectively. For *RH* =80% and T_e=3℃ the hourly water consumptions are noted as 1247ml, 1376ml, 1505ml, and 1591ml, with hourly power savings of 225W, 251W, 382W, and 612W, respectively. The corresponding power savings at T_e=12℃ are 158W, 239W, 282W, and 450W, respectively.

With a low makeup water requirement (approximately 11-76L per day), the proposed system appears well-suited for countries with very hot and/or humid climates such as India, Saudi Arabia, Brazil, etc. The comparison of monthly water consumption (MWC) and monthly energy savings (MES) for different months of the cooling season is illustrated in Fig. 5.13. The maximum energy savings of ₹2236.15 are achieved in May, while the minimum energy savings of ₹745.38 are observed in August.

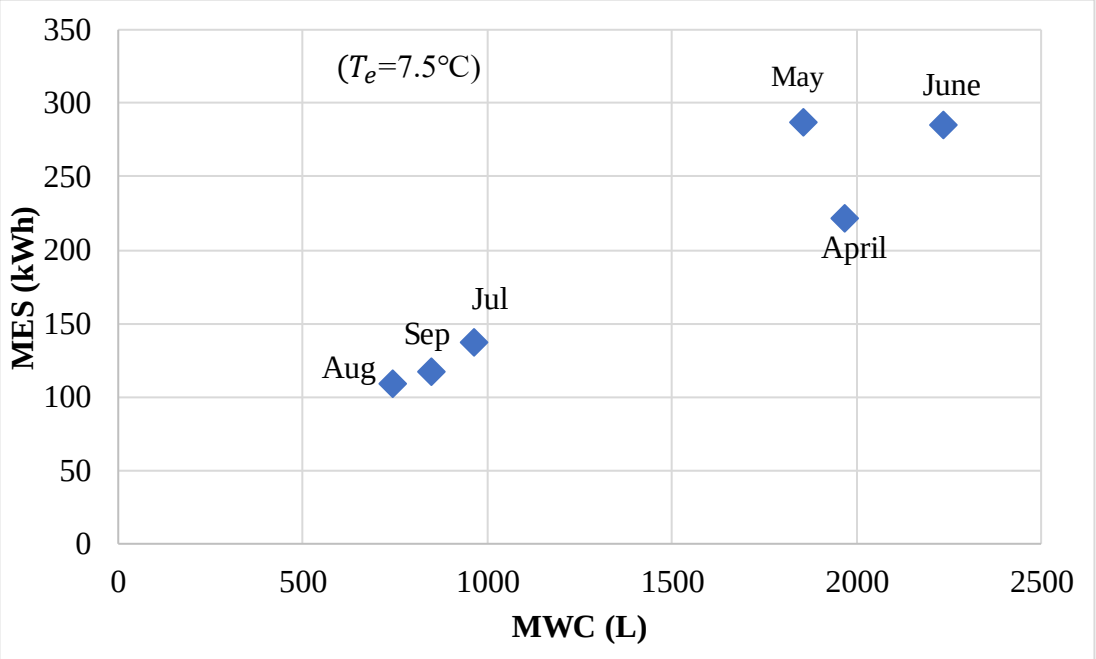

Fig.5.13 Monthly energy savings and water consumption at $T_e = 7.5℃$

5.8.1 Impact on energy/water costs

The ratio of water consumed to energy-saved at $T_e = 3℃$ and $12℃$ is represented by Fig.5.14 (a) and (b), respectively. The minimum ratio of water

consumed to energy-saved (5.5L/kWh) is seen in hot-humid climate (June), while the highest (9.8L/kWh) is in hot-dry situation (April). The highest water cost (₹74.46) is incurred in May, presumably due to the extremely hot as well as dry condition.

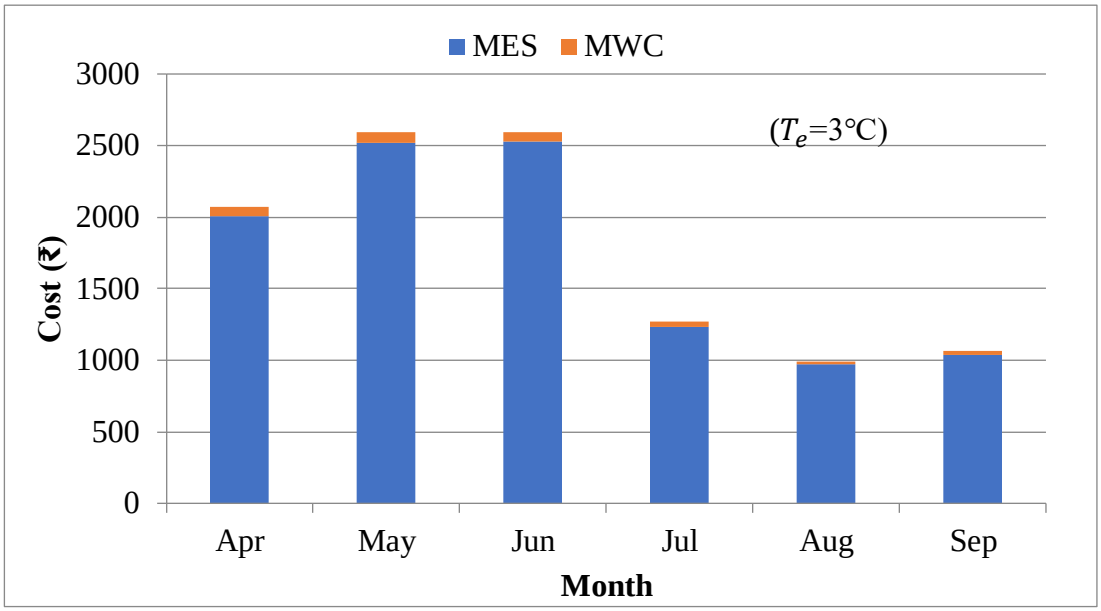

(a)

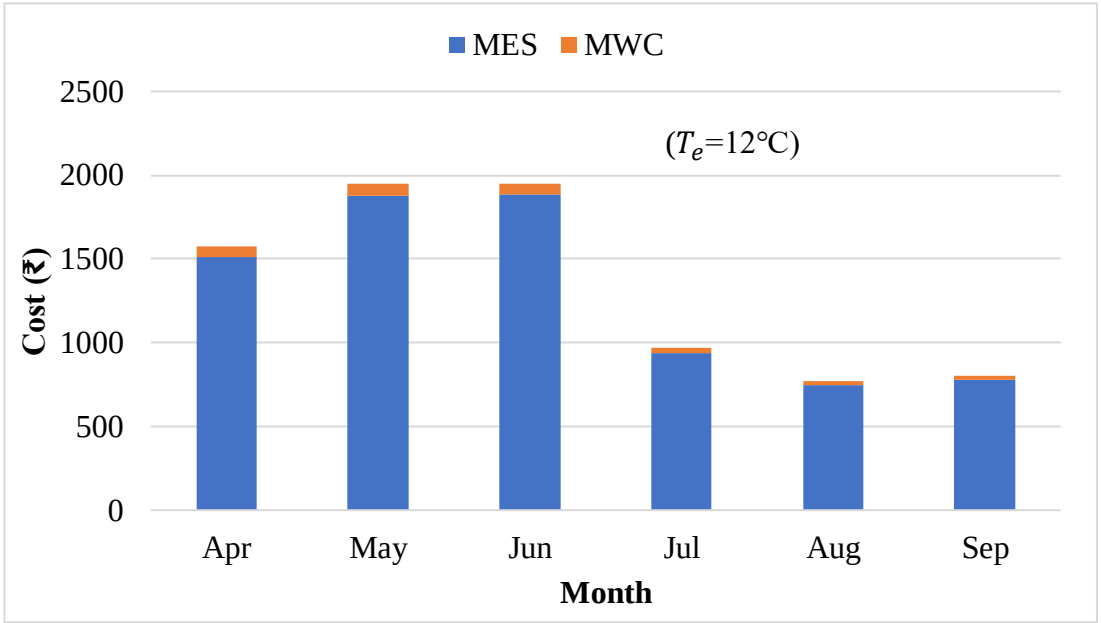

(b)

Fig.5.14 Comparison of monthly energy savings and water costs at (a) $T_e = 3℃$ and (b) $T_e = 12℃$

5.9 Optimization Using Box-Behnken Design Methodology

The Box-Behnken design, integrated into the Design Expert software, optimizes the three control factors – $T_a, RH,$ and T_e - concurrently to maximize the objective function COP and minimize TCR. COP gauges cycle performance, serving as a basis for efficient energy utilization, while TCR determines the economic efficiency of the system. Utilizing the Box-Behnken design technique ensures obtaining optimum response values, with equal consideration given to all control factors and responses.

Table 5.7(a) outlines the optimization criteria for DEC-SAC, while Table 5.7(b) presents individual optimal solutions for various choices. Thermodynamic optimization results in the highest COP enhancement for DEC-SAC over CSAC. Notably, optimizing the system economically decreases the total cost rate (maximized ΔTCR) as well as diminishes exergy destruction in DEC-SAC (maximized $\Delta E_{D,t}$). Thermoeconomic optimization achieves maximized outputs at an extreme ambient condition: (T_a=45℃, RH =20%).

Table 5.7(a) Multi objective optimization criteria

Parameter	Criteria	Lower Limit	Upper Limit	Lower Weight	Upper Weight	Importance
T_a(℃)	is in range	30	45	1	1	3
RH (%)	is in range	20	80	1	1	3
T_e(℃)	is in range	3	12	1	1	3

Table 5.7(b) Multi objective optimization results

Goal	T_a(℃)	RH (%)	T_e(℃)	$(+)\Delta COP$ (%)	$(-)\Delta TCR$ (%)	$(-)\Delta E_{D,t}$ (%)
Thermodynamic	45	20	4.4	64.45	22.34	54.45
Economic	45	20	5.5	63.84	23.15	54.51
Thermoeconomic	45	20	4.4	64.23	22.91	54.42

5.10 Payback of DEC-SAC System

The payback period calculation for the proposed DEC-SAC system considers the following parameters:

Ambient temperature (T_a) = 37.5℃ and relative humidity (RH) at 50% (average operating condition).

Saturation efficiency of the cooling pad is set at 0.65 [79],

Annual operation of the air conditioner is estimated at 1600 hours [125].

The unit cost of electrical energy is ₹7.5 based on average electricity tariff in New Delhi as on 1st January,2024.

The total modification cost includes structure and piping cost (₹4500), pump cost (₹150), and cooling pad cost (₹100). The approximate cost of running the 12W pump for 1600 hours is ₹150. Assuming negligible water cost, the total cost of the DEC system is approximately ₹4900. The total annual electrical energy savings amount to 224kWh. Consequently, the cost of the DEC system could be recovered within 2.9 years.

CHAPTER 6

CONCLUSIONS AND DIRECTIONS FOR FUTURE RESEARCH

This chapter summarizes the main findings of the study and indicates directions for future research work.

6.1 Conclusions

In this study, we explore the thermo-economics-based performance of a split air conditioner utilizing a direct evaporative cooler (DEC) in comparison to a conventional split air conditioner (CSAC). Through multi-objective optimization, the Box-Behnken design technique is employed to identify the optimal solution among conflicting objective functions. The key findings of the investigation are summarized as follows:

1. The performance of DEC-SAC is enhanced with increased evaporative cooling, particularly effective in hot-dry conditions with high ambient temperature (T_a) and low relative humidity (RH). Notably, the maximum and minimum reductions in ambient temperature are observed as 14℃ (T_a=45℃, RH=20%) and 3℃ (T_a=30℃, RH =80%), respectively.
2. The goodness-of-fit evaluation, represented by close matches between R^2 values for the data set and R_a^2 values, confirms the suitability of the second-order polynomial quadratic equation for modeling. The proposed model establishes a robust relationship between simulated and predicted data points.

3. The *COP* of the DEC-SAC system improves by 3.53% (T_a=30℃, RH =80%, T_e=12℃) to 65.21% (T_a=45℃, RH =20%, T_e=3℃), leading to a corresponding reduction in *TCR* ranging from 2.23% to 23.20%. DEC-SAC consistently outperforms CSAC across the entire range of input parameters. Ambient temperature emerges as the most influential factor.
4. Employing DEC-SAC results in highest monthly energy savings of 325.01kWh at T_e=3℃ in hot-dry condition (May month), while the minimum monthly energy savings of 94.58kWh at T_e=12℃ occur in the most humid condition (August month). Corresponding energy saving to water cost ratios are 40.92 and 29.97. At the mean evaporator temperature (T_e=7.5℃), DEC-SAC could save 892.4kWh electric energy and 731.7kg of CO_2 in a year against CSAC.
5. The sustainability index increases with rising ambient temperature, with DEC-SAC sustainability indices being 7.08% to 44.18% higher than those of CSAC for the given input parameters.
6. Multi-objective optimization of DEC-SAC yields the optimum outputs. Thermo-economically optimized system is obtained at T_a=45℃, RH =20%, and T_e=4.4℃, achieving maximized *COP* enhancement (64.23%), reduced *TCR* (22.91%), and decreased $E_{D,t}$ (54.45%).
7. The estimated NPV, IRR, and SPP for the DEC-SAC system at T_a=37.5℃, varying T_e from 3℃ to 12℃, and RH from 20% to 80% are ₹5,12,395-₹1,60,260, 59%-27%, and 1.21-2.99 years, respectively.
8. The cost of the proposed system is recoverable within 2.9 years, considering the average operating parameters.

In conclusion, the DEC significantly enhances the thermodynamic output of the SAC under all climate conditions, with optimal effectiveness observed when outdoor temperatures are elevated and relative humidity is low.

6.2 Suggestions/Directions for Future Research

1. Passive cooling methods may be explored to decrease indoor cooling load which will reduce energy demand.
2. Some electronic device may be introduced to automatically switch off/on the water circulating pump and fan when the compressor stops/starts.
3. The system may be modified so that some of the cool air from DEC is allowed to enter the cooling room, especially in hot-dry season to reduce cooling load on the air conditioner.
4. Experiments may be carried out in different cities to obtain actual results in real environment.

REFERENCES

[1] X. She *et al.*, "Energy-efficient and -economic technologies for air conditioning with vapor compression refrigeration: A comprehensive review," *Appl. Energy*, vol. 232, no. April, pp. 157–186, 2018, doi: 10.1016/j.apenergy.2018.09.067.

[2] A. Sethi, E. Vera Becerra, S. F. Yana Motta, and M. W. Spatz, "Low GWP R22 replacement for air conditioning in high ambient conditions," *Int. J. Refrig.*, vol. 57, pp. 26–34, 2015, doi: 10.1016/j.ijrefrig.2015.05.013.

[3] Z. F. Dupont J. L., Domanski P., Lebrun P., "38th Informatory Note on Refrigeration Technologies - The Role of Refrigeration in the Global Economy," 2019. doi: http://dx.doi.org/10.18462/iif.NItec38.06.2019.

[4] Y. H. Yau and H. L. Pean, "The performance study of a split type air conditioning system in the tropics, as affected by weather," *Energy Build.*, vol. 72, no. 2014, pp. 1–7, 2014, doi: 10.1016/j.enbuild.2013.12.010.

[5] J. Singh, S. S. Mantha, and V. M. Phalle, "Energy & Buildings Characterizing domestic electricity consumption in the Indian urban household sector," vol. 170, pp. 74–82, 2018, doi: 10.1016/j.enbuild.2018.04.002.

[6] K. Srithar, T. Rajaseenivasan, M. Arulmani, R. Gnanavel, M. Vivar, and M. Fuentes, "Energy recovery from a vapour compression refrigeration system using humidi fi cation dehumidi fi cation desalination," *Desalination*, vol. 439, no. March, pp. 155–161, 2018, doi: 10.1016/j.desal.2018.04.008.

[7] F. and C. C. Ministry of Environment and Government of India, “India Cooling Action Plan (ICAP): Operationalizing Space Cooling Recommendations,” 2019. [Online]. Available: http://ozonecell.nic.in/wp-content/uploads/2021/10/India-Cooling-Action-Plan-Booklet-SP.pdf

[8] B. A. Qureshi and S. M. Zubair, “Performance degradation of a vapor compression refrigeration system under fouled conditions ´ rioration de la performance d ’ un syste ` me frigorifique a compression de vapeur sous des conditions d ’ encrassement,” *Int. J. Refrig.*, vol. 34, no. 4, pp. 1016–1027, 2011, doi: 10.1016/j.ijrefrig.2011.02.012.

[9] G. Bejarano, J. A. Alfaya, M. G. Ortega, and M. Vargas, “On the difficulty of globally optimally controlling refrigeration systems Number of Transfer Units,” *Appl. Therm. Eng.*, vol. 111, pp. 1143–1157, 2017, doi: 10.1016/j.applthermaleng.2016.10.007.

[10] N. Shah, W. Y. Park, and C. Ding, “Trends in best-in-class energy-efficient technologies for room air conditioners,” *Energy Reports*, vol. 7, pp. 3162–3170, 2021, doi: 10.1016/j.egyr.2021.05.016.

[11] I. E. A. IEA, “Market Report Series energy efficiency 2018,” 2018. [Online]. Available: https://www.iea.org/reports/energy-efficiency-2018

[12] Y. Yao, Z. Zhang, and X. Hu, “Experimental contrast on the cooling performance of direct evaporative all fresh air handling units with R32 and R410A,” *Procedia Eng.*, vol. 205, pp. 802–809, 2017, doi: 10.1016/j.proeng.2017.10.013.

[13] V. H. Panato, M. P. Porto, and E. P. B. Filho, “Experimental performance of an R-22-based refrigeration system for use with R-1270 , R-438A , R-404A and R-134a Performance expérimentale d ’ un système frigorifique au R-22 en vue de son fonctionnement avec du R-1270 , du R-438A , du R-404A et du R-134a,” *Int. J. Refrig.*, vol. 83, pp. 108–117, 2017, doi: 10.1016/j.ijrefrig.2017.07.010.

[14] D. Sánchez *et al.*, “Energy performance evaluation of R1234yf , R1234ze (E), R600a , R290 and R152a as low-GWP R134a alternatives Évaluation de la performance énergétique du R1234yf , du R1234ze (E), du R600a , du R290 et du R152a comme alternatives à faible GWP au R134a,” *Int. J. Refrig.*, vol. 74, no. 2017, pp. 269–282, 2017, doi: 10.1016/j.ijrefrig.2016.09.020.

[15] R. Ben Jemaa, R. Mansouri, I. Boukholda, A. Bellagi, and U. R. Thermique, “ScienceDirect Energy and exergy investigation of R1234ze as R134a replacement in vapor compression chillers,” *Int. J. Hydrogen Energy*, vol. 42, no. 17, pp. 12877–12887, 2016, doi: 10.1016/j.ijhydene.2016.12.010.

[16] S. Daviran, A. Kasaeian, S. Golzari, O. Mahian, S. Nasirivatan, and S. Wongwises, “A comparative study on the performance of HFO-1234yf and HFC-134a as an alternative in automotive air conditioning systems,” *Appl. Therm. Eng.*, vol. 110, pp. 1091–1100, 2017, doi: 10.1016/j.applthermaleng.2016.09.034.

[17] C. Yıldırım, D. B. Özkan, and C. Onan, “Theoretical study of R32 to replace R410A in variable refrigerant flow systems,” *Int. J. Ambient Energy*, vol. 39, no. 1, pp. 87–92, 2018, doi: 10.1080/01430750.2016.1269682.

[18] X. Xu, Y. Hwang, and R. Radermacher, “Performance comparison of R410A and R32 in vapor injection cycles,” *Int. J. Refrig.*, vol. 36, no. 3, pp. 892–903, May 2013, doi: 10.1016/j.ijrefrig.2012.12.010.

[19] B. O. Bolaji and Z. Huan, “Computational analysis of the performance of ozone-friendly R22 alternative refrigerants in vapour compression air-Conditioning systems,” *Environ. Prot. Eng.*, vol. 38, no. 4, pp. 41–52, 2012, doi: 10.5277/EPE120404.

[20] A. Kumar and R. C. Gupta, “Impact Factor: 1.852 A Performance of a Window Air Conditioner Using Alternative Refrigerants R22 AND R410A,” *C) Int. J. Eng. Sci. Res. Technol.*, vol. 2, no. 7, pp. 1842–1848, 2013.

[21] P. A. Domanski, D. Yashar, and M. Kim, “Performance of a finned-tube evaporator optimized for different refrigerants and its effect on system efficiency * ´ vaporateur a ` tubes a ` ailettes optimise ´ pour Performance d ’ un e ` nes et impact sur l ’ efficacite ´ du syste ` me plusieurs frigor,” vol. 28, pp. 820–827, 2005, doi: 10.1016/j.ijrefrig.2005.02.003.

[22] S. Bobbo *et al.*, “Energetic and Exergetic Analysis of Low Global Warming Potential Refrigerants as Substitutes for R410A in Ground Source Heat Pumps,” *Energies*, vol. 12, no. 18, 2019, doi: 10.3390/en12183538.

[23] N. Zheng, Y. Hwang, and L. Zhao, “Thermodynamic Performance Assessment of R32 and R1234yf Mixtures as Alternatives of R410A,” *12th IEA Heat Pump Conf. 2017*, no. May, pp. 1–8, 2017, [Online]. Available: http://hpc2017.org/wp-content/uploads/2017/05/O.4.1.2-Thermodynamic-

Performance-Assessment-of-R32-and-R1234yf.pdf

[24] C. E. Vincent and M. K. Heun, “Thermoeconomic Analysis & Design of Domestic Refrigeration Systems,” 2006.

[25] N. Nethaji, T. Mohideen, and M. Nethaji, “Energy conservation in room air conditioner unit by recovering cold energy from condensate,” *Int. J. Refrig.*, vol. 104, pp. 95–102, 2019, doi: 10.1016/j.ijrefrig.2019.05.005.

[26] J. A. R. P. J.V.C. Vargas , Buzelin, L.O.S., S.C. Amico, “Experimental development of an intelligent refrigeration system,” *Int. J. Refrig.*, vol. 28, no. 2, pp. 165–175, 2005, [Online]. Available: https://doi.org/10.1016/j.ijrefrig.2004.08.013

[27] K. Harby, “Hydrocarbons and their mixtures as alternatives to environmental unfriendly halogenated refrigerants: An updated overview,” *Renew. Sustain. Energy Rev.*, vol. 73, no. June 2017, pp. 1247–1264, 2017, [Online]. Available: https://doi.org/10.1016/j.rser.2017.02.039

[28] B. C. Sami Missaoui, Zied Driss, Romdhane Ben Slama, “Experimental and numerical analysis of a helical coil heat exchanger for domestic refrigerator and water heating,” *Int. J. Refrig.*, vol. 133, no. January, pp. 276–288, 2022, doi: doi: 10.1016/2021.10.015.

[29] B. C. Sami Missaoui, Zied Driss, Romdhane Ben Slama, “Numerical analysis of the heat pump water heater with immersed helically coiled tubes,” *J. Energy Storage*, vol. 39, no. July, p. 102547, 2021, doi: 10.1016/2021.102547.

[30] Nannan Dai and Shuhong Li, “Simulation and performance analysis on condenser coil in household heat pump water heater,” *Sustain. Cities Soc.*, vol. 36, no. January, pp. 176–184, 2018, doi: 10.1016/2017.10.020.

[31] M. Katiyar and S. Agarwal, “An Overview of Passive Cooling Techniques in Buildings: Design Concepts and Architectural Interventions,” *Civ. Eng. Archit.*, vol. 55, no. 1, pp. 84–97, 2012, doi: 10.5281/zenodo.3379579.

[32] D. K. Bhamare, M. K. Rathod, and J. Banerjee, “Passive cooling techniques for building and their applicability in different climatic zones—The state of art,” *Energy Build.*, vol. 198, pp. 467–490, 2019, doi: 10.1016/j.enbuild.2019.06.023.

[33] G. S. N. and K. S. C. Kumar R., “Performance evaluation of multi-passive solar applications of a non air-conditioned building,” *Int. J. Environ. Technol. Manag.*, vol. 5, no. 1, pp. 60–75, 2005.

[34] M. M., *Energy efficient buildings of India*, 2001st ed. Tata Energy Research Institute, New Delhi, 2001.

[35] S. S. Chauhan and S. P. S. Rajput, “Experimental analysis of an evaporative–vapour compression based combined air conditioning system for required comfort conditions,” *Appl. Therm. Eng.*, vol. 115, pp. 326–336, 2017, doi: 10.1016/j.applthermaleng.2016.12.072.

[36] M. Krarti and N. Howarth, “Transitioning to high efficiency air conditioning in Saudi Arabia: A benefit cost analysis for residential buildings,” *J. Build. Eng.*, vol. 31, no. April, p. 101457, 2020, doi: 10.1016/j.jobe.2020.101457.

[37] A. Khosravi, R. N. N. Koury, and L. Machado, “Thermo-economic analysis and sizing of the components of an ejector expansion refrigeration system Analyse thermo-économique et dimensionnement des composants d ’ un système frigorifique à détente par éjecteur,” *Int. J. Refrig.*, vol. 86, pp. 463–479, 2018, doi: 10.1016/j.ijrefrig.2017.11.007.

[38] M. Dixit, A. Arora, and S. C. Kaushik, “Thermodynamic and thermoeconomic analyses of two stage hybrid absorption compression refrigeration system,” *Appl. Therm. Eng.*, vol. 113, pp. 120–131, 2017, doi: 10.1016/j.applthermaleng.2016.10.206.

[39] Z. Yang, C. Du, H. Xiao, B. Li, W. Shi, and B. Wang, “A novel integrated index for simultaneous evaluation of the thermal comfort and energy efficiency of air-conditioning systems,” *J. Build. Eng.*, vol. 57, no. April, p. 104885, 2022, doi: 10.1016/j.jobe.2022.104885.

[40] A. O. Elsayed and T. S. Kayed, “Dynamic performance analysis of inverter-driven split air conditioner,” *Int. J. Refrig.*, vol. 118, pp. 443–452, 2020, doi: 10.1016/j.ijrefrig.2020.05.014.

[41] D. Ha and J. H. Jeong, “Performance characteristics of a combined air conditioner and refrigerator system interconnected via an intercooler,” *Int. J. Refrig.*, vol. 49, pp. 57–68, 2015, doi: 10.1016/j.ijrefrig.2014.10.013.

[42] R. Opoku, E. A. Adjei, D. K. Ahadzie, and K. A. Agyarko, “Energy efficiency , solar energy and cost saving opportunities in public tertiary institutions in developing countries : The case of KNUST , Ghana,” *Alexandria Eng. J.*, vol.

59, no. 1, pp. 417–428, 2020, doi: 10.1016/j.aej.2020.01.011.

[43] M. D. D'Accadia and F. De Rossi, "Thermoeconomic optimization of a refrigeration plant," *Int. J. Refrig.*, vol. 21, no. 1, pp. 42–54, 1998, doi: 10.1016/S0140-7007(97)00071-6.

[44] R. S. Mitishita, E. M. Barreira, C. O. R. Negrão, and C. J. L. Hermes, "Thermoeconomic design and optimization of frost-free refrigerators," *Appl. Therm. Eng.*, vol. 50, no. 1, pp. 1376–1385, 2013, doi: 10.1016/j.applthermaleng.2012.06.024.

[45] S. Sanaye and H. R. Malekmohammadi, "Thermal and economical optimization of air conditioning units with vapor compression refrigeration system," *Appl. Therm. Eng.*, vol. 24, no. 13, pp. 1807–1825, 2004, doi: 10.1016/j.applthermaleng.2003.12.017.

[46] Y. Sahebi and A. Motallebi, "Economical and Exergical Analysis of Refrigeration Systems," *Middle-East J. Sci. Res.*, vol. 9, no. 3, pp. 285–290, 2011.

[47] M. Marwan *et al.*, "Temperature Control Strategy to Mitigate Electrical Energy Cost for Air Conditioning," *e-Prime - Adv. Electr. Eng. Electron. Energy*, vol. 7, no. December 2023, p. 100410, 2024, doi: 10.1016/j.prime.2023.100410.

[48] G. Q. Zhang, L. Wang, L. Liu, and Z. Wang, "Thermoeconomic optimization of small size central air conditioner," *Appl. Therm. Eng.*, vol. 24, no. 4, pp. 471–485, 2004, doi: 10.1016/j.applthermaleng.2003.10.009.

[49] A. Stegou-Sagia and N. Paignigiannis, “Evaluation of mixtures efficiency in refrigerating systems,” *Energy Convers. Manag.*, vol. 46, no. 17, pp. 2787–2802, Oct. 2005, doi: 10.1016/j.enconman.2005.01.007.

[50] A. Arora and S. C. Kaushik, “SHORT COMMUNICATION Energy and exergy analyses of a two-stage vapour compression refrigeration system,” no. August 2009, pp. 907–923, 2010, doi: 10.1002/er.

[51] B. B. Arora, S. K. Kalla, and J. A. Usmani, “Available from: Suneel K Kalla Retrieved on: 12 August,” 2016.

[52] A. Arora, B. B. Arora, B. D. Pathak, H. L. Sachdev, and A. Arora, “Exergy analysis of Vapour Compression Refrigeration system with R-22, R-407C and R-410A’,” 2007.

[53] J. U. Ahamed, R. Saidur, and H. H. Masjuki, “A review on exergy analysis of vapor compression refrigeration system,” *Renew. Sustain. Energy Rev.*, vol. 15, no. 3, pp. 1593–1600, 2011, doi: 10.1016/j.rser.2010.11.039.

[54] M. H. Yang and R. H. Yeh, “Performance and exergy destruction analyses of optimal subcooling for vapor-compression refrigeration systems,” *Int. J. Heat Mass Transf.*, vol. 87, pp. 1–10, Aug. 2015, doi: 10.1016/j.ijheatmasstransfer.2015.03.085.

[55] S. Anand and S. K. Tyagi, “Exergy analysis and experimental study of a vapor compression refrigeration cycle: A technical note,” in *Journal of Thermal Analysis and Calorimetry*, Nov. 2012, pp. 961–971. doi: 10.1007/s10973-011-1904-z.

[56] A. Yataganbaba and A. Kilicarslan, “Exergy analysis of R1234yf and R1234ze as R134a replacements in a two evaporator vapour ˙ rfan Kurtbas Analyse exergétique des substituts R1234yf et R1234ze au R134a dans un système frigorifique à compression de vapeur à double évaporateur,” vol. 60, pp. 26–37, 2015, doi: 10.1016/j.ijrefrig.2015.08.010.

[57] A. E. Özgür, A. Kabul, and Ö. Kizilkan, “Exergy analysis of refrigeration systems using an alternative refrigerant (HFO-1234yF) to R-134a,” *Int. J. Low-Carbon Technol.*, vol. 9, no. 1, pp. 56–62, 2014, doi: 10.1093/ijlct/cts054.

[58] G. Pottker and P. Hrnjak, “Effect of the condenser subcooling on the performance of vapor compression systems,” *Int. J. Refrig.*, vol. 50, no. 217, pp. 156–164, 2015, doi: 10.1016/j.ijrefrig.2014.11.003.

[59] R. Selbaş, Ö. Kizilkan, and A. Şencan, “Thermoeconomic optimization of subcooled and superheated vapor compression refrigeration cycle,” *Energy*, vol. 31, no. 12, pp. 2108–2128, 2006, doi: 10.1016/j.energy.2005.10.015.

[60] S. K. Tyagi, G. Lin, S. C. Kaushik, and J. Chen, “Thermoeconomic optimization of an irreversible Stirling cryogenic refrigerator cycle,” *Int. J. Refrig.*, vol. 27, no. 8, pp. 924–931, 2004, doi: 10.1016/j.ijrefrig.2004.04.016.

[61] H. M. Getu and P. K. Bansal, “Thermodynamic analysis of an R744-R717 cascade refrigeration system,” *Int. J. Refrig.*, vol. 31, no. 1, pp. 45–54, 2008, doi: 10.1016/j.ijrefrig.2007.06.014.

[62] S. A. Klein, D. T. Reindl, and K. Brownell, “Refrigeration system performance using liquid-suction heat exchangers,” *Int. J. Refrig.*, vol. 23, no. 8, pp. 588–

596, 2000, doi: 10.1016/S0140-7007(00)00008-6.

[63] H. Cho, H. Lee, and C. Park, “Performance characteristics of an automobile air conditioning system with internal heat exchanger using refrigerant R1234yf,” *Appl. Therm. Eng.*, vol. 61, no. 2, pp. 563–569, 2013, doi: 10.1016/j.applthermaleng.2013.08.030.

[64] M. Yang and R. Yeh, “International Journal of Heat and Mass Transfer Performance and exergy destruction analyses of optimal subcooling for vapor-compression refrigeration systems,” *Int. J. Heat Mass Transf.*, vol. 87, pp. 1–10, 2015, doi: 10.1016/j.ijheatmasstransfer.2015.03.085.

[65] Y. E. Güzelel, U. Olmuş, and O. Büyükalaca, “Simulation of a desiccant air-conditioning system integrated with dew-point indirect evaporative cooler for a school building,” *Appl. Therm. Eng.*, vol. 217, no. August, 2022, doi: 10.1016/j.applthermaleng.2022.119233.

[66] L. Zhao, W. J. Cai, X. D. Ding, and W. C. Chang, “Decentralized optimization for vapor compression refrigeration cycle,” *Appl. Therm. Eng.*, vol. 51, no. 1–2, pp. 753–763, 2013, doi: 10.1016/j.applthermaleng.2012.10.001.

[67] L. Geng, H. Liu, X. Wei, Z. Hou, and Z. Wang, “Energy and exergy analyses of a bi-evaporator compression/ejection refrigeration cycle,” *Energy Convers. Manag.*, vol. 130, pp. 71–80, 2016, doi: 10.1016/j.enconman.2016.10.016.

[68] S. A. Tassou and T. Q. Qureshi, “Comparative performance evaluation of positive displacement compressors in variable-speed refrigeration applications,” *Int. J. Refrig.*, vol. 21, no. 1, pp. 29–41, 1998, doi:

10.1016/S0140-7007(97)00082-0.

[69] J. Jabardo, W. Mamani, and M. R. Ianella, “Modeling experimental evaluation of an automotive air conditioning system with a variable capacity compressor,” *Int. J. Refrig.*, vol. 25, no. 8, pp. 1157–1172, 2002, doi: 10.1016/S0140-7007(02)00002-6.

[70] R. Khatri and A. Joshi, “Energy Performance Comparison of Inverter based Variable Refrigerant Flow Unitary AC with Constant Volume Unitary AC,” *Energy Procedia*, vol. 109, no. November 2016, pp. 18–26, 2017, doi: 10.1016/j.egypro.2017.03.038.

[71] V. Oruç and A. G. Devecioɨlu, “Thermodynamic performance of air conditioners working with R417A and R424A as alternatives to R22,” *Int. J. Refrig.*, vol. 55, pp. 120–128, 2015, doi: 10.1016/j.ijrefrig.2015.03.021.

[72] K. Almutairi, G. Thoma, J. Burek, S. Algarni, and D. Nutter, “Life cycle assessment and economic analysis of residential air conditioning in Saudi Arabia,” *Energy Build.*, vol. 102, pp. 370–379, 2015, doi: 10.1016/j.enbuild.2015.06.004.

[73] S. A. Borikar *et al.*, “Case Studies in Thermal Engineering A case study on experimental and statistical analysis of energy consumption of domestic refrigerator,” *Case Stud. Therm. Eng.*, vol. 28, no. October, p. 101636, 2021, doi: 10.1016/j.csite.2021.101636.

[74] C. Nikolaidis and D. Probert, “Exergy-method analysis of a two-stage vapour-compression refrigeration-plants performance,” *Appl. Energy*, vol. 60, no. 4, pp.

241–256, 1998.

[75] A. Arora and S. C. Kaushik, “Theoretical analysis of a vapour compression refrigeration system with R502, R404A and R507A,” *Int. J. Refrig.*, vol. 31, no. 6, pp. 998–1005, 2008, doi: 10.1016/j.ijrefrig.2007.12.015.

[76] C. Aprea, A. Maiorino, and R. Mastrullo, “Change in energy performance as a result of a R422D retrofit : An experimental analysis for a vapor compression refrigeration plant for a walk-in cooler,” *Appl. Energy*, vol. 88, no. 12, pp. 4742–4748, 2011, doi: 10.1016/j.apenergy.2011.06.049.

[77] A. Fouda and Z. Melikyan, “A simplified model for analysis of heat and mass transfer in a direct evaporative cooler,” *Appl. Therm. Eng.*, vol. 31, no. 5, pp. 932–936, 2011, doi: 10.1016/j.applthermaleng.2010.11.016.

[78] H. Liu, Q. Zhou, Y. Liu, P. Wang, and D. Wang, “Experimental study on cooling performance of air conditioning system with dual independent evaporative condenser,” *Int. J. Refrig.*, vol. 55, pp. 85–92, 2015, doi: 10.1016/j.ijrefrig.2015.03.012.

[79] J. M. Wu, X. Huang, and H. Zhang, “Theoretical analysis on heat and mass transfer in a direct evaporative cooler,” *Appl. Therm. Eng.*, vol. 29, no. 5–6, pp. 980–984, 2009, doi: 10.1016/j.applthermaleng.2008.05.016.

[80] W. Ketwong, T. Deethayat, and T. Kiatsiriroat, “Case Studies in Thermal Engineering Performance enhancement of air conditioner in hot climate by condenser cooling with cool air generated by direct evaporative cooling,” *Case Stud. Therm. Eng.*, vol. 26, no. January, p. 101127, 2021, doi:

10.1016/j.csite.2021.101127.

[81] G. P. Maheshwari, F. Al-Ragom, and R. K. Suri, “Energy-saving potential of an indirect evaporative cooler,” *Appl. Energy*, vol. 69, no. 1, pp. 69–76, 2001, doi: 10.1016/S0306-2619(00)00066-0.

[82] G. Heidarinejad, M. Bozorgmehr, S. Delfani, and J. Esmaeelian, “Experimental investigation of two-stage indirect / direct evaporative cooling system in various climatic conditions,” *Build. Environ.*, vol. 44, no. 10, pp. 2073–2079, 2009, doi: 10.1016/j.buildenv.2009.02.017.

[83] S. Delfani, J. Esmaeelian, H. Pasdarshahri, and M. Karami, “Energy saving potential of an indirect evaporative cooler as a pre-cooling unit for mechanical cooling systems in Iran,” *Energy Build.*, vol. 42, no. 11, pp. 2169–2176, 2010, doi: 10.1016/j.enbuild.2010.07.009.

[84] H. Yan, Y. Chen, and Y. Min, “Performance analysis of small-scale direct expansion air conditioning system with indirect evaporative cooler as dedicated ventilator,” *Build. Environ.*, vol. 208, no. September 2021, p. 108603, 2022, doi: 10.1016/j.buildenv.2021.108603.

[85] S. Thiangchanta, T. Anh, P. Suttakul, and Y. Mona, “ScienceDirect Energy reduction of split-type air conditioners using a pre-cooling system for the condenser,” *Energy Reports*, vol. 7, pp. 1–6, 2021, doi: 10.1016/j.egyr.2021.05.055.

[86] H. Yang, N. Pei, M. Fan, L. Liu, and D. Wang, “Experimental study on an air-cooled air conditioning unit with spray evaporative cooling system Étude

expérimentale d ’ une unité de conditionnement d ’ air à condenseur à air avec système de refroidissement évaporatif par aspersion,” *Int. J. Refrig.*, vol. 131, pp. 645–656, 2021, doi: 10.1016/j.ijrefrig.2021.06.011.

[87] G. Heidarinejad, M. Bozorgmehr, S. Delfani, and J. Esmaeelian, “Experimental investigation of two-stage indirect/direct evaporative cooling system in various climatic conditions,” *Build. Environ.*, vol. 44, no. 10, pp. 2073–2079, 2009, doi: 10.1016/j.buildenv.2009.02.017.

[88] Y. Yang, C. Ren, C. Yang, M. Tu, B. Luo, and J. Fu, “Energy and exergy performance comparison of conventional, dew point and new external-cooling indirect evaporative coolers,” *Energy Convers. Manag.*, vol. 230, p. 113824, 2021, doi: 10.1016/j.enconman.2021.113824.

[89] V. V. Rao and S. P. Datta, “A feasibility assessment of single to multi / hybrid evaporative coolers for building air-conditioning across diverse climates in India,” *Appl. Therm. Eng.*, vol. 168, no. November 2019, p. 114813, 2020, doi: 10.1016/j.applthermaleng.2019.114813.

[90] S. Vaisi and H. Taheri, “Developing the water-energy nexus performance of direct evaporative coolers in a hot and dry climate: Toward a green space cooling,” *Water-Energy Nexus*, vol. 6, pp. 244–254, 2023, doi: 10.1016/j.wen.2023.11.002.

[91] M. C. Ndukwu *et al.*, “Analysis of the influence of outdoor surface heat flux on the inlet water and the exhaust air temperature of the wetting pad of a direct evaporative cooling system,” *Appl. Therm. Eng.*, vol. 226, no. November 2022,

p. 120292, 2023, doi: 10.1016/j.applthermaleng.2023.120292.

[92] T. A. Jacob, N. Shah, and W. Y. Park, “Evaluation of hybrid evaporative-vapor compression air conditioners for different global climates,” *Energy Convers. Manag.*, vol. 249, no. July, p. 114841, 2021, doi: 10.1016/j.enconman.2021.114841.

[93] Z. Yang *et al.*, “Experimental performance analysis of hybrid air conditioner in cooling season,” *Build. Environ.*, vol. 204, no. April, p. 108160, 2021, doi: 10.1016/j.buildenv.2021.108160.

[94] M. Krarti *et al.*, “Energy performance of hybrid evaporative-vapor compression air conditioning systems for Saudi residential building stocks,” *J. Build. Eng.*, vol. 69, no. January, 2023, doi: 10.1016/j.jobe.2023.106344.

[95] B. J. Kim, S. Y. Jo, and J. W. Jeong, “Energy performance enhancement in air-source heat pump with a direct evaporative cooler-applied condenser,” *Case Stud. Therm. Eng.*, vol. 35, no. May, p. 102137, 2022, doi: 10.1016/j.csite.2022.102137.

[96] M. Jradi and S. Riffat, “Experimental and numerical investigation of a dew-point cooling system for thermal comfort in buildings,” *Appl. Energy*, vol. 132, pp. 524–535, 2014, doi: 10.1016/j.apenergy.2014.07.040.

[97] Y. Yang, C. Ren, Z. Wang, and B. Luo, “Theoretical performance analysis of a new hybrid air conditioning system in hot-dry climate,” *Int. J. Refrig.*, vol. 116, pp. 96–107, 2020, doi: 10.1016/j.ijrefrig.2020.03.015.

[98] A. A. Eidan, J. Alwan, P. Ferrão, J. Fournier, B. Lacarrière, and O. Le Corre, "ScienceDirect ScienceDirect ScienceDirect Enhancement of the Performance Characteristics for Air- Conditioning System by Using Direct Evaporative Cooling in Hot Assessing the feasibility Climates of using the heat demand-outdoor b heat demand forecast tem," *Energy Procedia*, vol. 142, pp. 3998–4003, 2017, doi: 10.1016/j.egypro.2017.12.311.

[99] A. Çag and S. Ali, "Engineering Science and Technology , an International Journal Performance testing and optimization of a split-type air conditioner with evaporatively-cooled condenser," vol. 32, 2022, doi: 10.1016/j.jestch.2021.09.010.

[100] C. Sheng and A. G. A. Nnanna, "Empirical correlation of cooling ef fi ciency and transport phenomena of direct evaporative cooler," *Appl. Therm. Eng.*, vol. 40, pp. 48–55, 2012, doi: 10.1016/j.applthermaleng.2012.01.052.

[101] A. R. Al-badri and A. A. Y. Al-waaly, "The influence of chilled water on the performance of direct evaporative cooling," *Energy Build.*, vol. 155, pp. 143–150, 2017, doi: 10.1016/j.enbuild.2017.09.021.

[102] S. S. Chauhan and S. P. S. Rajput, "Thermodynamic analysis of the evaporative-vapour compression based combined air conditioning system for hot and dry climatic conditions," *J. Build. Eng.*, vol. 4, pp. 200–208, 2015, doi: 10.1016/j.jobe.2015.09.010.

[103] P. Martínez, J. Ruiz, C. G. Cutillas, P. J. Martínez, A. S. Kaiser, and M. Lucas, "Experimental study on energy performance of a split air-conditioner by using

variable thickness evaporative cooling pads coupled to the condenser," *Appl. Therm. Eng.*, vol. 105, pp. 1041–1050, 2016, doi: 10.1016/j.applthermaleng.2016.01.067.

[104] A. Pakari and S. Ghani, "Comparison of 1D and 3D heat and mass transfer models of a counter flow dew point evaporative cooling system: Numerical and experimental study," *Int. J. Refrig.*, vol. 99, pp. 114–125, 2019, doi: 10.1016/j.ijrefrig.2019.01.013.

[105] S. S. Chauhan and S. P. S. Rajput, "Parametric analysis of a combined dew point evaporative-vapour compression based air conditioning system," *Alexandria Eng. J.*, vol. 55, no. 3, pp. 2333–2344, 2016, doi: 10.1016/j.aej.2016.05.005.

[106] C. Liang, Y. Wang, and X. Li, "Energy-efficient air conditioning system using a three-fluid heat exchanger for simultaneous temperature and humidity control," *Energy Convers. Manag.*, vol. 270, no. August, p. 116236, 2022, doi: 10.1016/j.enconman.2022.116236.

[107] T. Wang, C. Sheng, and A. G. A. Nnanna, "Experimental investigation of air conditioning system using evaporative cooling condenser," *Energy Build.*, vol. 81, pp. 435–443, 2014, doi: 10.1016/j.enbuild.2014.06.047.

[108] P. Sarntichartsak and S. Thepa, "Modeling and experimental study on the performance of an inverter air conditioner using R-410A with evaporatively cooled condenser," *ATE*, vol. 51, no. 1–2, pp. 597–610, 2013, doi: 10.1016/j.applthermaleng.2012.08.063.

[109] E. Hajidavalloo and H. Eghtedari, "Performance improvement of air-cooled

refrigeration system by using evaporatively cooled air condenser," *Int. J. Refrig.*, vol. 33, no. 5, pp. 982–988, 2010, doi: 10.1016/j.ijrefrig.2010.02.001.

[110] E. D. V. B. Ankit Sethi, "Genetron Properties 1.4.1." Honeywell International, Inc. - Buffalo Research Laboratory 20 Peabody St, Buffalo, NY, 14210, 2010. [Online]. Available: https://www.honeywell-refrigerants.com/europe/genetron-refrigerants-modeling-software-download/

[111] "Psychrometric Calculator." 2020.

[112] M. K. Marc A.Rosen,Ibrahim Dincer, "Role of exergy in increasing efficiency and sustainability and reducing environmental impact," *Energy Policy*, vol. 36, no. 1, pp. 128–137, 2008, doi: https://doi.org/10.1016/j.enpol.2007.09.006.

[113] K. Mansuriya, V. K. Patel, B. D. Raja, and A. Mudgal, "Assessment of liquid desiccant dehumidi fi cation aided vapor-compression refrigeration system based on thermo-economic approach," *Appl. Therm. Eng.*, vol. 164, no. April 2019, p. 114542, 2020, doi: 10.1016/j.applthermaleng.2019.114542.

[114] A. P. S. Kakaç, H. Liu, *Heat exchangers: selection, rating, and thermal design*, THIRD. CRC Press Taylor & Francis Group, 2012.

[115] G. A. Florides and S. A. Kalogirou, "Design and construction of a LiBr – water absorption machine," vol. 44, pp. 2483–2508, 2003, doi: 10.1016/S0196-8904(03)00006-2.

[116] M. Aminyavari, B. Najafi, A. Shirazi, and F. Rinaldi, "Exergetic, economic and environmental (3E) analyses, and multi-objective optimization of a CO2/NH3

cascade refrigeration system," *Appl. Therm. Eng.*, vol. 65, no. 1–2, pp. 42–50, 2014, doi: 10.1016/j.applthermaleng.2013.12.075.

[117] A. H. Mosaffa, L. G. Farshi, C. A. I. Ferreira, and M. A. Rosen, "Exergoeconomic and environmental analyses of CO 2 / NH 3 cascade refrigeration systems equipped with different types of flash tank intercoolers," *Energy Convers. Manag.*, vol. 117, pp. 442–453, 2016, doi: 10.1016/j.enconman.2016.03.053.

[118] S. Kashyap, J. Sarkar, and A. Kumar, "Exergy, economic, environmental and sustainability analyses of possible regenerative evaporative cooling device topologies," *Build. Environ.*, vol. 180, no. June, p. 107033, 2020, doi: 10.1016/j.buildenv.2020.107033.

[119] R. Roy and B. K. Mandal, "Thermo-economic assessment and multi-objective optimization of vapour compression refrigeration system using Low GWP refrigerants," *2019 8th Int. Conf. Model. Simul. Appl. Optim. ICMSAO 2019*, pp. 0–4, 2019, doi: 10.1109/ICMSAO.2019.8880390.

[120] E. Bellos, C. Tzivanidis, and G. Tsifis, "Energetic, Exergetic, Economic and Environmental (4E) analysis of a solar assisted refrigeration system for various operating scenarios," *Energy Convers. Manag.*, vol. 148, pp. 1055–1069, 2017, doi: 10.1016/j.enconman.2017.06.063.

[121] G. Zhang *et al.*, "Proposal and exergetic / net present value optimization of a novel integrated process into a two-stage geothermal flash cycle , involving bi-evaporator refrigeration unit : Application of non-dominated sorting genetic

algorithm (NSGA-II + LINMAP) method," *Process Saf. Environ. Prot.*, vol. 179, no. September, pp. 735–753, 2023, doi: 10.1016/j.psep.2023.09.025.

[122] S. Sholahudin and N. Giannetti, "Optimization of a cascade refrigeration system using refrigerant C 3 H 8 in high temperature circuits (HTC) and a mixture of C 2 H 6 / CO 2 in low temperature circuits (LTC)," *Appl. Therm. Eng.*, vol. 104, pp. 96–103, 2016, doi: 10.1016/j.applthermaleng.2016.05.059.

[123] S. Sanaye and M. Taheri, "Modeling and multi-objective optimization of a modified hybrid liquid desiccant heat pump (LD-HP) system for hot and humid regions," *Appl. Therm. Eng.*, vol. 129, pp. 212–229, 2018, doi: 10.1016/j.applthermaleng.2017.09.116.

[124] R. D. Misra, P. K. Sahoo, S. Sahoo, and A. Gupta, "Thermoeconomic optimization of a single effect water / LiBr vapour absorption refrigeration system ´ conomique d ' un syste ` me frigorifique a Optimisation thermoe ` eau / LiBr a ` simple effet absorption a," vol. 26, pp. 158–169, 2003.

[125] BEE Govt. of India, "Schedule - 19." Bureau of Energy Efficiency, Govt. of India, New Delhi,India, pp. 1–12, 2015. [Online]. Available: https://www.beestarlabel.com/content/files/inverter ac schedule final.pdf

[126] J. Ramachander, S. K. Gugulothu, G. R. K. Sastry, J. Kumar Panda, and M. S. Surya, "Performance and emission predictions of a CRDI engine powered with diesel fuel: A combined study of injection parameters variation and Box-Behnken response surface methodology based optimization," *Fuel*, vol. 290, no. November 2020, p. 120069, 2021, doi: 10.1016/j.fuel.2020.120069.

[127] H. Khurana, R. Majumdar, and S. K. Saha, “Response Surface Methodology-based prediction model for working fluid temperature during stand-alone operation of vertical cylindrical thermal energy storage tank,” *Renew. Energy*, vol. 188, pp. 619–636, 2022, doi: 10.1016/j.renene.2022.02.040.

[128] A. Lateef, M. Talib, W. Assad, T. Mechanics, and E. T. College-basra, “Thermal and exergy analysis of optimal performance and refrigerant for an air conditioner split unit under different Iraq climatic conditions,” *Therm. Sci. Eng. Prog.*, vol. 19, no. June, p. 100595, 2020, doi: 10.1016/j.tsep.2020.100595.

[129] Indian Meteorological Department, “Weather Data,” 2023. https://mausam.imd.gov.in

[130] Indian Meteorological Department, “Weather Data,” 2022. https://www.indianclimate.com/relative-humidity-data.php?request=5DWH4PLGSL (accessed Jun. 27, 2022).

MEASURED DATA AND UNCERTAINTY (MONTH WISE)

April

		CSAC			DEC SAC		
T_a (± 0.1°C)	RH ($\pm 1\%$)	T_e (± 0.1°C)	T_k (± 0.1°C)	Power ($\pm 0.1kW$)	T_e (± 0.1°C)	T_k (± 0.1°C)	Power ($\pm 0.1kW$)
32.9	22	3.3	47.9	1.909	3.1	37	1.372
34.6	21	3.4	49.6	2.018	3.3	37.7	1.407
35.6	19	3.1	50.6	2.085	2.9	38.3	1.439
37	18	3.2	52	2.182	3.1	39.3	1.492
38	17	3.2	53	2.255	3.1	40	1.53
38.5	19	3.1	53.5	2.292	3.4	40.2	1.541
37.6	18	3.3	52.6	2.225	3.1	39.4	1.497
36.8	20	2.9	51.8	2.168	3.2	38.9	1.471
37.1	19	3.1	52.1	2.19	3.2	39.3	1.492
37.8	21	3.1	52.8	2.24	3.1	39.5	1.503
37.6	18	3.4	52.6	2.225	3.3	39.5	1.503
32.9	22	12.4	47.9	1.46	12.3	39.7	1.062
34.6	21	11.9	49.6	1.554	11.8	40.3	1.089
35.6	19	12.3	50.6	1.612	12.2	42	1.166
37	18	11.8	52	1.696	12	42.9	1.208
38	17	12.2	53	1.758	12.1	42.3	1.179
38.5	19	12	53.5	1.79	12.1	43.4	1.231
37.6	18	12.1	52.6	1.733	11.9	42.6	1.193
36.8	20	11.9	51.8	1.684	11.7	41.7	1.152
37.1	19	11.7	52.1	1.702	12.1	42	1.166
37.8	21	12.1	52.8	1.745	12.3	41.9	1.161
37.6	18	12.3	52.6	1.733	12.1	41.9	1.161

May

		CSAC			DEC SAC		
T_a (± 0.1°C)	RH ($\pm 1\%$)	T_e (± 0.1°C)	T_k (± 0.1°C)	Power ($\pm 0.1kW$)	T_e (± 0.1°C)	T_k (± 0.1°C)	Power ($\pm 0.1kW$)
34.1	25	2.9	49.1	1.986	3.1	38.2	1.372
35.8	22	3.1	50.8	2.099	3.2	39.1	1.407
37.9	18	3.1	52.9	2.247	3.3	39.9	1.439
42.7	18	3.4	57.7	2.63	2.9	43.2	1.492
44.1	19	3.1	59.1	2.755	3.1	44.2	1.53

44.8	24	3.2	59.8	2.82	3.1	44.5	1.541
44.1	21	2.9	59.1	2.755	3.4	44.1	1.497
43.7	20	3.1	58.7	2.719	3.1	43.8	1.471
43	19	3.1	58	2.656	3.2	43.4	1.492
44.9	21	3.4	59.9	2.83	2.9	44.5	1.503
41.1	23	3.2	56.1	2.495	3.1	41.7	1.503
34.1	25	12.3	49.1	1.526	12.1	38.2	0.998
35.8	22	11.8	50.8	1.624	11.9	39.1	1.036
37.9	18	12.2	52.9	1.752	11.7	39.9	1.071
42.7	18	12	57.7	2.081	12.1	43.2	1.222
44.1	19	12.1	59.1	2.188	12.3	44.2	1.27
44.8	24	12.1	59.8	2.244	3.1	44.5	1.285
44.1	21	11.9	59.1	2.188	3.4	44.1	1.265
43.7	20	11.7	58.7	2.157	3.1	43.8	1.251
43	19	12.1	58	2.103	3.2	43.4	1.231
44.9	21	12.4	59.9	2.252	2.9	44.5	1.285
41.1	23	12.2	56.1	1.965	3.1	41.7	1.204

June

		CSAC			DEC SAC		
T_a (± 0.1°C)	RH ($\pm 1\%$)	T_e (± 0.1°C)	T_k (± 0.1°C)	Power ($\pm 0.1kW$)	T_e (± 0.1°C)	T_k (± 0.1°C)	Power ($\pm 0.1kW$)
29.5	59	3.4	44.5	1.794	3.5	38.8	1.465
30.2	56	3.2	45.2	1.838	3.2	38.8	1.465
31.7	51	3.3	46.7	1.936	3.3	39.7	1.514
33.3	47	3.2	48.3	2.046	3.4	41	1.586
34.8	42	3.1	49.8	2.154	3.1	41.3	1.603
35.2	41	3.3	50.2	2.184	3.3	41.6	1.62
35.5	39	3.4	50.5	2.207	3.4	41.7	1.626
35.9	37	3.1	50.9	2.237	3.1	41.6	1.62
36	37	3.1	51	2.245	3.2	41.7	1.626
36.1	37	3.2	51.1	2.253	3.2	41.8	1.629
36.2	37	3.2	51.2	2.261	3.1	41.8	1.629
29.5	59	12.2	44.5	1.348	12.1	38.8	1.065
30.2	56	12	45.2	1.387	11.9	38.8	1.065
31.7	51	12.1	46.7	1.471	11.7	39.7	1.107
33.3	47	12.1	48.3	1.565	11.9	41	1.169
34.8	42	11.9	49.8	1.658	12.2	41.3	1.184
35.2	41	11.7	50.2	1.684	12	41.6	1.199
35.5	39	11.9	50.5	1.703	12.1	41.7	1.204
35.9	37	11.7	50.9	1.729	12.1	41.6	1.199
36	37	12.1	51	1.736	11.9	41.7	1.204
36.1	37	12.3	51.1	1.743	11.7	41.8	1.206

36.2	37	12.1	51.2	1.749	12.1	41.8	1.206

July

		CSAC			DEC SAC		
T_a (± 0.1°C)	RH ($\pm 1\%$)	T_e (± 0.1°C)	T_k (± 0.1°C)	Power ($\pm 0.1kW$)	T_e (± 0.1°C)	T_k (± 0.1°C)	Power ($\pm 0.1kW$)
34.8	49	3.1	49.8	1.591	2.9	42.4	1.591
36	46	3.2	51	1.634	3.1	43.2	1.634
37.6	43	3.3	52.6	1.679	3.1	44	1.679
39.3	41	2.9	54.3	1.735	3.4	45	1.735
40.9	39	3.1	55.9	1.812	3.1	46.3	1.812
39.5	42	3.1	54.5	1.753	3.2	45.3	1.753
38.1	45	3.4	53.1	1.718	2.9	44.7	1.718
36.7	48	3.1	51.7	1.684	3.1	44.1	1.684
34.3	56	3.2	49.3	1.601	3.1	42.6	1.601
31.8	64	2.9	46.8	1.538	3.4	41.4	1.538
29.4	72	3.1	44.4	1.701	3.2	39.8	1.514
34.8	49	12.1	49.8	1.611	2.9	42.4	1.184
36	46	11.9	51	1.681	3.1	43.2	1.222
37.6	43	11.7	52.6	1.783	3.1	44	1.26
39.3	41	12.1	54.3	1.898	3.4	45	1.309
40.9	39	12.4	55.9	2.012	3.1	46.3	1.375
39.5	42	12.2	54.5	1.931	3.2	45.3	1.324
38.1	45	12.1	53.1	1.851	2.9	44.7	1.295
36.7	48	11.9	51.7	1.774	3.1	44.1	1.265
34.3	56	11.7	49.3	1.643	3.1	42.6	1.193
31.8	64	11.9	46.8	1.512	3.4	41.4	1.138
29.4	72	11.7	44.4	1.393	3.2	39.8	1.107

August

		CSAC			DEC SAC		
T_a (± 0.1°C)	RH ($\pm 1\%$)	T_e (± 0.1°C)	T_k (± 0.1°C)	Power ($\pm 0.1kW$)	T_e (± 0.1°C)	T_k (± 0.1°C)	Power ($\pm 0.1kW$)
31.6	53	3.4	46.6	1.83	3.5	40	1.53
32	52	3.2	47	1.854	3.2	40.2	1.541
33.1	49	3.3	48.1	1.922	3.3	40.8	1.575
34.3	46	3.2	49.3	1.999	3.4	41.5	1.614
35.4	44	3.1	50.4	2.072	3.1	42.1	1.649
36.1	42	3.3	51.1	2.119	3.3	42.4	1.667
36.7	40	3.4	51.7	2.161	3.4	42.8	1.69

37.4	38	3.1	52.4	2.211	3.1	43.2	1.714
35.6	44	3.1	50.6	2.085	3.2	42.2	1.655
33.8	50	3.2	48.8	1.966	3.2	41.5	1.614
32	56	3.2	47	1.854	3.1	40.6	1.575
31.6	53	11.7	46.6	1.391	12	40	1.121
32	52	11.9	47	1.412	12.1	40.2	1.131
33.1	49	11.7	48.1	1.471	12.1	40.8	1.16
34.3	46	12.1	49.3	1.537	11.9	41.5	1.194
35.4	44	12.3	50.4	1.6	11.7	42.1	1.224
36.1	42	12.1	51.1	1.641	11.9	42.4	1.239
36.7	40	12.1	51.7	1.677	11.7	42.8	1.259
37.4	38	11.9	52.4	1.72	12.1	43.2	1.28
35.6	44	11.7	50.6	1.612	11.9	42.2	1.229
33.8	50	11.9	48.8	1.509	11.7	41.5	1.194
32	56	11.7	47	1.412	11.8	40.6	1.16

September

		CSAC			**DEC SAC**		
$\boldsymbol{T_a}$ **(±0.1°C)**	$\boldsymbol{RH}$ **(±1%)**	$\boldsymbol{T_e}$ **(±0.1°C)**	$\boldsymbol{T_k}$ **(±0.1°C)**	**Power** $(\pm 0.1 kW)$	$\boldsymbol{T_e}$ **(±0.1°C)**	$\boldsymbol{T_k}$ **(±0.1°C)**	**Power** $(\pm 0.1 kW)$
31.9	48	3.3	46.9	1.95	3.4	39.7	1.45
33.4	43	3.4	48.4	2.053	3.1	40.3	1.481
35.7	38	3.1	50.7	2.222	3.3	42	1.569
38	34	3.3	53	2.405	3.4	42.9	1.618
40.3	29	3.4	55.3	2.605	3.1	42.3	1.585
39.7	28	3.1	54.7	2.551	3.2	43.4	1.645
39.1	27	3.2	54.1	2.498	3.5	42.6	1.601
38.5	25	3.5	53.5	2.447	3.2	41.7	1.553
37.9	29	3.2	52.9	2.397	3.3	42	1.569
37.2	32	3.3	52.2	2.34	3.4	41.9	1.564
36.6	35	3.4	51.6	2.292	3.1	41.9	1.564
31.9	48	12.2	46.9	1.482	12.1	39.7	1.062
33.4	43	12.1	48.4	1.571	11.9	40.3	1.089
35.7	38	12.1	50.7	1.716	11.7	42	1.166
38	34	12.1	53	1.873	11.9	42.9	1.208
40.3	29	11.9	55.3	2.044	12.2	42.3	1.179
39.7	28	11.7	54.7	1.998	12.3	43.4	1.231
39.1	27	11.9	54.1	1.953	12.1	42.6	1.193
38.5	25	11.7	53.5	1.909	12.1	41.7	1.152
37.9	29	12.1	52.9	1.866	11.9	42	1.166
37.2	32	12.3	52.2	1.817	11.7	41.9	1.161
36.6	35	12.1	51.6	1.776	12.1	41.9	1.161

REFRIGERANT PROPERTIES FOR THE MEASURED DATA

April ($T_e = 3$°C)

T_k (°C)	$h_{e,i}$ (kJ/kg)	$s_{e,i}$ (kJ/kg-K)	$h_{e,o}$ (kJ/kg)	$s_{e,o}$ (kJ/kg-K)	$h_{c,o}$ (kJ/kg)	$s_{c,o}$ (kJ/kg-K)	Q_k (W)	$h_{k,o}$ (kJ/kg)	$s_{k,o}$ (kJ/kg-K)
CSAC									
47.9	292.73	1.3356	522.03	2.1658	600.49	2.2408	6979.41	292.73	1.3041
49.6	296.57	1.3495	522.03	2.1658	603.91	2.2444	7088.46	296.57	1.3156
50.6	298.87	1.3578	522.03	2.1658	605.94	2.2465	7155.29	298.87	1.3224
52	302.12	1.3696	522.03	2.1658	608.83	2.2496	7252.46	302.12	1.3321
53	304.48	1.3782	522.03	2.1658	610.92	2.2519	7324.65	304.48	1.339
53.5	305.67	1.3825	522.03	2.1658	611.97	2.253	7361.66	305.67	1.3425
52.6	303.53	1.3747	522.03	2.1658	610.08	2.251	7295.49	303.53	1.3362
51.8	301.65	1.3679	522.03	2.1658	608.41	2.2492	7238.32	301.65	1.3307
52.1	302.36	1.3705	522.03	2.1658	609.03	2.2498	7259.58	302.36	1.3328
52.8	304.01	1.3765	522.03	2.1658	610.5	2.2514	7310.02	304.01	1.3376
52.6	303.53	1.3747	522.03	2.1658	610.08	2.251	7295.49	303.53	1.3362
DEC-SAC									
37	269.38	1.2511	522.03	2.1658	582.35	2.2271	6441.61	269.38	1.2326
37.7	270.83	1.2563	522.03	2.1658	583.74	2.2286	6477.5	270.83	1.2371
38.3	272.07	1.2608	522.03	2.1658	584.94	2.2299	6508.78	272.07	1.241
39.3	274.15	1.2683	522.03	2.1658	586.95	2.2322	6562.02	274.15	1.2474
40	275.61	1.2736	522.03	2.1658	588.38	2.2337	6600.15	275.61	1.252
40.2	276.03	1.2751	522.03	2.1658	588.79	2.2342	6611.17	276.03	1.2533
39.4	274.36	1.2691	522.03	2.1658	587.16	2.2324	6567.42	274.36	1.2481
38.9	273.31	1.2653	522.03	2.1658	586.15	2.2313	6540.56	273.31	1.2449
39.3	274.15	1.2683	522.03	2.1658	586.95	2.2322	6562.02	274.15	1.2474
39.5	274.56	1.2698	522.03	2.1658	587.36	2.2326	6572.84	274.56	1.2487
39.5	274.56	1.2698	522.03	2.1658	587.36	2.2326	6572.84	274.56	1.2487

May

T_k (°C)	$h_{e,i}$ (kJ/kg)	$s_{e,i}$ (kJ/kg-K)	$h_{e,o}$ (kJ/kg)	$s_{e,o}$ (kJ/kg-K)	$h_{c,o}$ (kJ/kg)	$s_{c,o}$ (kJ/kg-K)	Q_k (W)	$h_{k,o}$ (kJ/kg)	$s_{k,o}$ (kJ/kg-K)
CSAC									
49.1	295.43	1.3454	522.03	2.1658	602.9	2.2433	7055.8	295.43	1.3122
50.8	299.33	1.3595	522.03	2.1658	606.35	2.247	7168.91	299.33	1.3238
52.9	304.24	1.3773	522.03	2.1658	610.71	2.2517	7317.32	304.24	1.3383
57.7	315.99	1.4198	522.03	2.1658	621.08	2.2631	7699.82	315.99	1.3726
59.1	319.58	1.4328	522.03	2.1658	624.23	2.2667	7825	319.58	1.383
59.8	321.4	1.4394	522.03	2.1658	625.83	2.2685	7890.32	321.4	1.3883

59.1	319.58	1.4328	522.03	2.1658	624.23	2.2667	7825	319.58	1.383
58.7	318.54	1.4291	522.03	2.1658	623.32	2.2657	7788.53	318.54	1.38
58	316.75	1.4226	522.03	2.1658	621.75	2.2639	7726.07	316.75	1.3749
59.9	321.66	1.4404	522.03	2.1658	626.06	2.2688	7899.8	321.66	1.389
56.1	311.98	1.4053	522.03	2.1658	617.55	2.2592	7564.84	311.98	1.361
					DEC-SAC				
38.2	271.86	1.26	522.03	2.1658	581.99	2.2221	6446.31	271.86	1.2403
39.1	273.73	1.2668	522.03	2.1658	583.65	2.2237	6490.42	273.73	1.2462
39.9	275.4	1.2729	522.03	2.1658	585.13	2.2252	6530.44	275.4	1.2513
43.2	282.41	1.2982	522.03	2.1658	591.34	2.2314	6704.17	282.41	1.2729
44.2	284.57	1.3061	522.03	2.1658	593.26	2.2333	6759.8	284.57	1.2794
44.5	285.22	1.3084	522.03	2.1658	593.83	2.2339	6776.77	285.22	1.2814
44.1	284.35	1.3053	522.03	2.1658	593.06	2.2331	6754.17	284.35	1.2788
43.8	283.7	1.3029	522.03	2.1658	592.49	2.2325	6737.38	283.7	1.2768
43.4	282.84	1.2998	522.03	2.1658	591.72	2.2318	6715.18	282.84	1.2742
44.5	285.22	1.3084	522.03	2.1658	593.83	2.2339	6776.77	285.22	1.2814
41.7	279.2	1.2866	522.03	2.1658	591.88	2.2377	6695.82	279.2	1.263

June

T_k	$h_{e,i}$	$s_{e,i}$	$h_{e,o}$	$s_{e,o}$	$h_{c,o}$	$s_{c,o}$	Q_k	$h_{k,o}$	$s_{k,o}$
(°C)	**(kJ/kg)**	**(kJ/kg-K)**	**(kJ/kg)**	**(kJ/kg-K)**	**(kJ/kg)**	**(kJ/kg-K)**	**(W)**	**(kJ/kg)**	**(kJ/kg-K)**
					CSAC				
44.5	285.22	1.3084	522.03	2.1658	597.8	2.2445	6863.84	285.22	1.2814
45.2	286.75	1.3139	522.03	2.1658	599.31	2.2462	6908.07	286.75	1.286
46.7	290.05	1.3259	522.03	2.1658	602.6	2.2501	7006.11	290.05	1.296
48.3	293.62	1.3389	522.03	2.1658	606.18	2.2543	7115.94	293.62	1.3068
49.8	297.03	1.3512	522.03	2.1658	609.62	2.2585	7224.29	297.03	1.317
50.2	297.95	1.3545	522.03	2.1658	610.55	2.2596	7254.13	297.95	1.3197
50.5	298.64	1.357	522.03	2.1658	611.25	2.2604	7276.78	298.64	1.3217
50.9	299.56	1.3604	522.03	2.1658	612.19	2.2616	7307.35	299.56	1.3245
51	299.79	1.3612	522.03	2.1658	612.42	2.2619	7315.05	299.79	1.3252
51.1	300.02	1.362	522.03	2.1658	612.66	2.2622	7322.8	300.02	1.3259
51.2	300.26	1.3629	522.03	2.1658	612.89	2.2624	7330.55	300.26	1.3265
					DEC-SAC				
38.8	273.1	1.2646	522.03	2.1658	585.94	2.231	6535.23	273.1	1.2442
38.8	273.1	1.2646	522.03	2.1658	585.94	2.231	6535.23	273.1	1.2442
39.7	274.98	1.2714	522.03	2.1658	587.77	2.2331	6583.71	274.98	1.25
41	277.72	1.2813	522.03	2.1658	590.43	2.236	6655.88	277.72	1.2585
41.3	278.35	1.2836	522.03	2.1658	591.05	2.2367	6672.9	278.35	1.2604
41.6	278.99	1.2859	522.03	2.1658	591.67	2.2374	6690.07	278.99	1.2624
41.7	279.2	1.2866	522.03	2.1658	591.88	2.2377	6695.82	279.2	1.263
41.6	278.99	1.2859	522.03	2.1658	591.67	2.2374	6690.07	278.99	1.2624
41.7	279.2	1.2866	522.03	2.1658	591.88	2.2377	6695.82	279.2	1.263

41.8	279.31	1.287	522.03	2.1658	591.98	2.2378	6698.71	279.31	1.2634
41.8	279.31	1.287	522.03	2.1658	591.98	2.2378	6698.71	279.31	1.2634

July

T_k	$h_{e,i}$	$s_{e,i}$	$h_{e,o}$	$s_{e,o}$	$h_{c,o}$	$s_{c,o}$	Q_k	$h_{k,o}$	$s_{k,o}$
(°C)	**(kJ/kg)**	**(kJ/kg-K)**	**(kJ/kg)**	**(kJ/kg-K)**	**(kJ/kg)**	**(kJ/kg-K)**	**(W)**	**(kJ/kg)**	**(kJ/kg-K)**
				CSAC					
49.8	297.03	1.3512	522.03	2.1658	606.94	2.2516	7162.36	297.03	1.317
51	299.79	1.3612	522.03	2.1658	609.33	2.254	7242.73	299.79	1.3252
52.6	303.53	1.3747	522.03	2.1658	612.84	2.258	7361.36	303.53	1.3362
54.3	307.59	1.3894	522.03	2.1658	616.66	2.2624	7494.84	307.59	1.3482
55.9	311.49	1.4036	522.03	2.1658	620.34	2.2667	7628.09	311.49	1.3596
54.5	308.07	1.3912	522.03	2.1658	618.13	2.2655	7535.64	308.07	1.3496
53.1	304.72	1.379	522.03	2.1658	615.84	2.264	7444.94	304.72	1.3397
51.7	301.42	1.3671	522.03	2.1658	613.61	2.2627	7358.59	301.42	1.33
49.3	295.89	1.3471	522.03	2.1658	609.39	2.2595	7208.95	295.89	1.3136
46.8	290.27	1.3267	522.03	2.1658	604.98	2.256	7061.14	290.27	1.2967
44.4	285	1.3076	522.03	2.1658	600.71	2.2525	6926.13	285	1.2808
				DEC-SAC					
42.4	280.69	1.292	522.03	2.1658	589.82	2.2298	6660.71	280.69	1.2676
43.2	282.41	1.2982	522.03	2.1658	591.34	2.2314	6704.17	282.41	1.2729
44	284.13	1.3045	522.03	2.1658	592.87	2.2329	6748.55	284.13	1.2781
45	286.31	1.3124	522.03	2.1658	594.8	2.2349	6805.39	286.31	1.2847
46.3	289.16	1.3227	522.03	2.1658	597.33	2.2375	6881.63	289.16	1.2934
45.3	286.96	1.3147	522.03	2.1658	595.38	2.2355	6822.74	286.96	1.2867
44.7	285.65	1.31	522.03	2.1658	594.22	2.2343	6788.17	285.65	1.2827
44.1	284.35	1.3053	522.03	2.1658	593.06	2.2331	6754.17	284.35	1.2788
42.6	281.12	1.2936	522.03	2.1658	590.2	2.2302	6671.49	281.12	1.2689
41.4	278.56	1.2843	522.03	2.1658	587.93	2.2279	6607.62	278.56	1.2611
39.7	274.98	1.2714	522.03	2.1658	587.77	2.2331	6583.71	274.98	1.25

August

T_k	$h_{e,i}$	$s_{e,i}$	$h_{e,o}$	$s_{e,o}$	$h_{c,o}$	$s_{c,o}$	Q_k	$h_{k,o}$	$s_{k,o}$
(°C)	**(kJ/kg)**	**(kJ/kg-K)**	**(kJ/kg)**	**(kJ/kg-K)**	**(kJ/kg)**	**(kJ/kg-K)**	**(W)**	**(kJ/kg)**	**(kJ/kg-K)**
				CSAC					
46.6	289.83	1.3251	522.03	2.1658	597.92	2.2381	6899.63	289.83	1.2954
47	290.71	1.3283	522.03	2.1658	598.71	2.2389	6923.86	290.71	1.298
48.1	293.17	1.3372	522.03	2.1658	600.89	2.2412	6991.95	293.17	1.3054
49.3	295.89	1.3471	522.03	2.1658	603.3	2.2437	7068.8	295.89	1.3136
50.4	298.41	1.3562	522.03	2.1658	605.53	2.2461	7141.75	298.41	1.3211

51.1	300.02	1.362	522.03	2.1658	606.97	2.2476	7189.5	300.02	1.3259
51.7	301.42	1.3671	522.03	2.1658	608.2	2.249	7231.27	301.42	1.33
52.4	303.06	1.373	522.03	2.1658	609.66	2.2505	7281.06	303.06	1.3348
50.6	298.87	1.3578	522.03	2.1658	605.94	2.2465	7155.29	298.87	1.3224
48.8	294.75	1.3429	522.03	2.1658	602.29	2.2427	7036.44	294.75	1.3102
47	290.71	1.3283	522.03	2.1658	598.71	2.2389	6923.86	290.71	1.298
					DEC-SAC				
40	275.61	1.2736	522.03	2.1658	588.38	2.2337	6600.15	275.61	1.252
40.2	276.03	1.2751	522.03	2.1658	588.79	2.2342	6611.17	276.03	1.2533
40.8	277.29	1.2797	522.03	2.1658	590.02	2.2356	6644.6	277.29	1.2572
41.5	278.78	1.2851	522.03	2.1658	591.46	2.2372	6684.33	278.78	1.2617
42.1	280.05	1.2897	522.03	2.1658	592.71	2.2386	6719	280.05	1.2656
42.4	280.69	1.292	522.03	2.1658	593.34	2.2393	6736.56	280.69	1.2676
42.8	281.55	1.2951	522.03	2.1658	594.18	2.2403	6760.21	281.55	1.2702
43.2	282.41	1.2982	522.03	2.1658	595.03	2.2413	6784.13	282.41	1.2729
42.2	280.27	1.2905	522.03	2.1658	592.92	2.2389	6724.84	280.27	1.2663
41.5	278.78	1.2851	522.03	2.1658	591.46	2.2372	6684.33	278.78	1.2617
40.6	277.29	1.2797	522.03	2.1658	590.02	2.2356	6644.6	277.29	1.2572

September

T_k	$h_{e,i}$	$s_{e,i}$	$h_{e,o}$	$s_{e,o}$	$h_{c,o}$	$s_{c,o}$	Q_k	$h_{k,o}$	$s_{k,o}$
(°C)	**(kJ/kg)**	**(kJ/kg-K)**	**(kJ/kg)**	**(kJ/kg-K)**	**(kJ/kg)**	**(kJ/kg-K)**	**(W)**	**(kJ/kg)**	**(kJ/kg-K)**
					CSAC				
46.9	290.49	1.3275	522.03	2.1658	603.04	2.2506	7019.54	290.49	1.2974
48.4	293.85	1.3397	522.03	2.1658	606.41	2.2546	7123	293.85	1.3075
50.7	299.1	1.3587	522.03	2.1658	611.71	2.261	7292	299.1	1.3231
53	304.48	1.3782	522.03	2.1658	617.21	2.2678	7475.18	304.48	1.339
55.3	310.02	1.3982	522.03	2.1658	622.93	2.2749	7674.73	310.02	1.3553
54.7	308.56	1.3929	522.03	2.1658	621.41	2.273	7620.95	308.56	1.351
54.1	307.11	1.3877	522.03	2.1658	619.92	2.2711	7568.42	307.11	1.3468
53.5	305.67	1.3825	522.03	2.1658	618.44	2.2693	7517.08	305.67	1.3425
52.9	304.24	1.3773	522.03	2.1658	616.97	2.2675	7466.88	304.24	1.3383
52.2	302.59	1.3713	522.03	2.1658	615.28	2.2654	7409.73	302.59	1.3335
51.6	301.19	1.3662	522.03	2.1658	613.84	2.2636	7361.88	301.19	1.3293
					DEC-SAC				
39.7	274.98	1.2714	522.03	2.1658	584.76	2.2248	6520.37	274.98	1.25
40.3	276.24	1.2759	522.03	2.1658	585.87	2.2259	6550.75	276.24	1.2539
42	279.84	1.2889	522.03	2.1658	589.06	2.2291	6639.31	279.84	1.265
42.9	281.76	1.2959	522.03	2.1658	590.77	2.2308	6687.77	281.76	1.2709
42.3	280.48	1.2913	522.03	2.1658	589.63	2.2296	6655.34	280.48	1.267
43.4	282.84	1.2998	522.03	2.1658	591.72	2.2318	6715.18	282.84	1.2742
42.6	281.12	1.2936	522.03	2.1658	590.2	2.2302	6671.49	281.12	1.2689

41.7	279.2	1.2866	522.03	2.1658	588.5	2.2285	6623.41	279.2	1.263
42	279.84	1.2889	522.03	2.1658	589.06	2.2291	6639.31	279.84	1.265
41.9	279.63	1.2882	522.03	2.1658	588.87	2.2289	6634	279.63	1.2643
41.9	279.63	1.2882	522.03	2.1658	588.87	2.2289	6634	279.63	1.2643

April ($\boldsymbol{T_e = 12}$℃)

T_k (°C)	$h_{e,i}$ (kJ/kg)	$s_{e,i}$ (kJ/kg-K)	$h_{e,o}$ (kJ/kg)	$s_{e,o}$ (kJ/kg-K)	$h_{c,o}$ (kJ/kg)	$s_{c,o}$ (kJ/kg-K)	Q_k (W)	$h_{k,o}$ (kJ/kg)	$s_{k,o}$ (kJ/kg-K)
CSAC									
47.9	292.73	1.3255	523.52	2.1347	582.56	2.1929	6530.02	292.73	1.3041
49.6	296.57	1.339	523.52	2.1347	585.69	2.1962	6624.23	296.57	1.3156
50.6	298.87	1.3471	523.52	2.1347	587.55	2.1982	6681.92	298.87	1.3224
52	302.12	1.3585	523.52	2.1347	590.19	2.2011	6765.74	302.12	1.3321
53	304.48	1.3668	523.52	2.1347	592.1	2.2032	6827.96	304.48	1.339
53.5	305.67	1.3709	523.52	2.1347	593.06	2.2043	6859.84	305.67	1.3425
52.6	303.53	1.3634	523.52	2.1347	591.33	2.2024	6802.83	303.53	1.3362
51.8	301.65	1.3569	523.52	2.1347	589.81	2.2007	6753.55	301.65	1.3307
52.1	302.36	1.3593	523.52	2.1347	590.38	2.2013	6771.87	302.36	1.3328
52.8	304.01	1.3651	523.52	2.1347	591.72	2.2028	6815.35	304.01	1.3376
52.6	303.53	1.3634	523.52	2.1347	591.33	2.2024	6802.83	303.53	1.3362
DEC-SAC									
37	269.38	1.2437	523.52	2.1347	565.27	2.1785	6054.22	269.38	1.2326
37.7	270.83	1.2487	523.52	2.1347	566.54	2.1799	6085.24	270.83	1.2371
38.3	272.07	1.2531	523.52	2.1347	567.64	2.1812	6112.28	272.07	1.241
39.3	274.15	1.2604	523.52	2.1347	569.48	2.1832	6158.26	274.15	1.2474
40	275.61	1.2655	523.52	2.1347	570.78	2.1847	6191.17	275.61	1.252
40.2	276.03	1.267	523.52	2.1347	571.15	2.1851	6200.68	276.03	1.2533
39.4	274.36	1.2611	523.52	2.1347	569.67	2.1834	6162.92	274.36	1.2481
38.9	273.31	1.2575	523.52	2.1347	568.74	2.1824	6139.72	273.31	1.2449
39.3	274.15	1.2604	523.52	2.1347	569.48	2.1832	6158.26	274.15	1.2474
39.5	274.56	1.2619	523.52	2.1347	569.85	2.1836	6167.6	274.56	1.2487
39.5	274.56	1.2619	523.52	2.1347	569.85	2.1836	6167.6	274.56	1.2487

May

T_k (°C)	$h_{e,i}$ (kJ/kg)	$s_{e,i}$ (kJ/kg-K)	$h_{e,o}$ (kJ/kg)	$s_{e,o}$ (kJ/kg-K)	$h_{c,o}$ (kJ/kg)	$s_{c,o}$ (kJ/kg-K)	Q_k (W)	$h_{k,o}$ (kJ/kg)	$s_{k,o}$ (kJ/kg-K)
CSAC									
49.1	295.43	1.335	523.52	2.1347	584.76	2.1952	6596.03	295.43	1.3122
50.8	299.33	1.3487	523.52	2.1347	587.92	2.1987	6693.68	299.33	1.3238
52.9	304.24	1.3659	523.52	2.1347	591.91	2.203	6821.65	304.24	1.3383

57.7	315.99	1.4071	523.52	2.1347	601.38	2.2136	7150.7	315.99	1.3726
59.1	319.58	1.4197	523.52	2.1347	604.25	2.2169	7258.17	319.58	1.383
59.8	321.4	1.4261	523.52	2.1347	605.7	2.2186	7314.2	321.4	1.3883
59.1	319.58	1.4197	523.52	2.1347	604.25	2.2169	7258.17	319.58	1.383
58.7	318.54	1.4161	523.52	2.1347	603.42	2.2159	7226.87	318.54	1.38
58	316.75	1.4098	523.52	2.1347	601.99	2.2143	7173.25	316.75	1.3749
59.9	321.66	1.427	523.52	2.1347	605.91	2.2188	7322.33	321.66	1.389
56.1	311.98	1.3931	523.52	2.1347	598.16	2.21	7034.7	311.98	1.361
				DEC-SAC					
38.2	271.86	1.2524	523.52	2.1347	565.53	2.1754	6067.9	271.86	1.2403
39.1	273.73	1.2589	523.52	2.1347	567.06	2.1769	6106.24	273.73	1.2462
39.9	275.4	1.2648	523.52	2.1347	568.43	2.1783	6141.01	275.4	1.2513
43.2	282.41	1.2894	523.52	2.1347	574.15	2.1841	6291.77	282.41	1.2729
44.2	284.57	1.2969	523.52	2.1347	575.91	2.1859	6339.98	284.57	1.2794
44.5	285.22	1.2992	523.52	2.1347	576.44	2.1865	6354.68	285.22	1.2814
44.1	284.35	1.2962	523.52	2.1347	575.73	2.1858	6335.1	284.35	1.2788
43.8	283.7	1.2939	523.52	2.1347	575.2	2.1852	6320.55	283.7	1.2768
43.4	282.84	1.2909	523.52	2.1347	574.5	2.1845	6301.31	282.84	1.2742
44.5	285.22	1.2992	523.52	2.1347	576.44	2.1865	6354.68	285.22	1.2814
41.7	279.2	1.2781	523.52	2.1347	573.97	2.1883	6273.7	279.2	1.263

June

T_k	$h_{e,i}$	$s_{e,i}$	$h_{e,o}$	$s_{e,o}$	$h_{c,o}$	$s_{c,o}$	Q_k	$h_{k,o}$	$s_{k,o}$
(°C)	**(kJ/kg)**	**(kJ/kg-K)**	**(kJ/kg)**	**(kJ/kg-K)**	**(kJ/kg)**	**(kJ/kg-K)**	**(W)**	**(kJ/kg)**	**(kJ/kg-K)**
					CSAC				
44.5	285.22	1.2992	523.52	2.1347	579.36	2.1946	6418.44	285.22	1.2814
45.2	286.75	1.3046	523.52	2.1347	580.74	2.1962	6456.5	286.75	1.286
46.7	290.05	1.3162	523.52	2.1347	583.73	2.1997	6540.82	290.05	1.296
48.3	293.62	1.3287	523.52	2.1347	586.98	2.2036	6635.19	293.62	1.3068
49.8	297.03	1.3406	523.52	2.1347	590.09	2.2074	6728.21	297.03	1.317
50.2	297.95	1.3438	523.52	2.1347	590.93	2.2085	6753.81	297.95	1.3197
50.5	298.64	1.3463	523.52	2.1347	591.56	2.2092	6773.24	298.64	1.3217
50.9	299.56	1.3495	523.52	2.1347	592.41	2.2103	6799.46	299.56	1.3245
51	299.79	1.3503	523.52	2.1347	592.63	2.2106	6806.07	299.79	1.3252
51.1	300.02	1.3511	523.52	2.1347	592.84	2.2108	6812.71	300.02	1.3259
51.2	300.26	1.3519	523.52	2.1347	593.05	2.2111	6819.35	300.26	1.3265
					DEC-SAC				
38.8	273.1	1.2567	523.52	2.1347	568.56	2.1822	6135.12	273.1	1.2442
38.8	273.1	1.2567	523.52	2.1347	568.56	2.1822	6135.12	273.1	1.2442
39.7	274.98	1.2633	523.52	2.1347	570.22	2.1841	6176.99	274.98	1.25
41	277.72	1.2729	523.52	2.1347	572.65	2.1868	6239.26	277.72	1.2585
41.3	278.35	1.2751	523.52	2.1347	573.22	2.1875	6253.94	278.35	1.2604
41.6	278.99	1.2774	523.52	2.1347	573.78	2.1881	6268.74	278.99	1.2624

41.7	279.2	1.2781	523.52	2.1347	573.97	2.1883	6273.7	279.2	1.263
41.6	278.99	1.2774	523.52	2.1347	573.78	2.1881	6268.74	278.99	1.2624
41.7	279.2	1.2781	523.52	2.1347	573.97	2.1883	6273.7	279.2	1.263
41.8	279.31	1.2785	523.52	2.1347	574.07	2.1884	6276.19	279.31	1.2634
41.8	279.31	1.2785	523.52	2.1347	574.07	2.1884	6276.19	279.31	1.2634

July

T_k	$h_{e,i}$	$s_{e,i}$	$h_{e,o}$	$s_{e,o}$	$h_{c,o}$	$s_{c,o}$	Q_k	$h_{k,o}$	$s_{k,o}$
(°C)	**(kJ/kg)**	**(kJ/kg-K)**	**(kJ/kg)**	**(kJ/kg-K)**	**(kJ/kg)**	**(kJ/kg-K)**	**(W)**	**(kJ/kg)**	**(kJ/kg-K)**
				CSAC					
49.8	297.03	1.3406	523.52	2.1347	588.05	2.202	6681.45	297.03	1.317
51	299.79	1.3503	523.52	2.1347	590.26	2.2043	6751.15	299.79	1.3252
52.6	303.53	1.3634	523.52	2.1347	593.47	2.208	6853.22	303.53	1.3362
54.3	307.59	1.3777	523.52	2.1347	596.94	2.2121	6967.94	307.59	1.3482
55.9	311.49	1.3914	523.52	2.1347	600.28	2.216	7082.35	311.49	1.3596
54.5	308.07	1.3794	523.52	2.1347	598.14	2.2146	7000.82	308.07	1.3496
53.1	304.72	1.3676	523.52	2.1347	595.94	2.213	6920.87	304.72	1.3397
51.7	301.42	1.356	523.52	2.1347	593.76	2.2115	6844.46	301.42	1.33
49.3	295.89	1.3366	523.52	2.1347	589.75	2.208	6712.79	295.89	1.3136
46.8	290.27	1.3169	523.52	2.1347	585.54	2.2044	6582.48	290.27	1.2967
44.4	285	1.2985	523.52	2.1347	581.47	2.2007	6463.22	285	1.2808
				DEC-SAC					
42.4	280.69	1.2833	523.52	2.1347	572.75	2.1827	6254.08	280.69	1.2676
43.2	282.41	1.2894	523.52	2.1347	574.15	2.1841	6291.77	282.41	1.2729
44	284.13	1.2954	523.52	2.1347	575.56	2.1856	6330.23	284.13	1.2781
45	286.31	1.303	523.52	2.1347	577.33	2.1874	6379.46	286.31	1.2847
46.3	289.16	1.313	523.52	2.1347	579.66	2.1898	6445.46	289.16	1.2934
45.3	286.96	1.3053	523.52	2.1347	577.86	2.188	6394.49	286.96	1.2867
44.7	285.65	1.3007	523.52	2.1347	576.8	2.1869	6364.55	285.65	1.2827
44.1	284.35	1.2962	523.52	2.1347	575.73	2.1858	6335.1	284.35	1.2788
42.6	281.12	1.2848	523.52	2.1347	573.1	2.183	6263.44	281.12	1.2689
41.4	278.56	1.2759	523.52	2.1347	571.01	2.1809	6208.03	278.56	1.2611
39.8	274.98	1.2633	523.52	2.1347	570.22	2.1841	6176.99	274.98	1.25

August

T_k	$h_{e,i}$	$s_{e,i}$	$h_{e,o}$	$s_{e,o}$	$h_{c,o}$	$s_{c,o}$	Q_k	$h_{k,o}$	$s_{k,o}$
(°C)	**(kJ/kg)**	**(kJ/kg-K)**	**(kJ/kg)**	**(kJ/kg-K)**	**(kJ/kg)**	**(kJ/kg-K)**	**(W)**	**(kJ/kg)**	**(kJ/kg-K)**
				CSAC					
46.6	289.83	1.3154	523.52	2.1347	580.2	2.1904	6461.03	289.83	1.2954
47	290.71	1.3185	523.52	2.1347	580.92	2.1912	6481.99	290.71	1.298
48.1	293.17	1.3271	523.52	2.1347	582.92	2.1933	6540.86	293.17	1.3054

49.3	295.89	1.3366	523.52	2.1347	585.13	2.1956	6607.25	295.89	1.3136
50.4	298.41	1.3455	523.52	2.1347	587.17	2.1978	6670.24	298.41	1.3211
51.1	300.02	1.3511	523.52	2.1347	588.49	2.1993	6711.44	300.02	1.3259
51.7	301.42	1.356	523.52	2.1347	589.62	2.2005	6747.47	301.42	1.33
52.4	303.06	1.3618	523.52	2.1347	590.95	2.2019	6790.39	303.06	1.3348
50.6	298.87	1.3471	523.52	2.1347	587.55	2.1982	6681.92	298.87	1.3224
48.8	294.75	1.3327	523.52	2.1347	584.21	2.1947	6579.31	294.75	1.3102
47	290.71	1.3185	523.52	2.1347	580.92	2.1912	6481.99	290.71	1.298
				DEC-SAC					
40	275.61	1.2655	523.52	2.1347	570.78	2.1847	6191.17	275.61	1.252
40.2	276.03	1.267	523.52	2.1347	571.15	2.1851	6200.68	276.03	1.2533
40.8	277.29	1.2714	523.52	2.1347	572.27	2.1864	6229.53	277.29	1.2572
41.5	278.78	1.2766	523.52	2.1347	573.59	2.1879	6263.8	278.78	1.2617
42.1	280.05	1.2811	523.52	2.1347	574.73	2.1892	6293.69	280.05	1.2656
42.4	280.69	1.2833	523.52	2.1347	575.3	2.1899	6308.82	280.69	1.2676
42.8	281.55	1.2863	523.52	2.1347	576.07	2.1907	6329.2	281.55	1.2702
43.2	282.41	1.2894	523.52	2.1347	576.84	2.1916	6349.8	282.41	1.2729
42.2	280.27	1.2818	523.52	2.1347	574.92	2.1894	6298.71	280.27	1.2663
41.5	278.78	1.2766	523.52	2.1347	573.59	2.1879	6263.8	278.78	1.2617
40.6	277.29	1.2714	523.52	2.1347	572.27	2.1864	6229.53	277.29	1.2572

September

T_k	$h_{e,i}$	$s_{e,i}$	$h_{e,o}$	$s_{e,o}$	$h_{c,o}$	$s_{c,o}$	Q_k	$h_{k,o}$	$s_{k,o}$
(°C)	**(kJ/kg)**	**(kJ/kg-K)**	**(kJ/kg)**	**(kJ/kg-K)**	**(kJ/kg)**	**(kJ/kg-K)**	**(W)**	**(kJ/kg)**	**(kJ/kg-K)**
					CSAC				
46.9	290.49	1.3177	523.52	2.1347	584.13	2.2002	6552.36	290.49	1.2974
48.4	293.85	1.3295	523.52	2.1347	587.18	2.2039	6641.25	293.85	1.3075
50.7	299.1	1.3479	523.52	2.1347	591.99	2.2098	6786.3	299.1	1.3231
53	304.48	1.3668	523.52	2.1347	596.96	2.216	6943.3	304.48	1.339
55.3	310.02	1.3862	523.52	2.1347	602.12	2.2225	7114.1	310.02	1.3553
54.7	308.56	1.3811	523.52	2.1347	600.75	2.2208	7068.09	308.56	1.351
54.1	307.11	1.376	523.52	2.1347	599.4	2.219	7023.14	307.11	1.3468
53.5	305.67	1.3709	523.52	2.1347	598.06	2.2173	6979.19	305.67	1.3425
52.9	304.24	1.3659	523.52	2.1347	596.74	2.2157	6936.2	304.24	1.3383
52.2	302.59	1.3601	523.52	2.1347	595.21	2.2138	6887.23	302.59	1.3335
51.6	301.19	1.3552	523.52	2.1347	593.91	2.2121	6846.21	301.19	1.3293
					DEC-SAC				
39.7	274.98	1.2633	523.52	2.1347	568.08	2.178	6132.26	274.98	1.25
40.3	276.24	1.2677	523.52	2.1347	569.11	2.179	6158.65	276.24	1.2539
42	279.84	1.2803	523.52	2.1347	572.05	2.182	6235.52	279.84	1.265
42.9	281.76	1.2871	523.52	2.1347	573.62	2.1836	6277.55	281.76	1.2709
42.3	280.48	1.2826	523.52	2.1347	572.57	2.1825	6249.42	280.48	1.267

43.4	282.84	1.2909	523.52	2.1347	574.5	2.1845	6301.31	282.84	1.2742
42.6	281.12	1.2848	523.52	2.1347	573.1	2.183	6263.44	281.12	1.2689
41.7	279.2	1.2781	523.52	2.1347	571.53	2.1814	6221.72	279.2	1.263
42	279.84	1.2803	523.52	2.1347	572.05	2.182	6235.52	279.84	1.265
41.9	279.63	1.2796	523.52	2.1347	571.88	2.1818	6230.91	279.63	1.2643
41.9	279.63	1.2796	523.52	2.1347	571.88	2.1818	6230.91	279.63	1.2643

LIST OF PUBLICATIONS

Based on the present study, the following papers have been published.

Journal Papers

1. Gupta, S.K., Arora, B.B. & Arora, A. Effect of Evaporative Cooling of Condenser on the Performance of Air Conditioner. *Iran J Sci Technol Trans Mech Eng* **47**, 1661–1677 (2023). https://doi.org/10.1007/s40997-023-00631-3. (SCIE)
2. Gupta, S.K., Arora, B.B. & Arora, A. Effect of varying ambient conditions on the performance of air conditioner using evaporative cooler. *J Braz. Soc. Mech. Sci. Eng.* **45**, 625 (2023). https://doi.org/10.1007/s40430-023-04542-x. (SCIE)
3. Sunil Kumar Gupta, B.B. Arora, Akhilesh Arora, Thermo-economic assessment of air conditioner utilizing direct evaporative cooling: A comprehensive analysis, International Journal of Refrigeration, Volume 158, 2024, Pages 68-88, ISSN 0140-7007, https://doi.org/10.1016/ j.ijrefrig. 2023. 11.021. (SCIE)
4. Sunil Kumar Gupta, B.B. Arora, Akhilesh Arora, "Thermodynamic Performance Assessment of Air Conditioner Combining Evaporative and Passive Cooling" *J. Thermal Sci. Eng. Appl*. May 2024, 16(5): 051003, https://doi.org/10.1115/1.4064743. (SCIE)
5. Sunil Kumar Gupta, B.B. Arora, Akhilesh Arora, "Thermodynamic performance enhancement of an air conditioner with dew point evaporative cooler," *J. Eng. Sustain. Bldgs. Cities*. Feb 2024, 5(1): 014501 (9 pages), https://doi.org/10.1115/1.4063498. (Scopus)

Conference Papers

1. Sunil Kumar Gupta, B.B. Arora, Akhilesh Arora, "Economics-Based Payback and Life Cycle Cost Savings Assessment of Inverter Type Air Conditioners", 2021, *IOP Conf. Ser.: Mater. Sci. Eng.* 1206 012023DOI 10.1088/1757-899X/1206/1/012023 (ICRAMEN-2021).
2. Gupta, S.K., Arora, B.B., Arora, A. (2023), "Effect of Ambient Temperature on Thermodynamic Performance of a Split Type Air Conditioner" in *Recent Trends in Thermal and Fluid Sciences. Lecture Notes in Mechanical Engineering*. Springer, Singapore. https://doi.org/10.1007/978-981-19-3498-8_1 (INCOME-2021).
3. Sunil Kumar Gupta, B.B. Arora, Akhilesh Arora, "Effects of Design Variables on the Output Parameters of a Split Air Conditioner Replacing R410A with A New Refrigerant Mixture R454B", *Advances in Mechanical Engineering and Management*, Walnut Publications, ISBN-13: 978-1957302652 ISBN-10: 1957302658, 1 February 2023. (https://www.amazon.in/Advances-Mechanical-Engineering-Management-Ravindra/dp/1957302658) (MMPM-2021).

AUTHOR'S BIO-DATA

Mr. Sunil Kumar Gupta graduated in Mechanical Engineering from The Institution of Engineers (India), Kolkata in 1996. He obtained his Master of Engineering degree from the University of Delhi (Delhi College of Engineering) in 2002. He has more than 30 years of experience including 3 years in Heavy Engineering industry and 14 years in Industrial Training in the Institutes run by Govt. of Delhi.

Presently he is a regular faculty in Aryabhatt Institute of Technology, Department of Training and Technical Education, Govt. of Delhi (now a campus of Delhi Skill and Entrepreneurship University) since 2010. He is an Associate Member of The Institution of Engineers (India). He is also a member of ISHRAE. His area of interest is Energy Conservation in Refrigeration and Air-Conditioning. He has published four research papers in reputed SCI expanded journals and one technical brief in ASME journal. He has also presented three papers in International Conferences.